

CHEMOSTRATIGRAPHY AND GEOCHEMICAL CONSTRAINTS ON THE DEPOSITION
OF THE BAKKEN FORMATION, WILLISTON BASIN, EASTERN MONTANA AND
WESTERN NORTH DAKOTA

by

DAVID NYRUP MALDONADO

Presented to the Faculty of the Graduate School of
The University of Texas at Arlington in Partial Fulfillment
of the Requirements
for the Degree of

MASTER OF SCIENCE IN GEOLOGY

THE UNIVERSITY OF TEXAS AT ARLINGTON

December 2012

Copyright © by David Nyrup Maldonado 2012

All Rights Reserved



Acknowledgements

First, I would like to thank God for allowing me to return to school to finalize what has been a long and overdue achievement. I agree with the statement that timing is everything but hard work and perseverance played a very large role in completing this task. I would like to thank my advisor, Dr. Harry Rowe, for his patience, time, and energy during my attendance at the University of Texas at Arlington as a graduate student. This thesis would not have been possible without Dr. Rowe, Dr. Stephen C. Ruppel, and the Texas Bureau of Economic Geology in Austin, Texas. I would also like to extend thanks to Dr. John S. Wickham for his guidance and being a member of my thesis committee. I would also like to extend many thanks for Paula Burkhart our geoscience administrative assistant for her patience and understanding. I would also like to thank several members of the Texas Bureau of Economic Geology. I would also like to thank Kenneth Edwards and Josh Lambert for core handling assistance. I would also like to thank Brigham Exploration Inc., now Statoil, for contributing their cores to the Texas Bureau of Economic Geology in Austin, Texas. I would like to thank my family for their loving support and encouragement during my studies during these last several years. Finally, I would like to dedicate my academic career to the people for which I have the most love and respect, my parents.

December 5, 2012

Abstract

CHEMOSTRATIGRAPHY AND GEOCHEMICAL CONSTRAINTS ON THE DEPOSITION
OF THE BAKKEN FORMATION, WILLISTON BASIN, EASTERN MONTANA AND
WESTERN NORTH DAKOTA

David Nyrup Maldonado, MS

The University of Texas at Arlington, 2012

Supervising Professor: Harold Rowe

The late Devonian-early Mississippian Bakken Formation was deposited in a structural-sedimentary intracratonic basin that extends across a large part of modern day North Dakota, eastern Montana, and the southern portion of Canada's Saskatchewan Province. The deposition of the Bakken Formation occurred during a fascinating period of geologic time that is linked to one of the five major mass extinctions. The occurrences of these mass extinctions are recorded worldwide as organic rich mud rocks similar to the ones found in the Bakken Formation. Collectively, the Bakken Formation consists of a middle dolomitic siltstone that is representative of a transgressive deposit and is bound by regressive organic rich mud rocks deposits that were influenced by rapid flooding events induced by the late Devonian-early Mississippian seaway. Geochemical proxies, total organic carbon and stable isotopic results that were recovered from four cores provide insight into the paleoenvironmental conditions during the deposition of the Bakken Formation. Geochemical analysis and interpretation of sample suites exhibit aggregate mineralogical composition from related shifts in elemental concentrations in weight percent (wt. %) consisting of magnesium (Mg), calcium (Ca), silicon (Si),

aluminum (Al) and iron (Fe). The occurrence of chemostratigraphic shifts from concentrations of the Bakken Formation's bulk rock mineralogical composition represent facies changes of sedimentary packages within the middle Bakken and are linked to dolomite, calcite, quartz, pyrite, and clay (mainly illite) content. Furthermore, geochemical proxies of redox sensitive elements expressed as enrichment factors (EF) brought insight into the redox conditions during deposition of the upper and lower Bakken shales across the Williston Basin (e.g., Mo, U, V, Zn, Ni, and Cu). Molybdenum-total organic carbon (Mo-TOC) relationships, established two separate anoxic episodes that are represented by the Bakken shales and also provided insight into the degree of basin restriction the Williston Basin experienced during late-Devonian-early Mississippian time. Observed geochemical Mo-TOC relationships from the Bakken shales display similar trends of basin restriction comparable to modern silled basin analogues, specifically the Cariaco Basin (Algeo et al. 2006). The elemental shifts from Mo-TOC vs. depth profiles, demonstrate that the Bakken shales were deposited under semi-restricted conditions. Furthermore, Mo-TOC relationships also inferred water mass residence times and variable hydrographic mixing from deep basin waters from the Williston Basin. TOC and stable isotopic composition of TOC ($\delta^{13}\text{C}$) from the Bakken shales were utilized as geochemical proxies to examine the change and distribution of organic matter across the Williston Basin. Lastly, stable isotopic composition of TOC results potentially demonstrate a blend of kerogen source formed from marine organic matter (plankton) and land-plant lipids based on previous studies.

Table of Contents

Acknowledgements.....	iii
Abstract.....	iv
List of Illustrations.....	viii
List of Tables.....	xi
Chapter 1 Introduction.....	1
Purpose of Study.....	1
Previous Work.....	2
Regional Geology.....	6
Devonian-Carboniferous Paleoclimate.....	18
Research objectives.....	19
Chapter 2 Methods.....	21
Core Data Acquisition.....	21
Energy Dispersive X-ray Fluorescence (ED-XRF) Analysis.....	22
Mudstone Calibration of ED-XRF.....	24
Additional Geochemical Analysis.....	27
Chapter 3 Results.....	28
ED-XRF and Non-ED-XRF Data.....	28
Chemostratigraphic Applications.....	28
Diagrams.....	29
Chapter 4 Discussion.....	32
Major Elements.....	32
Three Forks Formation.....	32
Bakken Formation.....	44

Redox Indicators Geochemical Proxies.....	50
Basin Restriction (Mo/TOC)	55
Organic Composition (TOC and Stable isotopes of Organic Carbon)	66
Bakken Shale Kerogen type from $\delta^{13}\text{C}$	69
Chapter 5 Conclusion.....	75
Future Research.....	78
References.....	79
Biographical Information.....	91

List of Illustrations

Figure 1-1 Major Paleozoic structural trends7

Figure 1-2 Present day structural features, Western Interior, United States 8

Figure 1-3 Generalized regional Montana-North Dakota cross section A-A' 9

Figure 1-4 Regional paleogeography and paleostructure..... 12

Figure 1-5 Regional paleogeography and paleostructure..... 16

Figure 1-6 Stratigraphic column of the Williston Basin and Bakken Formation..... 17

Figure 2-1 Geographical location of cores in research study 21

Figure 2-2 Overview of ED-XRF instrumentation 23

Figure 4-1 Chemostratigraphic profile of major elements Three Forks Formation and lower Bakken Formation from west to east %Al, %Fe, %Ca, %Mg, %Si/%Al and %Si ... 33

Figure 4-2 Interpreted Upper-Devonian lithofacies map Three Forks Formation 34

Figure 4-3 Cross Plot of Core A of %Ti, Mo ppm, Rb ppm, V ppm, U ppm, Zr ppm and %K versus %Al..... 36

Figure 4-4 Cross Plot of Core B of %Ti, Mo ppm, Rb ppm, V ppm, U ppm, Zr ppm and %K versus %Al..... 37

Figure 4-5 Cross Plot of Core C of %Ti, Mo ppm, Rb ppm, V ppm, U ppm, Zr ppm and %K versus %Al 38

Figure 4-6 Cross Plot of Core D of %Ti, Mo ppm, Rb ppm, V ppm, U ppm, Zr ppm and %K versus %Al..... 39

Figure 4-7 Cross Plot for Core A of %Ca, %Mg, %Si, and %K versus %Al 40

Figure 4-8 Cross Plot for Core B of %Ca, %Mg, %Si, and %K versus %Al 41

Figure 4-9 Cross Plot for Core C of %Ca, %Mg, %Si, and %K versus %Al 42

Figure 4-10 Cross Plot for Core D of %Ca, %Mg, %Si, and %K versus %Al 43

Figure 4-11 Chemostratigraphic profile of major elements Bakken Formation from west to east %Al, %Fe, %Ca, %Mg, %Si/%Al and %Si	46
Figure 4-12 Gross thickness map of Bakken Formation.....	47
Figure 4-13 Cross-plots of %Si/%Al versus %TOC	49
Figure 4-14 Chemostratigraphic profile of trace elements expressed as enrichment factors (EF) redox character of the Bakken Formation from west to east in comparison with %TOC and Mo, U, Zn, Ni, and Cu.	52
Figure 4-15 Middle to Late Paleozoic axes for potential paleoceanic undercurrents during 1. Middle Devonian, 2. Upper Devonian and 3. Mississippian time	54
Figure 4-16 Cross plot for A of Mo ppm / %TOC.....	57
Figure 4-17 Cross plot for core C of Mo ppm / %TOC.....	58
Figure 4-18 Cross plot for core D of Mo ppm / %TOC.....	59
Figure 4-19 Eustatic sea level changes during late Phanerozoic	61
Figure 4-20 Chemostratigraphic profile of Mo ppm and TOC % versus depth for the upper Bakken shales	62
Figure 4-21 Chemostratigraphic profile of Mo ppm and TOC % versus depth for the lower Bakken shales	63
Figure 4-22 Total organic carbon and M verses depth below sediment water interface for the Cariaco Basin.....	64
Figure 4-23 Chemostratigraphic profile of covariant trace elements e.g. Mo ppm, U ppm, Cu ppm, Zn ppm, Ni ppm, with %TOC	67
Figure 4-24 Paleogeographical reconstruction of continents during Famennian-Tournaisian time, distribution of Devonian organic-rich marine mudrocks, and predicted	

positions of atmospheric pressures cells with associated surface winds responsible for upwelling locations	68
Figure 4-25 Carbon isotopes for Williston basin oil extract and rock samples	70
Figure 4-25 Occurences of $\delta^{13}\text{C}$ analyzed from the A, C, and D core for the Bakken shales	71

List of Tables

Table 2-1 Information from cores analyzed in research project.....22

Table 2-2 Lowest Detectable Measurements (LDM) for Elements Analyzed 26

Table 2-3 Subset types and numbers of analysis performed on three Bakken cores A, C,
and D 27

Table 4-1 Total Organic Carbon, TOC and Stable Carbon Isotopic, $\delta^{13}\text{C}$ data for core A
..... 72

Table 4-2 Total Organic Carbon, TOC and Stable Carbon Isotopic, $\delta^{13}\text{C}$ data for core C
..... 73

Table 4-3 Total Organic Carbon, TOC and Stable Carbon Isotopic, $\delta^{13}\text{C}$ data for core D
..... 74

Chapter 1

Introduction

Purpose of Study

Collectively, the Bakken Formation of the Williston Basin is made up of upper and lower organic rich mudrocks that are highly siliceous with a middle unit that consists of variable lithologies that contain calcite, dolomite, and quartz. Recently, mudrocks/shales have become popular because they provide insight into major processes of sedimentation, sea level changes, lateral continuity of correlatable key markers on a locally or regional scale, and they yield evidence of paleoxygenation of ancient basins. Furthermore, the study of mudrocks also provides evidence of compaction, thermal history, source, and hydrocarbon seal which aids in reservoir quality. Although numerous studies have been done on the Bakken Formation ranging from reservoir characterization, depositional history, structural occurrences, facies analysis, ichnofacies determination, Devonian eustatic sea level fluctuations in Euramerica and many more, there has never been a study conducted on the chemostratigraphy of the late Devonian-early Mississippian interval (Brown et al. 1982; Sandberg, C. A., et al., 1982; Johnson et al., 1985; Smith et al., 1995; Angulo et al., 2008; Kohlruss et al., 2009; Angulo et al., 2012). Deposition of the Bakken Formation was potentially controlled by basin subsidence, varying rates of sediment supply, temporal and spatial changes under marine conditions. The processes that contributed to the bulk geochemistry content of the Bakken formation could be potentially reconstructed by the use geochemical proxies (ie. Si/Al, Zr/Al, and Ti/Al) to show the occurrence of depositional sequences attributed to sedimentary influx from siliciclastics and carbonate sedimentation, eolian, volcanogenic, or biogenic sources (Ver Straeten, 2010). Studies have also shown that molybdenum

concentration data in conjunction with TOC (ie. trace metal conc./TOC) can provide insight into the degree of water mass restriction, chemical evolution of deep water restriction, and concentration amounts of redox sensitive elements preserved as a primary environmental signal (Algeo et. al. 2006; Rowe et. al 2008; and Rowe et. al. 2009). Conducting this kind of research has become important because chemostratigraphy could be utilized as an additional tool to identify elemental controls of mudrock deposition. Successful integration of geochemical inferences complement paleoenvironmental interpretations and help establish the framework for defining the extremes of water mass evolution and biogeochemical cycling in isolated paleo-marine depositional systems (Rowe et. al. 2008; Algeo et. al. 2008).

Previous Work

The application of redox sensitive elements i.e., S, Ba, V, Cr, Mn, Fe, Ni, Cu, Zn, U, & Mo, have recently been used in studies to determine sedimentation patterns of various detrital sources, biogenic input, dynamic redox conditions, and authigenic sediment sources (Clayton et al., 1978; Cawood et al., 2003; Grosjean et al., 2004, François et al., 2004, Riquier, L. et. al 2006). Elemental proxies such as such as total organic carbon and molybdenum (Mo-TOC) have been utilized to identify anoxic dominated sequences and to develop regression lines whose slopes (m) range from ~2 to 65 ($\times 10^{-4}$) yielding an understanding of slow evolving water mass characteristics from individual local basins to regional basins of the Devonian-Carboniferous North American Seaway (Algeo et. al. 2007). Normalization of isotopic and elemental proxies i.e. TOC & Mo, with Al are useful for quantifying the original framework of ancient sediments. This approach was used to discern the original organic matter in place of ancient black shales

to modern ones found in the Cariaco Basin. Strong correlations between TOC and trace elements V, Mo, and Co, but low Mn concentrations suggest deposition of an oxygen deficient setting (Wilde, et. al. 2004). The application of Mo concentrations has been also used to ascertain environmental differences between sulfidic bottom waters vs. sulfide pore waters beneath an oxygenated water column (Scott and Lyons, 2012). While existing concentrations of molybdenum in sediments suggest anoxic conditions (Dean et. al. 1997) higher concentrations of Mo have been found in anoxic basins where conditions are linked to intermixing of marine waters.

Redox-trace elements, Mo and U specifically, have been extensively utilized due to their long residence times (~ 800 kyr for Mo, ~ 450 kyr in oxic seawaters and are proxies indicators of paleoredox conditions (Dean et al., 1997; Algeo and Maynard 2005; Brumsack, 2006; Tribovillard et al., 2006; Algeo et. al, 2009). These trace elements also exhibit high authigenic enrichment under anoxic conditions because Mo becomes “reactive” when molybdate (MoO_4^{2-}) reacts with hydrogen sulfide (H_2S), facilitating the development of reactive thiomolybdates (TM's) ($\text{Mo O}_x\text{S}_{4-x}$; $x = 0$ to 3) are absorbed by humic material (Berrang and Grill 1974; Magyar et al., 1993; Helz et. al., 1996; Zheng et al., 2000. In recent or ancient restricted basins trace elemental proxies such as Mo, U and V serve as indicators of anoxic-euxinic conditions (Algeo and Lyons, 2006; Algeo and Maynard, 2008; Algeo and Tribovillard, 2009; Algeo and Rowe, 2011). These conditions exist in silled basins that experience basin restriction limiting deep water renewal times. Therefore, geochemical signatures of trace element enrichment can be utilized to identify paleoceanographic conditions of deep-water basin restriction, deep-water residence times and changes in deep-water chemical composition.

Studies have also been focused on using enrichment of molybdenum and uranium (Mo-U) covariation to link benthic redox conditions, operation of particle shuttles within the water column, and evolution of water chemistry (Tribovillard, N., et. al., 2011). Furthermore, the Mo-U linear relationship has been used to understand the attributes of water mass processes that reveal similar redox and hydrographic control patterns of recent and ancient low oxygen marine systems, i.e., Cariaco Basin, Black Sea, Late Pennsylvanian Midcontinent Sea (LPMS) and the Late Devonian Seaway (LDS) (Algeo et. al., 2008). Chemostratigraphic studies have also been applied to ancient and modern silled basins by utilizing other sedimentary trace metal concentrations such as Re with Mo, U, V, to identify benthic redox conditions, degree of water mass restriction, and chemical changes in aqueous chemistry and basin hydrography (Algeo et. al., 2008).

Chemostratigraphic studies have brought insight into not only the degree of water mass restriction of modern or ancient silled basins, but also insight into organic-rich mudrocks formation by integrating multiple sedimentary geochemical proxies as ratios (e.g. Mo/Al, Si/Al, Fe/Al, and carbon-sulfur-iron (TOC-S-F) (Dean et. al., 1989; Rowe et. al., 2008). Studies have also been conducted to demonstrate trace element anomalies during the Late Devonian 'punctata Event' of the Western Canada Sedimentary Basin (WCSB) (Śliwiński et. al. 2010). In this research global perturbation of the C-cycle during the Late Devonian was examined by chemostratigraphic profiles of Mg and its association with dolomitization of the Fairholme and South-Cairn Carbonate complexes of the WCSB. Minor and trace elements were used to elucidate oceanic bio-productivity (ie. Ni, Cu, P, Ba, Zn) variations of terrigenous siliciclastics entering the WCSB (ie. Al, Si, Ti, K, Cr, Zr, Co), and dominate redox conditions near the sediment-water interface (eg. U, Mo, V, Ni/Co, U/Th, V/Cr, V/V+Ni). Another important application of geochemical

proxies is the ability to infer the depositional environment in relation to potential orbital scale that may be related Milankovitch cycles through the chemical composition of sediments (Rachold & Brumsack, 2001). Chemical compositions linked to variations in carbonate content Ca/Al, detrital composition in the form of illite and quartz content (Ti/Al and Si/Al), the lack of enrichment of redox-sensitive trace elements (V, Cr, high Mn) content or nutrient-related trace elements (Ba, P, Zn), all construct Albanian sediments from the Lower Saxony Basin NW Germany. Carbonate content and Al normalized concentrations of detrital elements such as Si and Ti suggest carbonate cyclicity, cyclicity in detrital input and nutrient-related element abundances can be seen in a 60 m interval. Furthermore, spectral analysis results of the chemical data found within the sedimentological content of the Upper Albanian sediments are hypothesized as representing Milankovitch cycles of eccentricity, obliquity, and precession bands.

Studies have also been focused on determining the environmental conditions associated with the deposition of two Late Frasnian black Kellwasser horizons in a submarine-rise environment of the Harz Mountains, Germany (Riquier, L. et. al 2006). In this research three Late Devonian sections from the Harz Mountains were analyzed for major and trace element concentrations to elucidate two events of minimum detrital input with an increase in primary production. Elemental ratios of Ti/Al and Zr/Al were used to identify periods of nutrient enrichment. Additional geochemical data (U, V and Mo and redox indices U/Th, V/Cr, and Ni/Co) were also used to identify oxygen restricted conditions during Late Frasnian time (Riquier, L. et. al 2006).

Organic geochemical proxies like stable isotope ratios of carbon and nitrogen $\delta^{13}\text{C}$, $\delta^{15}\text{N}$ and carbon/nitrogen ratios (C/N) have been utilized to identify various sources of organic matter preserved in sediment through time (Meyers, 1994). Integrating

elemental and carbon isotope values allows for the identification of organic matter derived from settling sediment particles that is representative of a mixture of organic matter components. The importance of utilizing stable isotopic, carbon, and nitrogen ratios also plays a vital role in identifying the controls on the production and preservation of organic matter. Paleoenvironmental controls such as upwellings contribute to primary productivity of organic matter across modern and ancient shore lines, sea ways, and basins. Additional variables that impact the recycling of nutrients in open marine conditions are trade winds, waves, surface currents, and paleoclimatic changes. (Meyers, 1997). Surface oceanic currents during ancient glacial periods experienced stronger hydrographic circulation enhancing higher paleoproductivity vs. interglacial periods (Ganeshram, R. et. al. 1998). According to Lyle (1998), paleoproductivity is enhanced during glacial periods due to efficient nutrient recycling and greater deliveries of land derived nutrients.

Regional Geology

During the late Paleozoic one of the largest mass extinctions occurred which affected terrestrial and marine habitats. This mass extinction, known as the Hangenberg event, took place at the Famennian-Tournaisian boundary and marks a period in geologic record during the deposition of the Bakken Formation in the intra cratonic Williston Basin (Kaiser et al., 2011). The Williston basin began to develop during the late Cambrian convergence of the Churchill Hinterland with the Superior Province that formed the Trans-Hudson Orogen. The newly developed region encompassing the area of the Williston Basin is interpreted as being formed by various structural processes i.e. convergence, divergence, periods of uplift and subsidence (Crowley et. al., 1985). This

hypothesis was tested by fission-track dating of apatite samples of basement rocks beneath and adjacent to the basin. Crowley concluded that the timing of the uplift of the basement prior to subsidence of the Williston Basin coincides with the thermal-origin hypothesis of basin formation. Furthermore, a series of major Paleozoic structural trends, that currently control the structures and geometries of the Williston Basin, were developed during the rifting of ancient North American plates during the late Precambrian period (Gerhard, 1990) (Figure 1-1).

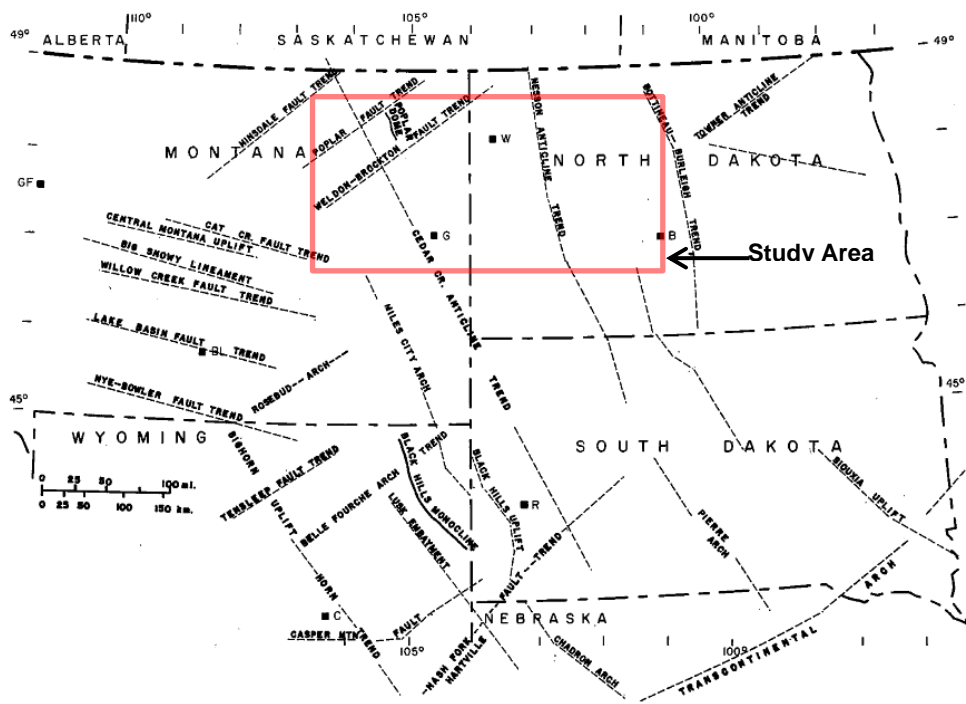


Figure 1-1 Major Paleozoic structural trends and study area (Brown et. al 1982).

During late Paleozoic time, the Antler and Ancestral Rocky Mountains orogenies developed a realignment of the already deformed deep-seated lineaments due to plate collisions from the paleo-west (Kluth, 1986). These deformations which were subsequently re-initiated during the Laramide Orogeny, and then again during early Tertiary time form structural features currently observed in the Williston Basin (Figure 1-

2). The Antler orogen to the West, the Acadian orogen to the East, and the Ellesmere orogen to the north surrounded the interior of North America which produced compressive stresses that translated laterally throughout the North American craton resulting in periodic adjustments of interior platforms, changes in relative base level, and fluctuating rates of clastic sedimentation into the Williston Basin (Sleep et al., 1980; Sandberg et al., 1982; Lambeck, 1983; DeRito et al., 1983; Quinlan and Beaumont, 1984; Johnson et al., 1985; Ross and Ross, 1985; Beaumont et al., 1987).

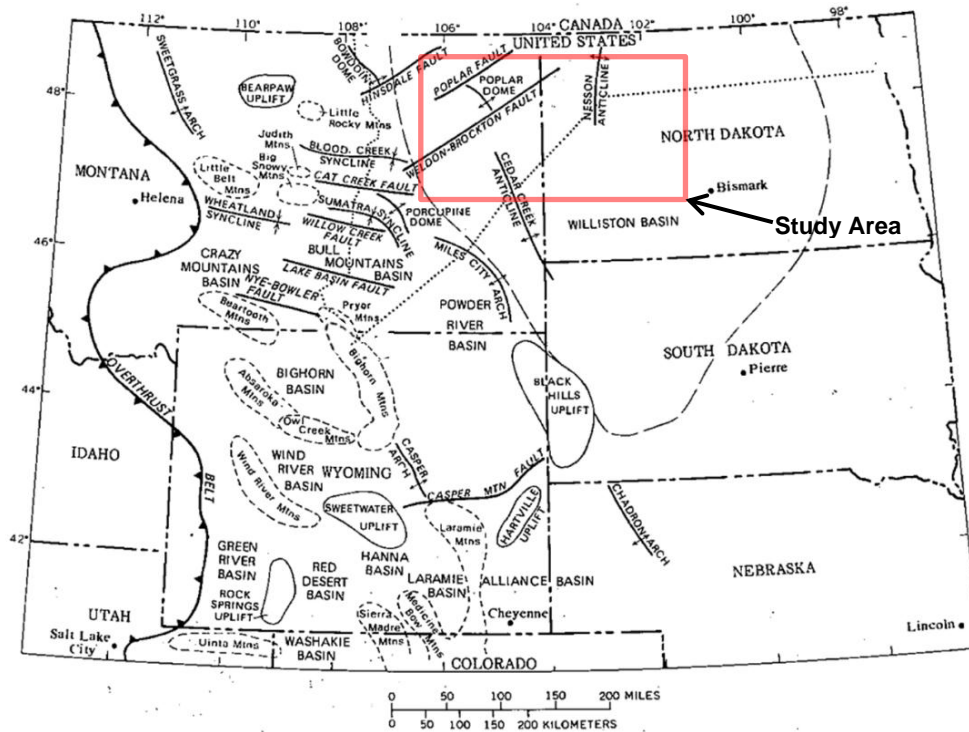


Figure 1-2 Present day structural features, Western Interior, United States. Modified after Peterson (1981).

Preserved sedimentary fill within the Williston basin consists of a complete rock record that ranges in thickness from 15,000 to 16,000 feet (Figure 1-3) (Carlson, 1960). The stratigraphic Cambrian to Quaternary sedimentary fill, constitute a cyclical deposition of carbonates and clastics that have been influenced by subsidence and tectonic

The cyclical pattern of sedimentary formations observed in the Williston basin can be interpreted as intermittent punctuated periods of deposition. During Cambrian time the region west of the Williston Basin was flooded during a highstand, with small punctuated transgressive-regression cycles, that is represented by the deposition of the Flathead Formation (Gerhard et al., 1982). The earliest transgression during Cambrian time is also represented by the Gross Ventre, Gallatin and Grove Creek Formation and their equivalents, Emmerson Formation. During Upper Cambrian time, the transgression had reached the Williston Basin and is manifested as the Deadwood Formation which mainly consists of sandstones, shales, and carbonates that were deposited on the structurally variable surface of Precambrian basement. Furthermore, the possible regressional sequences that may be missing could be attributed to regional widespread erosion (Peterson and MacCary, 1987; Gerhard and Anderson, 1988). During this time period, the sediment deposited at the center of the Williston basin is considered marginal marine to inner shelf deposits that are ~1000 ft. thick at the central part of the Williston Basin. The sedimentary fill that is linked to Ordovician-Silurian time is marked by secondary cyclical transgressive-regressive deposits that consist of carbonates and anhydrites (Vigrass, 1971). At this time period the circular shape and depocenter of the Williston Basin became clearly defined with ~2,500 ft. of sedimentary rock preserved at the center of the basin, with openings to the southwest and to the southeast (Gerhard and Anderson, 1988). The late Ordovician commenced with deposition of fluvial/deltaic sands and shales which are representative of transgressive basal siliciclastics belonging to the Winnipeg group. These deltaic sands were overlain by argillaceous shales from the Black Island Formation, deeper water marine shales-Icebox Formation; and argillaceous limes-Roughlock Formation (Ellingson, 1995). The end of the Winnipeg group is difficult

to identify within the Williston Basin in North Dakota because its contact with the Deadwood group consists of similar lithologies. However, in eastern Montana there is a sharp lithological contact that has been identified between them (Lochman-Balk and Wilson, 1967). The Red River Formation of the Big Horn group conformably overlies the Winnipeg group, which consists of cyclical equatorial shelf, and lagoonal deposits (Gerhard and Anderson, 1988), and is conformably overlain by subtle disconformities of cyclical carbonates and anhydrites belonging to the Stony Mountain and Stonewall Formations. The transgressive-regressive deposits observed within the Williston Basin are attributed to several possible factors such as local tectonics, continental glaciation, and climatic changes (Peterson and MacCary, 1987). During Silurian-Devonian time seaway reorientation occurred to the north and south of the Williston Basin due to structural movement along the Trans-Continental Arch. Silurian deposits which conformably overlie Ordovician deposits consist of transgressive-regressive peritidal/shallow marine cycles belonging to three units within the Interlake Group (LoBue, 1982). Karstification at the top of the Interlake Group is said to have occurred during Silurian time due to falling sea level followed by widespread erosion. The Silurian deposits were then followed by two regional sea-level rises and an unconformity that separates Devonian from younger Lower Mississippian deposits (Sloss, 1987; Gerhard et. al., 1990). During the initial transgression the Ashern Formation of the Elk Point Group is defined as three basal carbonate-evaporite deposits with varying lithologies that consist of dolostones and shales whose depositional environment is not clear (Rosenthal, 1987). However possible depositional processes could be attributed to transgressive infill of post-Silurian erosional surfaces that consisted of tidal flat deposits, sabkhas to non-marine environment (Lobdell, 1984). The following early to mid-Devonian transgressive-

regressive interval overlying the Ashern formation is the Winnipegosis Formation. The transgressive phase of the Winnipegosis Formation consists of shelf-deposited carbonates and reefs scattered throughout southeastern Saskatchewan. The regressive phase of the Winnipegosis formation has been described as subtidal and intertidal deposits with increasing anhydrite finally capped by halites of the mid-Devonian Prairie Evaporite Formation (Gendzwill, 1978, Martindale, 1987, and Perrin, 1982a). During the deposition of the Prairie Formation a reorientation of the Elk Point Basin, which consists of the Williston and Alberta Basins, occurred due to tectonic activity from the Transcontinental Arch in the south east (Figure 4-1).

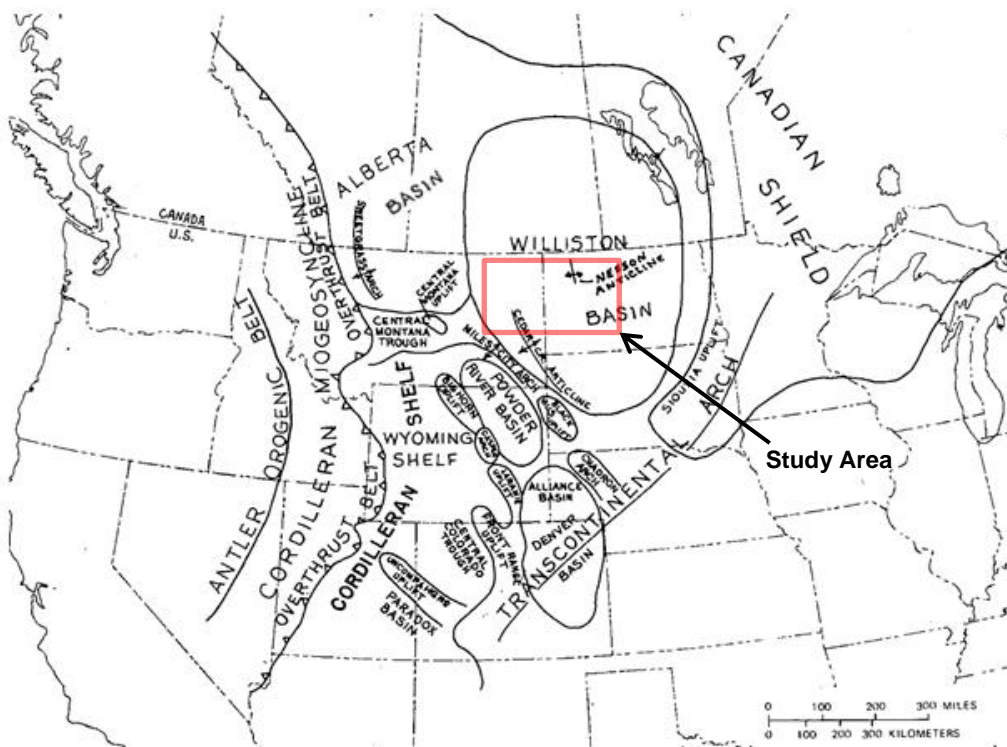


Figure 1-4 Regional paleogeography and paleostructure during Paleozoic time, Western Interior, United States (Peterson et al., 1987).

The tilting of the basins in a northwestward direction ensured increased basin restriction, salinity, and Prairie deposition. Following the deposition of the Prairie Formation, an unconformity can be identified by the presence of peritidal deposits in the form of red beds in North Dakota. These red beds are the first sequence found within the Manitoba Group and are followed by the Souris River Formation that consists of cyclical fine clastics which grade into dolomites and limestones, and are finally capped by anhydrite deposits. As the southerly encroachment of the Late Devonian seas continued, the deposition of the Duperow Formation began, which consists of shelf carbonates that are interbedded with peritidal and anhydrite deposits. (Wilson, 1967; Gerhard and Anderson, 1988). The Duperow Formation is conformably overlain by a series of carbonate-evaporite cycles belonging to the Birdbear Formation. The Birdbear Formation has been described as a transgressive-regressive cycle that was deposited in a low-energy subtidal and high energy intertidal, lagoonal depositional environment (Halabura, 1982). The Three Forks formation overlies the Birdbear Formation and consists of red and green shales, siltstones, sandstones, carbonate rocks and evaporite sequences that represent the final regression of Devonian sedimentation. Evidence of the final regressive cycle marks the upper section of the Three Forks Formation and has been interpreted as clastic material derived from a westward direction (Peterson and MacCary, 1987).

During Bakken deposition the semi-isolated Williston Basin was located close to the Equator (5° to 10°N) in a zone of prevailing east to west trade winds and occupied a position near the center of the Epicontinental Sea at the western margin of North America (Gerhard et. al. 1988; Richards, 1989; Smith et. al., 1995). During late Devonian-early Mississippian time, sediments were ushered into the Williston basin due to the reorientation of the Devonian-Carboniferous seaway through the central Montana trough.

Following the reorientation of the Devonian-Carboniferous seaway, major uplift and erosional events occurred along the margins of the basin during the transition from the Devonian to the Mississippian period (Gerhard and Anderson, 1988). The time interval between the end of the Three Forks Formation and the Bakken Formation represents the initial transgression of the advancing late-Devonian-early Mississippian seaway. The Bakken Formation straddles the Devonian/Mississippian boundary and is made up of three intervals known as the upper, middle and lower Bakken members (Meijer-Drees et.al., 1996). These intervals have been recognized as tripartite sequences of transgressive-regressive deposits, which overlap toward the basin margins. These deposits consist of two regionally distributed lower and upper organic-rich shales, known as the Bakken shales, and a dolomitic siltstone known as the middle Bakken. At the base of the lower Bakken shale Meijer-Drees and Johnston 1996, recovered late Devonian conodonts from this basal unit that overlies an erosional surface known as a sequence boundary. Smith and Bustin 1996, research also suggest that the lower Bakken was deposited at considerable water depths (200 m or more) influenced by low intensity bottom currents. Schieber 1998, also examined the lower Bakken shale and discovered thin lag deposits (coarse sand size) that contained reworked pyrite grains, pieces of pyritized shell material and quartz grains (reworked quartz-filled Tasminites cysts). The middle Bakken is composed of horizontally bedded mudstone at the base that grade into a wave-flaser bedded sandstone overlain by trough and tabular fine grained quartz sandstone that was deposited in a shoreface setting. Overlying the quartz sandstone is a final sedimentary package composed of horizontal bedded mudstones at the top of the middle Bakken member. Overall the middle Bakken collectively is representative of a mixed siliciclastic-carbonate system consisting of detrital grains, clay,

limestone and dolomite. The upper Bakken unit is the final transgressive interval that was deposited during an abrupt sea level rise and is the final succession within the Bakken formation. According to Smith et. al. (1995) the depositional environment of the Bakken formation has been interpreted as a deep marine-offshore/shoreface-deep-marine cycle. Following Bakken deposition a period of cyclic carbonate shelf sedimentation took place during early Mississippian time. The limestone deposition known as the Lodgepole Formation of the Madison Group represents sedimentation during a sustained transgression, which accumulated along the shelf edges of the Williston Basin and as isolated carbonate mounds (Precht, 1986; Gerhard et. al. 1988). The transgression reached its maximum at the end of Lodgepole deposition or early Mission Canyon Formation time.

According to Ellison 1950, Conant et. al. 1961, and Blatt et. al. 1991, the deposition of the Bakken Formation represents part of a vast interval of Late Devonian and Early Mississippian (Latest Famennian to earliest Tournaisian) black shale formation that includes the Exshaw Formation (Alberta Basin), Chattanooga Shale (Appalachian Basin), Antrim Shale (Michigan Basin), New Albany Shale (Illinois Basin), Ohio Shale (Appalachian Basin), Woodford Shale (Anadarko Basin/Arbuckle mountains and Permian Basin), that are found throughout the interior of North America. The vast shale succession that was deposited during this period are correlatable to the Hangenberg event named after the Hangenberg shale found in Rehinishces Schiefergebirge of Germany (Walliser, 1984). Similarly to the Bakken Shale, the Hangenberg Shale is also part of a synchronous global continuum of black mudrocks that reflect the wide spread generation of anoxic paleoenvironments and concurrent demise of late Devonian fauna (Caplan and Bustin, 1999). Globally, Devonian-Carboniferous black mudrocks include

the Hangenberg Shale from Montagne Noire, France, Cranic Alps, Bohemian region former Yugoslavia Domanik and equivalent formations of the Volga-Ural Platform, mudrocks and carbonates of the Pripyat, Dnieper-Donets Rift, Upper Devonian marine mudrocks

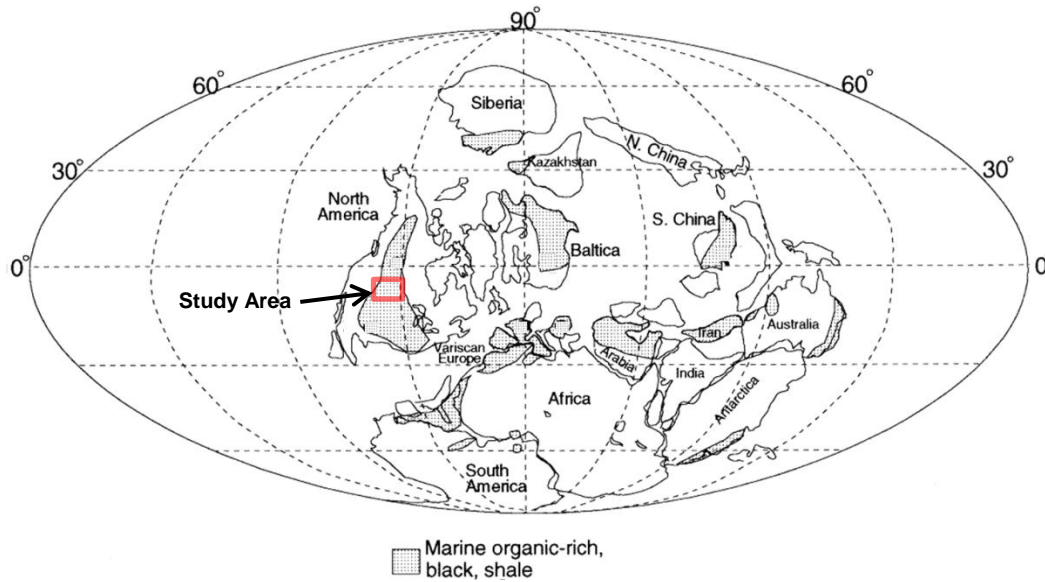


Figure 1-5 Geographical distribution of upper-Devonian organic rich mudrocks and paleogeographical reconstruction of continents during late Famennian-early Tournasian (Scotese and McKerrow, 1990).

of the Illizi Platform and Chanshun Shale of South China (Feist, 1990; Schonlaub, 1986; Schonlaub et al., 1992; Chlupac, 1988., Krstic et al., 1988; Ulmishek, 1988., Klemme and Ulmishek, 1991; Bai and Ning, 1988; Xu et al., 1989; and Wang et al., 1993), (Figure 1-5). The present research consists of the Bakken Formation, Figure 1-6; which unconformably overlies the truncated surfaces of the Upper Devonian Big Valley and Torquay (Saskatchewan), Lyleton (Manitoba) and Three Forks formations (North Dakota and Montana). The Bakken Formation is also conformably overlain by the Mississippian Lodgepole carbonates which is considered to be an abrupt or thin (<10 cm) gradational contact (Smith and Bustin, 2000).

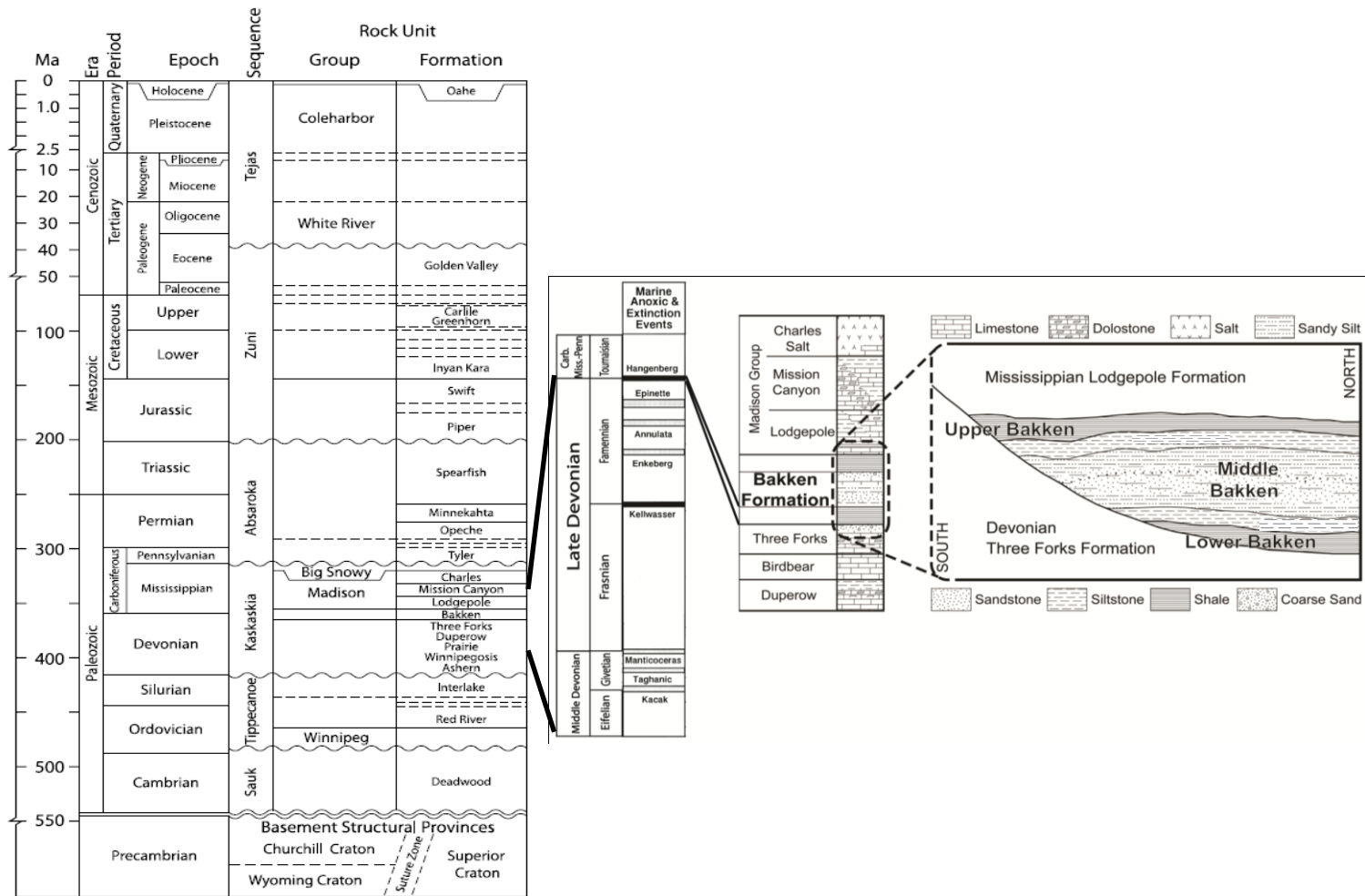


Figure 1-6. Stratigraphic column of the Williston Basin (modified from Carlson and Anderson, 1965; Murphy et al., 2009) with correlative interregional unconformities described by Sloss (1963) and schematic lithological profile of the Bakken Formation (Webster, 1984; Murphy et al., 2009, & Kuhn et al., 2010).

Devonian-Carboniferous Paleoclimate

Research suggest that the paleoclimate conditions during late Devonian-early Mississippian time were shaped by glaciation events derived from atmospheric CO₂ levels, latitudinal and location of glaciation, and pre-glacial conditions, contributed to the mass extinction at the Devonian-Carboniferous boundary (Cox et. al. 2001). The Devonian-Carboniferous boundary has also been recognized as a period of time that is linked to one of the largest biotic disturbances that took place during the Phanerozoic and also is commonly known as the D-C bio-event (McLaren et. al. 1990; Becker et. al. 1992, Sepkosk, 1996; Walliser, 1996b). Furthermore, glaciations also caused short term sea-level fluctuations (cyclothems) in North America during Famennian–Tournaisian stages (Veevers et. al. 1987) producing mass extinctions which have been tied to glacial melting. Sediments assigned to this interval of time occurred at equatorial and mid-latitudes as black organic-rich shales. The Hangenberg shale for example, is one of many late-Devonian-early Mississippian organic rich intervals that amassed a top of ramp and platform carbonates along continental shelves that serve as regional unconformities (House 1985). The increased burial of organic rich shale's during anoxic conditions produced long-term effects of atmospheric CO₂ drawdown initiating glaciation (Algeo and Scheckler 1998). Late Devonian glaciation occurred in the aftermath of a mass extinction, known as the Hangenberg event, which ultimately affected a large diverse group of land plants, marine invertebrates to include conodonts, trilobites, ammonoids, and to a lesser extent, acritarchs, foraminifera, ostracods, brachiopods, corals, and stromatoporoids (Kalvoda 1986; Wang et. al. 1993; Caplan and Bustin 1999). Mass extinctions during the late Devonian have been speculated to have occurred during two different extinction pulses. The first extinction primarily affected low-latitude shallow shelf organisms, while the second event occurred due to glacial melt which, coincides with positive δ¹³C enrichment from organic marine deposits that have been interpreted as

intervals of high productivity and increased carbon burial (McGhee 1996; Brenchley et al. 1995, Joachimski and Buggisch (2002). Previous interpretations of glacial episodes have been considered to have lasted 3 m.yr. to 0.5 m.yr, known as mini-glaciations. (Frakes et al. 1992; Martin 1996; Ziegler, McGhee 1996). Pulses of global regressional cycles during Devonian time can be observed in North America and are present on other continents such as Eurasia, Australia, and Africa. Globally, Devonian tectonics has been recorded on many continents to include the Acadian and Antler orogenies in North America and the Late Caledonian orogeny in other parts of the world. Based on these facts, regional and local eustatic sea level changes, tectonism, and regional climatic effects attributed to the transgressive-regressive cycles deposited during late Devonian-early Mississippian geologic time.

Research Objectives & Hypothesis

The current investigation consists of a geochemical and chemostratigraphic analysis of the Three Forks formation and the Bakken formation. The main emphasis for this research project however, is on the Bakken Formation with the under and overlying formations as secondary objectives. 1.) Elemental proxies and redox sensitive element concentrations observed within the Bakken formation across the Williston Basin, i.e. %Ca, %Al, %Si, %Fe, & % Mg, will demonstrate geochemical shifts due to high elemental concentrations to interpret correlative sedimentary packages across the Williston Basin. Elemental ratios, i.e., %Ca, %Al, %Si, % Mg, %K, %Ti, and Zr (ppm) versus % Al, will be used in this fashion to represent clay and non-clay in mineral phases throughout the Bakken Formation as well as mineralogy changes with respect to calcite, quartz, pyrite, and dolomite. 2.) Redox sensitive trace elements expressed as enrichment factors (EFs) for Mo, U, V, Zn, Ni, and Cu, will be utilized as geochemical proxies to examine the redox capacity of the lower and upper Bakken shales. According

to Algeo et. al. 2004, trace elements exhibiting large enrichment factors are considered to have a euxinic affinity. 3.) Modern basins will be used as analogues to compare basin geometry, hydrographic circulation, and basin restriction, to the Williston Basin. This will be accomplished by interpreting Mo/TOC relationships to shed some light into the deposition of the organic rich lower and upper Bakken shales. 4.) Geochemical proxies, i.e. Zn, Ni, Cu, and TOC, will also be utilized to demonstrate correlatable signatures associated with primary productivity within the lower and upper Bakken shales geochemical. 5.) Total organic carbon and stable isotopes of organic carbon will be analyzed to understand the distribution of organic matter concentrations across the Williston Basin as well as the source for the organic content within the lower and upper Bakken shales. 6.) Stable carbon isotope data, $\delta^{13}\text{C}$, derived will also be used to identify the organic carbon source and correlate kerogen type within the lower and upper Bakken shales.

Chapter 2
METHODS

Core data acquisition

Geochemical data were acquired from four drilled cores A, B, C, and D are geographically located in eastern Montana and North Dakota (Figure 2-1). The four cores were drilled in Sheridan, Roosevelt County, Montana and in Williams, Mountrail County, North Dakota. General information, Table 2-1, for each core that was drilled and recovered by Brigham Exploration and are currently housed at the Texas Bureau of Economic Geology (BEG) Core Research Center, at the Pickle Research Center, Austin, Texas. Access was granted to analyze the cores of the study through research scientist and mudrock project activity coordinator for the BEG, Dr. Stephen Ruppel.

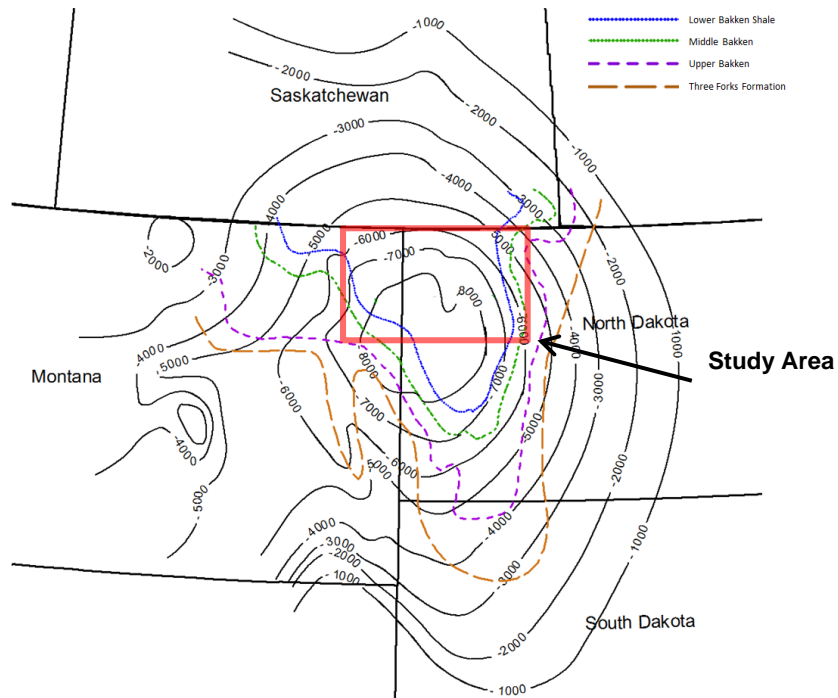


Figure 2-1 Geographical location of cores in research study, Mississippi structure map and erosional limits of the Bakken and Three Forks Formation (modified from Meissner, F.F., 1978).

Core Name	Total Interval Length (Feet)	Interval Analyzed (Depth in Feet)	XRF Unit Utilized
A	120	8,317-8,437	New BEG (ED-XRF)
B	120	9,862-9,982	New BEG (ED-XRF)
C	150	10,725-10,875	New BEG (ED-XRF)
D	183	10,056-10,239	New BEG (ED-XRF)

Table 2-1 Information from cores analyzed in research project regarding well name location, analyzed interval length and depth, and ED-XRF unit used for analysis.

Energy Dispersive X-ray Fluorescence (ED-XRF) Analysis

Core samples were marked for each of the 4 cores at a ~6 to one foot intervals prior to ED-XRF analysis. A Bruker Tracer III-V handheld energy-dispersive x-ray fluorescence (ED-XRF) instrument (Rowe et al., 2012) was utilized to measure metal concentrations for each sample marked from the 4 cores. Additional detailed sampling was undertaken to capture specific transition zones within the Bakken Formation. The ED-XRF was kept stationary by use of a platform supplied by Burkert, and the samples were placed in direct contact with the 3 X 4mm elliptical beam area of the instrument nose (Figure 2-3). Samples were placed on the nose of the instrument immediately above the 3 by 4 mm elliptical beam window and stabilized using a platform that surrounded the instrument's nose (Rowe et al., 2012).

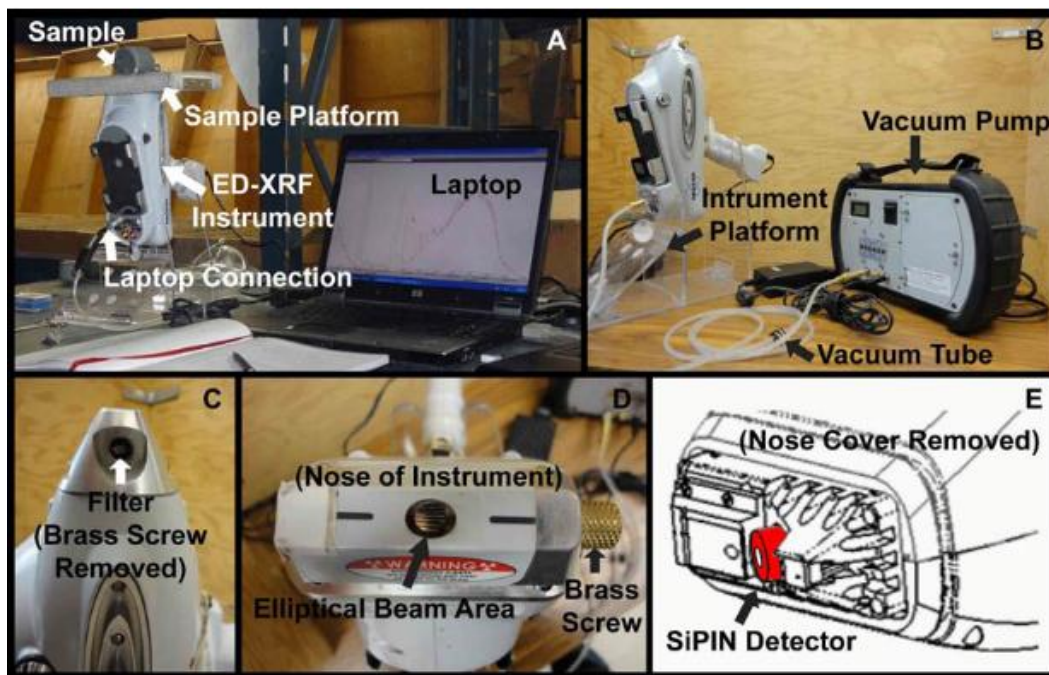


Figure 2-3 Overview of ED-XRF instrumentation illustrating A) core samples laid directly on nose of instrument with aid of a platform while data is recorded on a laptop, B) the instrument platform used in (A) to keep the instrument immobile and upright alongside the vacuum pump used in low-energy acquisitions, C) the filter used in high-energy acquisitions, D) the nose of the instrument where the beam is emitted, and E) the SiPIN detector below the beam area (drawing from Brüker manual, Kaiser, 2008).

A flat sample surface is needed in order to optimize measurement consistency and accuracy. Each core sample was specifically analyzed on the slabbed side whenever possible because the measurement sensitivity of the ED-XRF instrument decreases by the inverse square of the distance from the silicon detector (SiPIN).

Major element data measurements were acquired by using a low-energy, vacuum-pumped instrument setting. Each sample was analyzed for major and trace element concentrations for 240 seconds each. For additional information on energy dispersive X-ray fluorescence techniques and X-ray fluorescence in general, see Potts et. al. 1992 and Rowe et. al. 2012.

Low-energy spectrum acquisition includes elements that emit characteristic x-rays between 1.25 to 7.06 kV. In order to obtain the elements in this range, and allow for

backscatter that does not interfere with the peaks of interest associated with major and trace elements e. g. Mg, Ca, Si, Fe, Mo, U, V, Zn, and Ni , the voltage on the instrument was set to 15 kV. Two hand held ED-XRF instruments were used, the BEG and the UTA, and both instruments currents were set to 42 μ A; however, while the voltage settings remain constant for this elemental range, regardless of the Tracer III-V used, the current settings vary between instruments because of inter-instrument variability associated with the manufacture of the x-ray tube and electronics.

Trace element data acquisition was undertaken using a filtered, high-energy instrument setting. The characteristic x-rays between 6.92 and 19.80 kV were measured in the high-energy acquisition mode (40 kV and 28 μ A). For the trace element analyses, a Cu-Ti-Al filter inserted into the instrument was utilized to attenuate greatly the low-energy x-rays from reaching the detector.

Mudstone Calibration for ED-XRF

The functionality of the ED-XRF was tested at the beginning and end of each analysis session by the use of a quality control reference. These quality control references serve as calibrations for major and trace elemental analysis and were developed by utilizing a suite of ninety reference materials. These ninety reference materials include: five international shale standards, seven from the Devonian-Mississippian Ohio Shale, twenty from the Pennsylvanian Smithwick Formation of Central Texas, twenty-seven from Devonian-Mississippian Woodford Formation from West Texas, fifteen from the Late Cretaceous Eagle Ford formation of South Texas, and sixteen from the Mississippian Barnett Formation of North Central Texas (Rowe et. al. 2012). Each of the ninety reference materials was pressed in a Carver press to forty tons with a forty millimeter die using a boric acid backing. The reference material was then pulverized to a 200 mesh powder using a TM Engineering pulverizer with trace metal

grade stainless steel pulverizing cups and pucks. Eight grams of powdered reference material were utilized in each reference material. The finished reference pellets were analyzed for major and trace elements using wavelength-dispersive x-ray fluorescence (WD-XRF) and inductively-coupled plasma mass spectrometry (ICP-MS) (Rowe et. al. 2012).

The standard pellets were analyzed on the Bruker Tracer III-V for six minutes at three different locations on the pellet face under both low- and high-energy settings. All 270 raw x-ray spectra (90 references x 3 analyses) were loaded into Bruker's Cal process software along with the accepted (WD-XRF & ICP-MS) elemental concentrations for all standards. A low-energy and a high-energy calibration were developed by making inter-element corrections (slope and background) for each element in each calibration. Certain standards were omitted after the implementation of the inter-element corrections using statistical analysis for each element to determine the outliers with a standardized value greater than 3.0 standard deviations from the mean. The completed calibration yields quantified values using the raw ED-XRF spectra from unknown samples. The low energy calibration quantifies the following elements: Mg, Al, Si, P, S, K, Ca, Ba, Ti, V, Cr, Mn, and Fe. The high energy calibration quantifies the following elements: Ni, Cu, Zn, Th, Rb, U, Sr, Y, Zr, Nb, and Mo. The limits of determination of a method (LDM) for each element are provided in Table 2-2 (Rousseau, 2001). Rawspectra from unknowns are processed through a calibration spreadsheet (Rowe et. al. 2012).

Element	Accepted Value ^a	Instrument 1 (UTA-1)			Instrument 2 (1st UTA-2)		
		Measured Value ^b	σ (n=7) ^b	LDM ^c	Measured Value ^b	σ (n=7) ^b	LDM ^c
Mg (%)	0.67	0.8	0.09	0.17	0.85	0.14	0.28
Al (%)	4.96	5.39	0.14	0.28	5.32	0.11	0.22
Si (%)	32.6	33.7	0.2	0.05	33.1	0.4	0.8
P (%)	0.07	0.05	0.03	0.07	0.09	0.03	0.06
S (%)	3.34	2.18	0.1	0.2	2.27	0.09	0.18
K (%)	2.07	2.31	0.09	0.18	2.22	0.07	0.14
Ca (%)	0.13	0.23	0.03	0.06	0.24	0.02	0.04
Ti (%)	0.23	0.27	0.02	0.04	0.27	0.02	0.03
Mn (%)	0.015	0.012	0.001	0.002	0.013	0.001	0.003
Fe (%)	2.93	2.55	0.06	0.12	2.52	0.06	0.13
Ba (ppm)	2090	1884	376	753	1706	300	600
V (ppm)	928	1114	68	137	1110	80	159
Cr (ppm)	110	98	13	26	106	14	27
Ni (ppm)	130	153	26	52	150	20	40
Cu (ppm)	83	147	20	40	87	12	23
Zn (ppm)	823	844	96	191	880	74	147
Th (ppm)	8.4	9	1	2	9	1	2
Rb (ppm)	122	123	12	25	131	12	25
U (ppm)	18.1	17	6	11	22	4	8
Sr (ppm)	75.5	87	5	10	93	9	18
Y (ppm)	35.4	34	3	5	36	2	4
Zr (ppm)	80.3	95	7	13	96	6	13
Nb (ppm)	9	9	1	2	9	1	2
Mo (ppm)	79	83	4	9	82	3	6
a-Values for major elements from lithium borate-fused disc analysis by WD-XRF at SGS; values for trace elements (ppm) from sodium borate fusion dissolution and analysis by ICP-MS.							
b- Average HH-ED-XRF measured values (n=7) and standard deviations (s) for reference material RTC-W-260, a black shale from the Devonian Woodford Formation of West Texas.							
c- Limit of Determination of Method (LDM) calculated according to Rousseau (2001).							

Table 2-2. Lowest Detectable Measurements (LDM) for Elements Analyzed (Rowe et al. 2012).

Additional Geochemical Analysis: Sample Preparation

Drilled powdered samples from the back of each of the four cores A, B, C, and D were collected at ~6 inch intervals for the lower and upper Bakken Shales for additional analysis. Samples were collected and subsequently pulverized using a TM Engineering pulverizer with trace metal grade stainless steel pulverizing cups and pucks. The samples were then stored in standard plastic liquid sample cups.

Total organic carbon (TOC) and stable isotopic compositions of TOC ($\delta^{13}\text{C}$) were performed on powdered samples that were weighed into silver capsules (Costech Analytical, Inc. #41067) and subsequently acidified repeatedly with six percent (6%) sulfurous acid (H^2SO^3) in order to remove carbonate phases (Verardo et al., 1990). Samples were analyzed at the University of Texas at Arlington using a Costech 4010 elemental analyzer interfaced with a Thermo Finnigan Conflo IV device to a Thermo Finnigan Delta-V isotopic ratio mass spectrometer (IRMS). Isotopic results are reported in per mil (‰) relative to V-PDB for $\delta^{13}\text{C}$. The average standard deviations were 0.11‰ and 0.07‰ for $\delta^{13}\text{C}$ of USGS-40 glutamic acid (IAEA-8573), and 1.07% and 0.08% for the TOC of USGS-40. The average standard deviations for unknown samples analyzed in triplicate were 0.10‰ for $\delta^{13}\text{C}$, 0.12‰ $\delta^{15}\text{N}$, and 0.02% for TOC. A subset of samples was additionally analyzed for TOC and stable isotopic compositions of TOC ($\delta^{13}\text{C}$), Table 2-3.

Core Name	XRF	Total Organic Carbon (TOC)	Carbon Isotopes ($\delta^{13}\text{C}$)
A	88	36	36
C	121	66	66
D	132	50	50

Table 2-3. Subset types and numbers of analysis performed on three Bakken cores A, C, and D.

CHAPTER 3

RESULTS

ED-XRF and Non-ED-XRF Data

Elemental data were derived from 4 cores through various analysis described in Chapter two. All data were plotted in various formats to illustrate spatial trends of elements expressed in weight percent, parts per mil (‰), whole number ratio (C/N) and as enrichment factors (EF). Various trace element results were calculated as weight ratios expressed as enrichment factors (EF) to identify sample enrichment with respect to the average marine gray shale (Rowe et al., 2012). Enrichment factors were calculated in the following format:

$$EF_X = \left[\frac{X/Al_{sample}}{X/Al_{average-gray-shale}} \right]; \text{where } X = \text{an element (e.g., Mo, U, V, Zn, Ni, Cu)}.$$

Charts exclusively utilized to determine observed correlations or changes amongst chemofacies were plotted on cross plots and chemostratigraphic profiles versus core depth. Furthermore, all data are presented in weight percent, parts per million or a combination of both as ratios. Any negative values produced from these analysis which observed throughout the Bakken Formation were excluded on all plotted data sets.

Chemostratigraphic Applications

Geochemical data was produced from four analyzed cores that averaged 140' in thickness. The elemental data retrieved from these cores were utilized as elemental proxies to infer the paleodepositional environment of the Three Forks Formation, Bakken Formation and Lodgepole Formation. The chemostratigraphic shifts observed in Ca, Al, Si, Mg, and Fe will identify the mineralogical composition of sedimentary packages associated with calcite, illite or other clays, quartz, dolomite, and pyrite found within the

Bakken Formation. Variations in trace elemental proxy concentrations (Mo, U, V, & Zn) expressed as enrichment factors (EF) were applied in this research to determine redox conditions during deposition of the Bakken Formation. Results from total organic carbon (TOC) and stable isotope composition of TOC ($\delta^{13}\text{C}$) demonstrate the amount of organic carbon and its potential provenance for the lower and upper Bakken shales.

Diagrams

Chemostratigraphic profiles and cross-plots diagrams were utilized to identify changes in elemental concentrations and linear and non-linear trends to identify mineral phases versus %Al. Chemostratigraphic profiles were used to demonstrate concentrations of lateral variation of elemental concentration shifts to interpret correlative sedimentary packages across the Williston Basin. The presences of high concentrations of Ca, Si, Fe, & Mg within each core reveal changes in mineralogy that can be associated to calcite, illite, quartz, pyrite, and dolomite respectively. Cross-plots were used to graphically display elemental ratios of Ca, Al, Si, Mg, K, Ti, and Zr (ppm) versus % Al to determine linear trends, denote lack of enrichment or indicate mineralogy. Elemental ratios used in this fashion serve as representing clay and non-clay in mineral phases throughout the Bakken Formation. Also the element Al is commonly used as a proxy for fine-grained sediments due to it being a major component in clay minerals i.e. illite (Ver Straeten et. al. 2011). Cross-plots of %Si/%Al vs. %TOC will be examined to positive or negative relationship for the upper and lower Bakken shales. The abundance of some elements as related to the bulk mineralogy of their associated constituents will also be examined using Si/Al and %TOC vs. depth profiles to demonstrate a dilution relationship with respect to Si.

Chemostratigraphic shifts of redox-sensitive trace elements presented as enrichment factors (EFs) were used to evaluate the abundance of redox components e.g. (Mo, U, V, Zn, Ni, and Cu), within each core. Determining the redox conditions for which

the Bakken formation was deposited under allows for the identification of bottom water conditions. Recent research suggests that some trace elements may precipitate where free dissolved sulfide exist. Concentrations of enriched trace elements relative to their crustal abundances indicate that the host sediments accumulated under anoxic conditions (Calvert and Pedersen, 1993). The presence of these redox sensitive elements (Mo, U, V, Zn, Ni, and Cu) and their respective high concentrations within each core serve as indicators for anoxic-euxinic conditions during deposition of the Bakken shales. Sediments exhibiting enrichments in U, V, and Mo reflect euxinic conditions at the sediment-water interface or in the water column (Algeo and Maynard, 2004; Tribovillard et al., 2004). In the case of Ni and Cu for example, these trace elements are dominantly delivered to the sediments and are associated with organic matter (Tribovillard et al., 2006). Enrichment in Zn and Ni as observed within each core, is directly associated with the presence of organic matter in the form of micronutrients. Furthermore, redox-sensitive elements that have a strong affinity to euxinic conditions are Mo, U, Zn, and V.

This study also utilizes sedimentary Mo-TOC relationships to demonstrate hydrographic conditions in anoxic paleoenvironments. Abundant amounts of Mo are found naturally in seawater but undergoes enrichment in marine sediments under anoxic and euxinic conditions (Rowe et. al., 2009). A cross plot of molybdenum versus total organic carbon (TOC) represent degree of water mass restriction for the Williston basin during deposition of Late Devonian-Early Mississippian strata. Results from Mo-TOC cross plots were compared to similar cross plots of modern basins to compare basin geometry, hydrographic circulation, and basin restriction. The application of molybdenum-total organic carbon ratios as proxies have been utilized in studies to reveal strong correlation between degree of hydrographic restriction and scale of deep water renewal times (Lyons et. al., 2003 Rowe et. al., 2008). Molybdenum and TOC profiles

were examined to observe potential mixing of paleoceanic marine waters within the Williston Basin during late Devonian-early Mississippian time. Recent studies from Algeo and Lyons 2006 show that Mo-TOC concentrations have the potential to yield information about the temporal dynamics of basin hydrography. In their study positive covariation of raw Mo-TOC concentrations vs. depth, illustrate an exchange of deep marine waters from the Cariaco Basin with nutrient-rich intermediate waters from the Caribbean seas caused by recent post glacial eustatic transgressions.

Chemostratigraphic profiles of Zn, Ni, Cu, and TOC were utilized to demonstrate correlatable signatures associated with primary productivity events within the lower and upper Bakken shale's. Lastly, total organic carbon, %TOC and stable isotopes of organic carbon, $\delta^{13}C$ for the lower and upper Bakken shale's for the Anderson 28-33 1H, State 36 1 2H, and Richards 30 #1 cores were examined to understand the distribution of organic matter across the Williston Basin and identify the source for organic matter content source as related to kerogen type via oil type as identified in previous studies.

Chapter 4
DISCUSSION

Major Elements

Bulk mineralogy was identified for the Three Forks Formation, Bakken Formation and Lodgepole Formation. Elemental cross plots and chemostratigraphic profiles displaying concentrations for major elements e.g. Al, Ca, Mg, and Si were used to demonstrate correlative sedimentary packages across the Williston Basin with respect to the Three Forks Formation (Figure 4-1). The chemostratigraphic facies of the Three Forks Formation can be correlated to a minimal extent and display the aerial distribution of these facies across the Williston Basin (4-1). The Three Forks Formation displays an overall increase in Ca concentration from west to east whereas Mg concentrations display an inverse relationship. Correlative chemostratigraphic packages within the Three Forks Formation of Al and Si content can be observed on an elemental vs. depth profile from west to east. The Al and Si correlative geochemical shifts match very well which could possibly imply presence of clay. Inversely, Al and Si content diminish when Ca and Mg content increased within the Three Forks Formation from west to east.

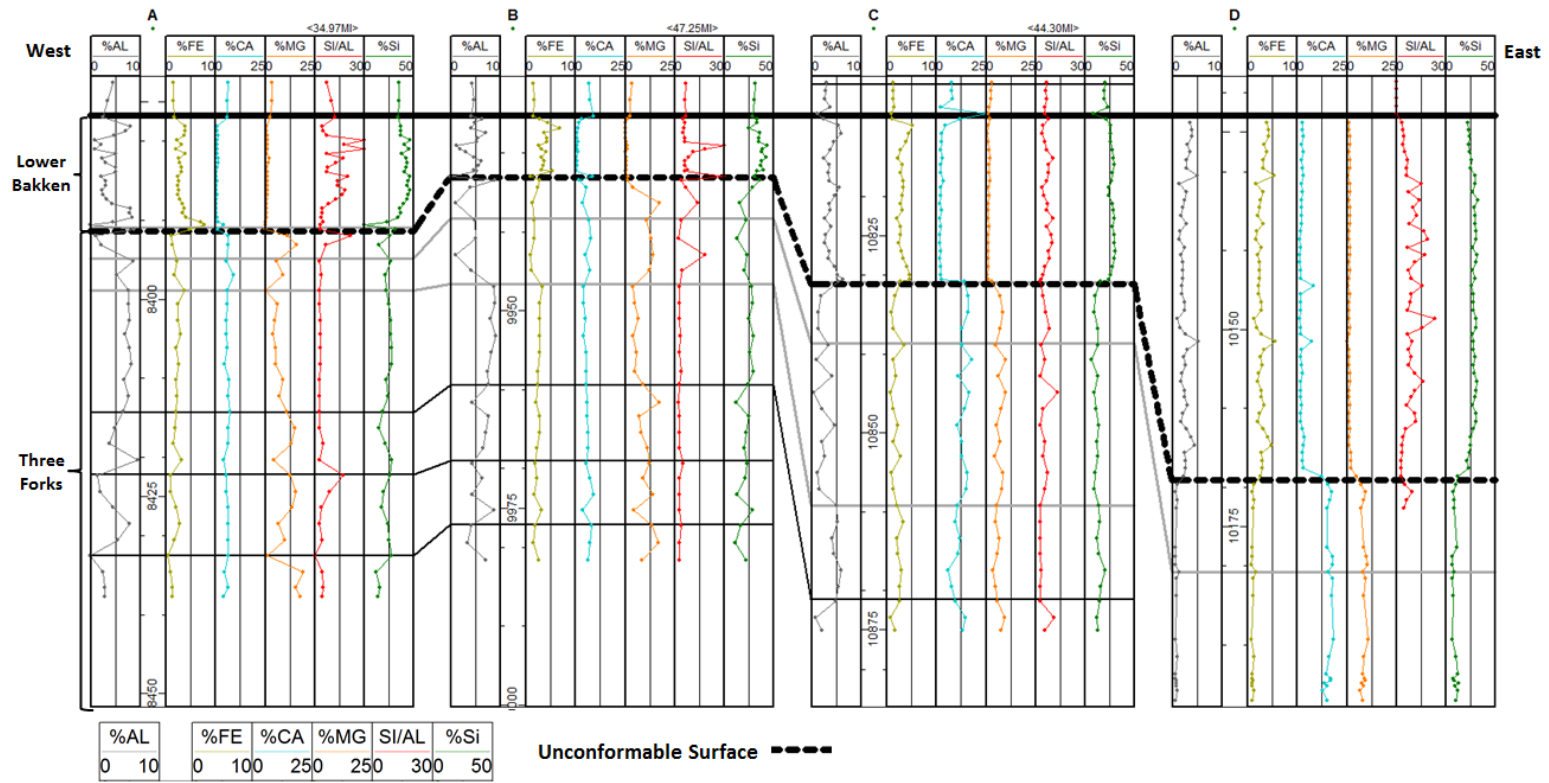


Figure 4-1 Chemostratigraphic profile of major elements from west to east for the Three Forks Formation and the lower Bakken shale i.e. %Al, %Fe, %Ca, %Mg, %Si/%Al and %Si.

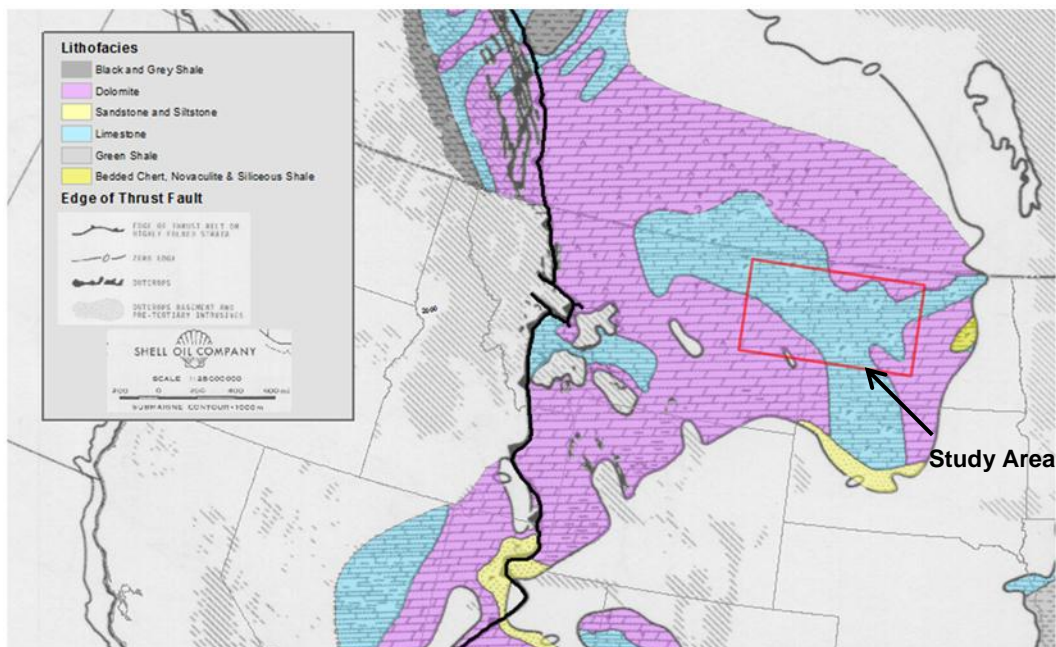


Figure 4-2 Interpreted Upper-Devonian lithofacies map Three Forks Formation equivalent (modified from Butler, et. al. 1961, Shell Oil Company).

Higher %Mg content is observed at the base of each core within the Three Forks Formation. Mg content then diminishes upward followed by a distinct spike before transitioning into lower Bakken shale. Upward diminishing Mg concentrations and increased Ca concentrations content from west to east are related to a facies change within the Three Forks Formation (Figure 4-2). To the west the Three Forks Formation contains higher Mg concentrations which could indicate the presence of dolomite. To the east Ca concentrations are higher and Mg content is lower indicating increased calcite and decreased dolomite content. Concentrations of Mg and Ca are also related to periods of episodic sea-level drops which effects include: (1) subaerial exposure of Famennian- and Frasnian-age (and possibly older) carbonate rocks commonly resulting in their karstification and phreatic zone brecciation; (2) deposition of evaporites in some basins as sea-level fell; (3) clastic wedge progradation; (4) an extensive (temporally and areally) lacuna within the Famennian and part of the Tournaisian, punctuated by thin

units of clastic rocks, carbonate, and evaporites deposited during interglacial events (Handford et. al., 1993 and Issacson, P.E. et. al. 1999).

Cross-plots of elemental ratios of K, Si, Rb, and Ti versus Al, displaying a positive linear trend is associated with trace and major elements linked to same derivation of source and linkage to the clay structure within of the Three Forks Formation for all 4 cores (Figures 4-3, 4-4, 4-5, and 4-6). In the case where Si/Al does not follow a linear trend then a Si dilution could be associated with the negative trend. Linear relationships between cross plots K, Si, Ti and Rb versus Al, can illustrate that these elements 1.) reside in the clay structure, or 2.) linked to mineralogical makeup under similar depositional controls (Rowe et. al., 2012). Elemental ratios of Ca/Al and Mg/Al display a negative correlation suggesting that during periods of calcite or dolomite accumulation, Al concentrations i.e. clay minerals, Illite was less prevalent (Figures 4-7, 4-8, 4-9, and 4-10).

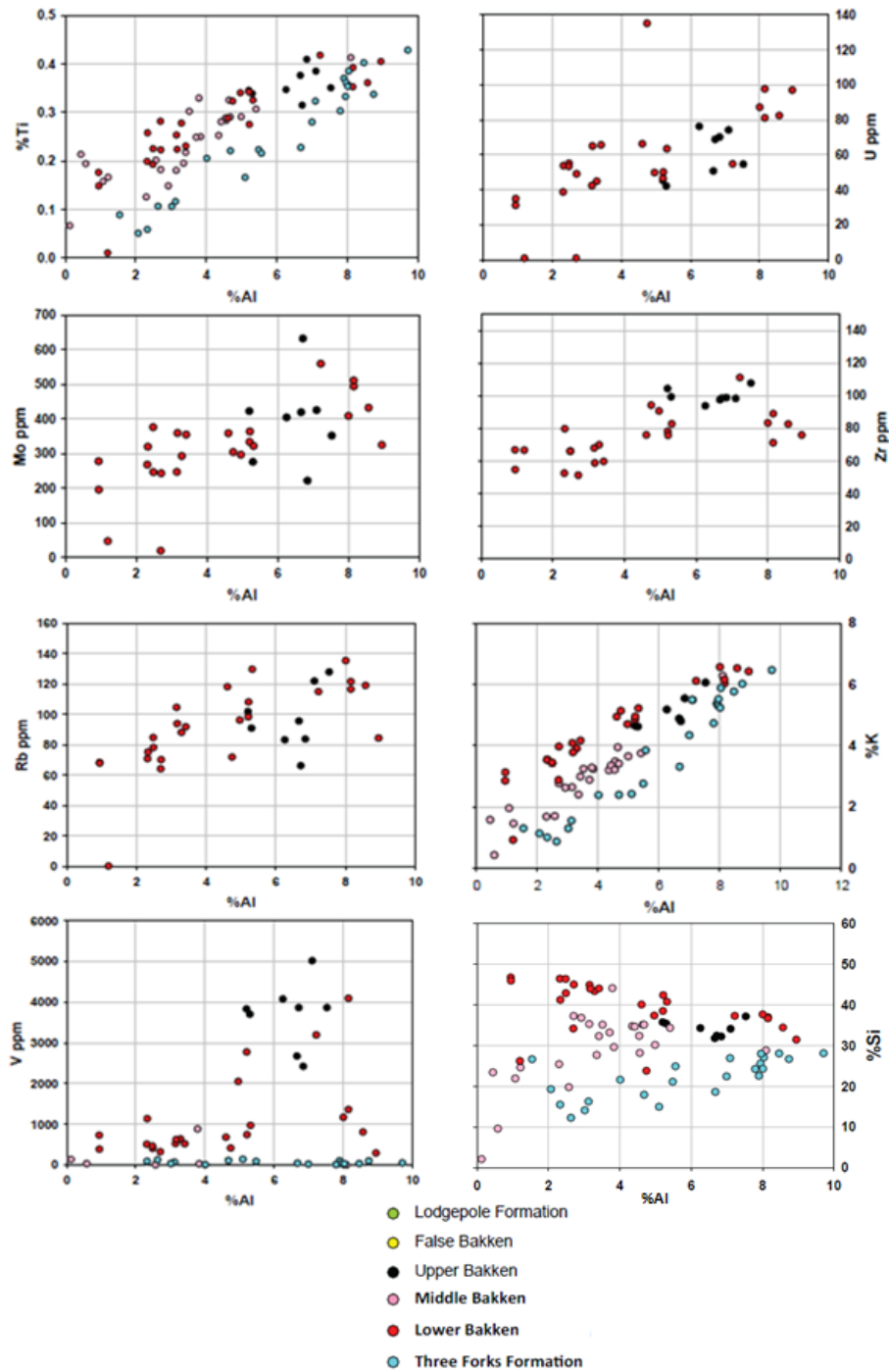


Figure 4-3. Cross plot for core A of %Ti, Mo ppm, Rb ppm, V ppm, U ppm, Zr ppm, %K, and %Si versus %Al.

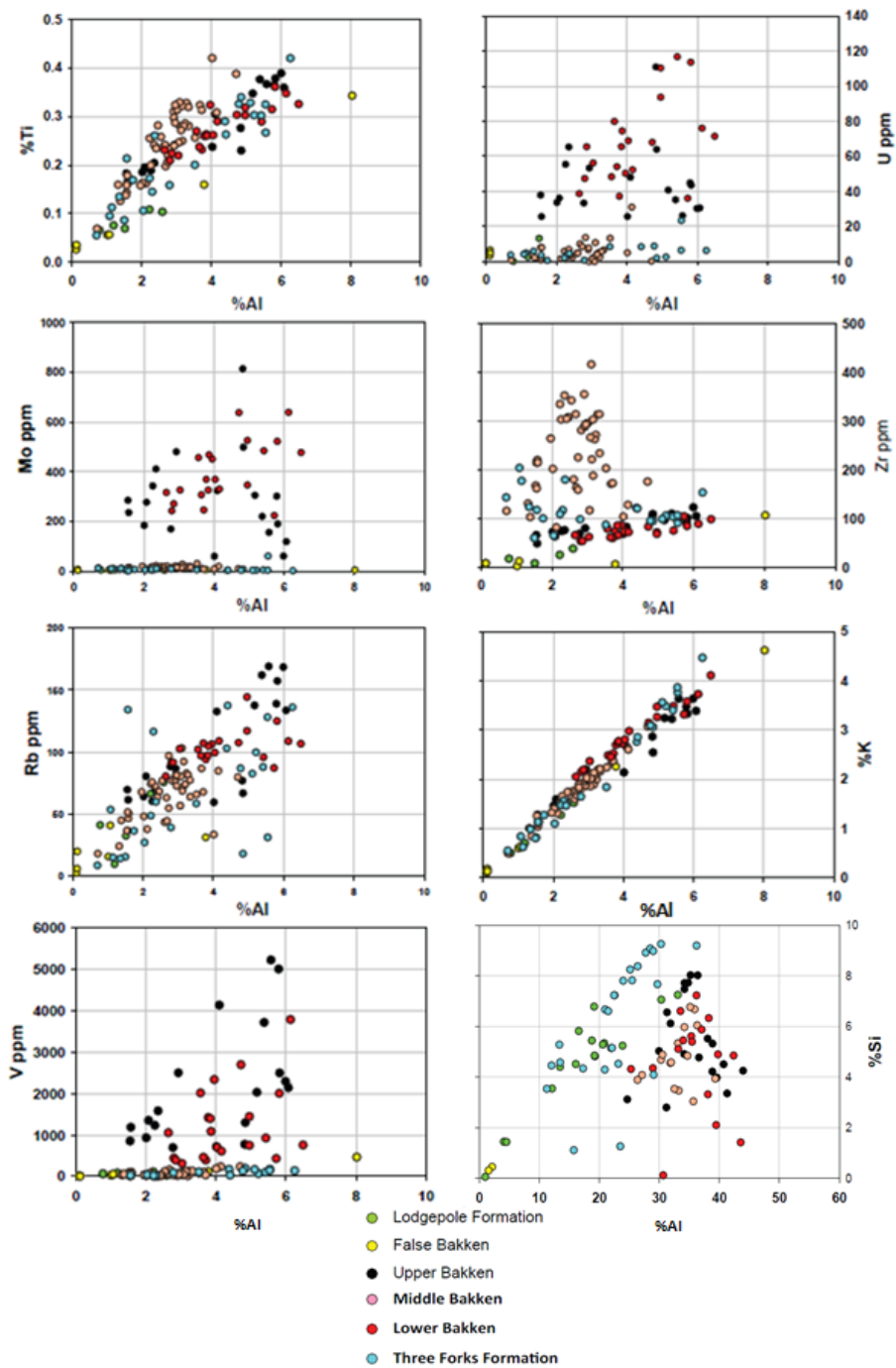


Figure 4-4. Cross plot for core B of %Ti, Mo ppm, Rb ppm, V ppm, U ppm, Zr ppm, %K, and %Si versus %Al.

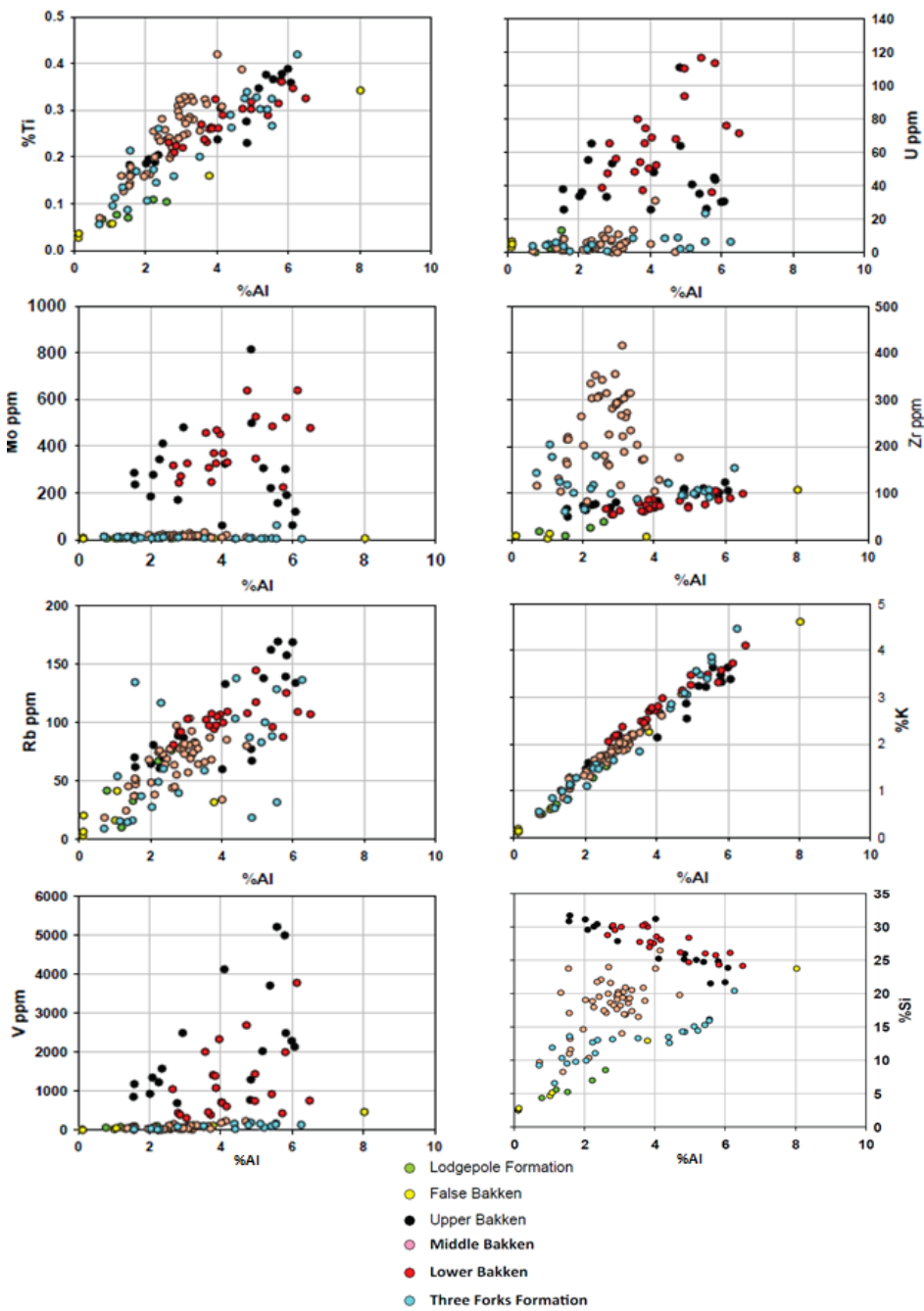


Figure 4-5. Cross plot for core C of %Ti, Mo ppm, Rb ppm, V ppm, U ppm, Zr ppm, %K, and %Si versus %Al.

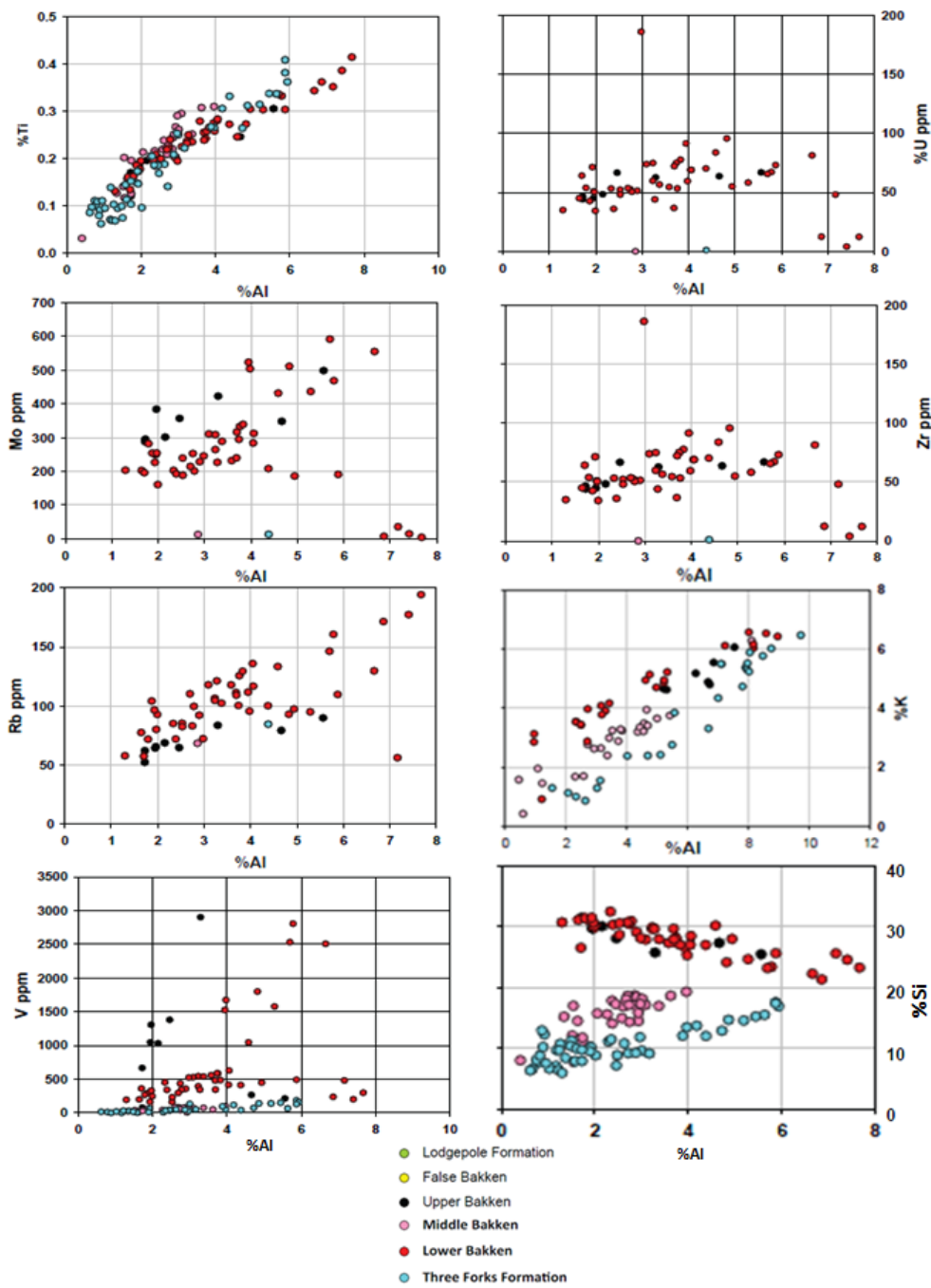


Figure 4-6. Cross plot for core D of %Ti, Mo ppm, Rb ppm, V ppm, U ppm, Zr ppm, %K, and %Si versus %Al.

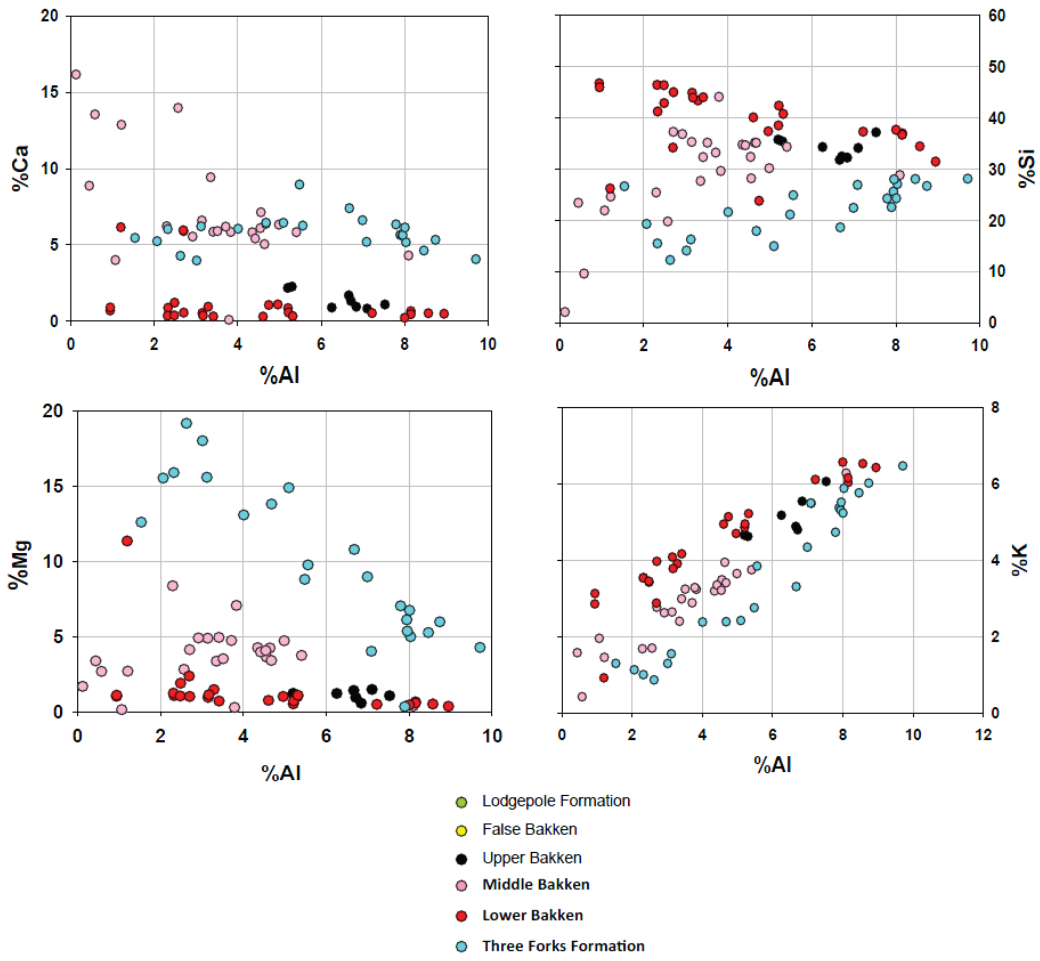


Figure 4-7. Cross plot for core A of %Ca, Mg%, %Si, and %K versus %Al.

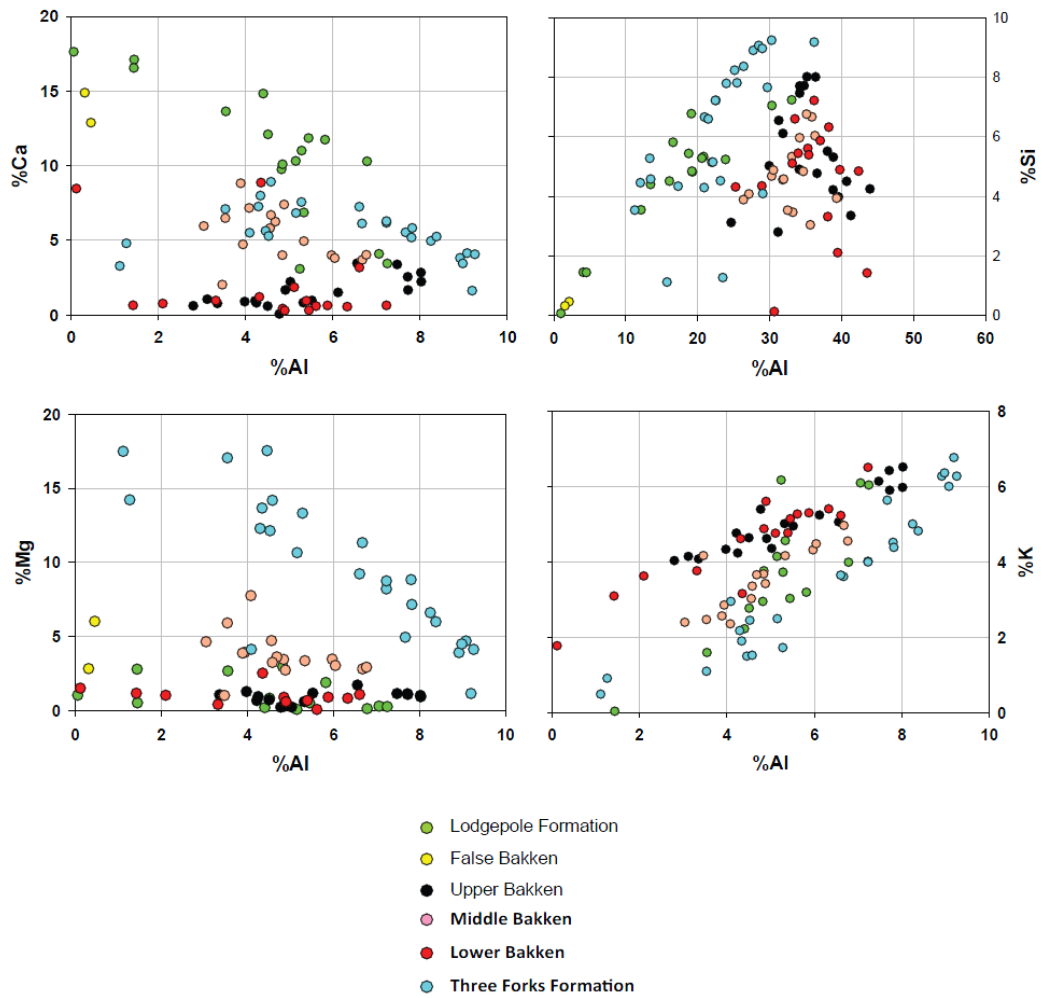


Figure 4-8 Cross plot for core B of %Ca, Mg%, %Si, and %K versus %Al.

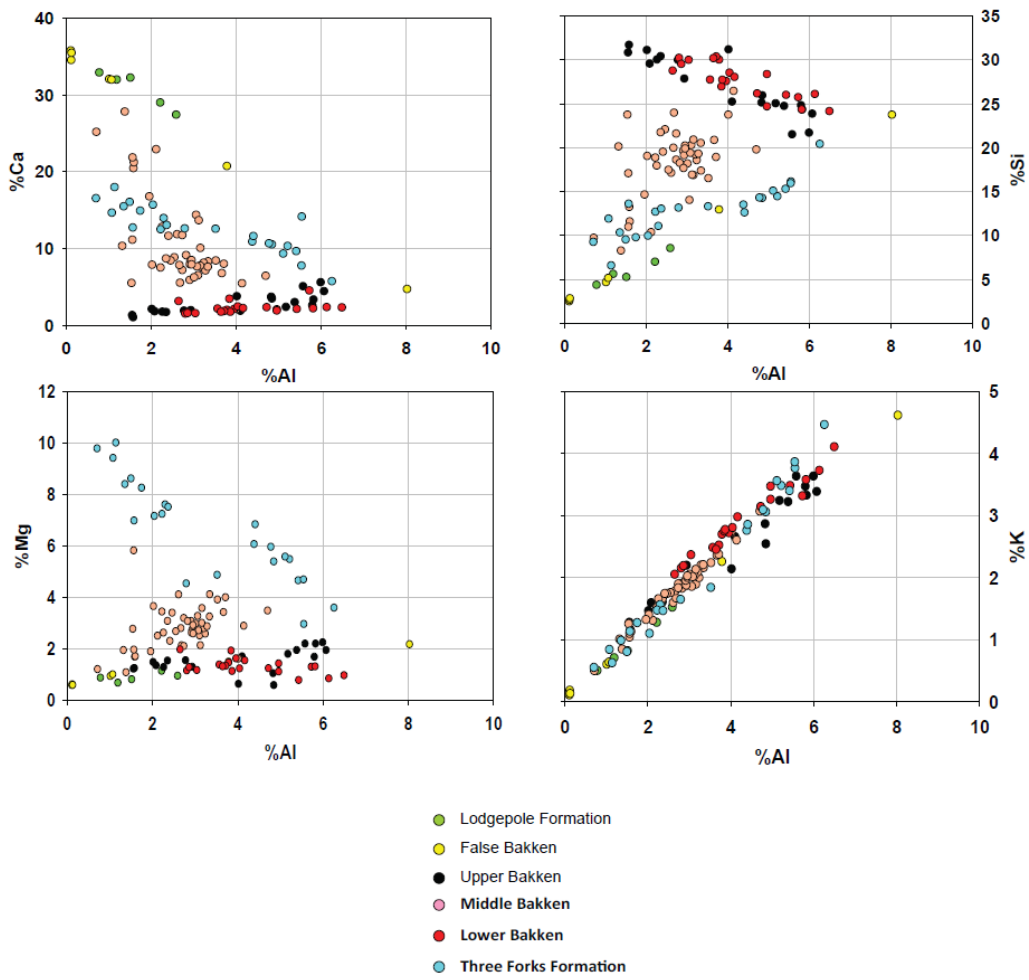


Figure 4-9. Cross plot for core B of %Ca, Mg%, %Si, and %K versus %Al.

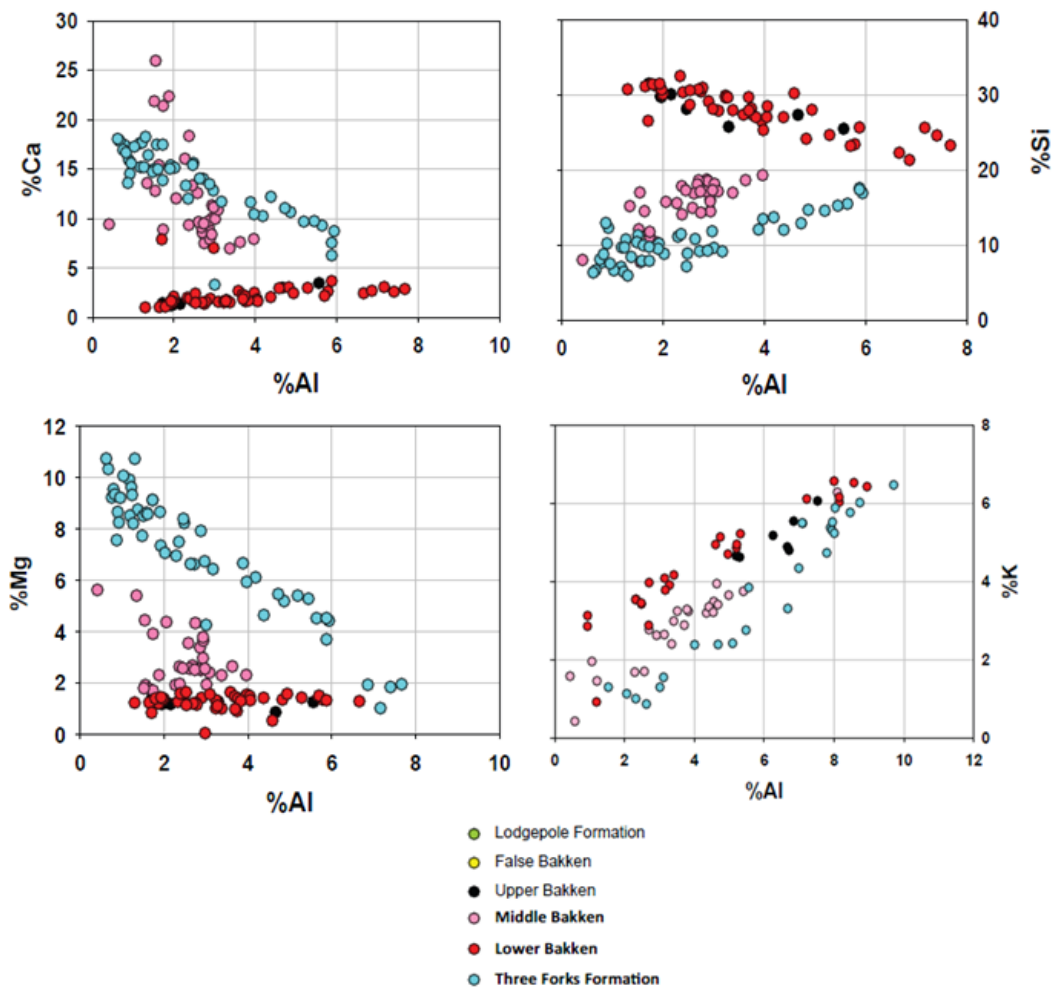


Figure 4-10. Cross plot for core D of %Ti, Mo ppm, Rb ppm, V ppm, U ppm, Zr ppm, %K, and %Si versus %Al.

Bakken Formation

Elemental shifts from chemostratigraphic profiles within the Bakken Formation can also be observed in each core (Figure 4-11). In each core the lower and upper Bakken shales display 0 to 2 weight percent Ca & Mg concentrations on average across the Williston Basin. However, the middle Bakken member displays much higher amounts of Ca and Mg ranging from 4 to 20 weight percent. These geochemical shifts could be attributed to changes in sedimentary facies within each core across the Williston Basin (Figure 4-11). The chemostratigraphy of the middle Bakken, specifically in the C and D core show higher concentrations of Ca and Mg. The concentration of Mg within the middle Bakken increases from west to east then diminishes while %Ca content increases across the Williston Basin. These geochemical shifts come about as a result of lithological changes within the middle Bakken that represent a transition from a dolomite to a dolostone facies with high amounts of calcite and quartz content. Significant facies variations have been observed from core descriptions of the middle Bakken as having 30 to 80 ft thick interbedded layers of calcareous siltstones to quartz sandstone, dolostone, silty limestone with silica, calcite or dolomite (LeFerver, 2005). The mineralogical make up these lithologies coincides well with the chemostratigraphic profiles observed in each core (Figure 4-11). In general, the middle Bakken can be interpreted as a mixed siliciclastic-carbonate system made up detrital Si, Ca, Mg, and Al-clay. Amounts of Al, Si, and Fe vary across the Williston Basin for the upper and lower Bakken shales. Concentrations of Al and Fe range between 2 to 8 weight percent and are consistent west to east. These amounts of %Al and %Fe could be attributed to clay types i.e. illite and pyrite within the upper and lower Bakken shales, respectively (Figure 4-11). Concentrations of %Si content observed in chemostratigraphic profiles within the lower and upper Bakken shales for cores A and B are located in eastern Montana, range between 30 to 50 weight percent. The %Si content observed in the C and D core

however, range between 25 to 32 weight percent. The amounts of Si content found within each core could be related to the geographical distribution of each location within the Williston Basin. The A and B cores for example, were drilled in eastern Montana closest to the inner edge of Bakken Formation limits (Figure 4-12).

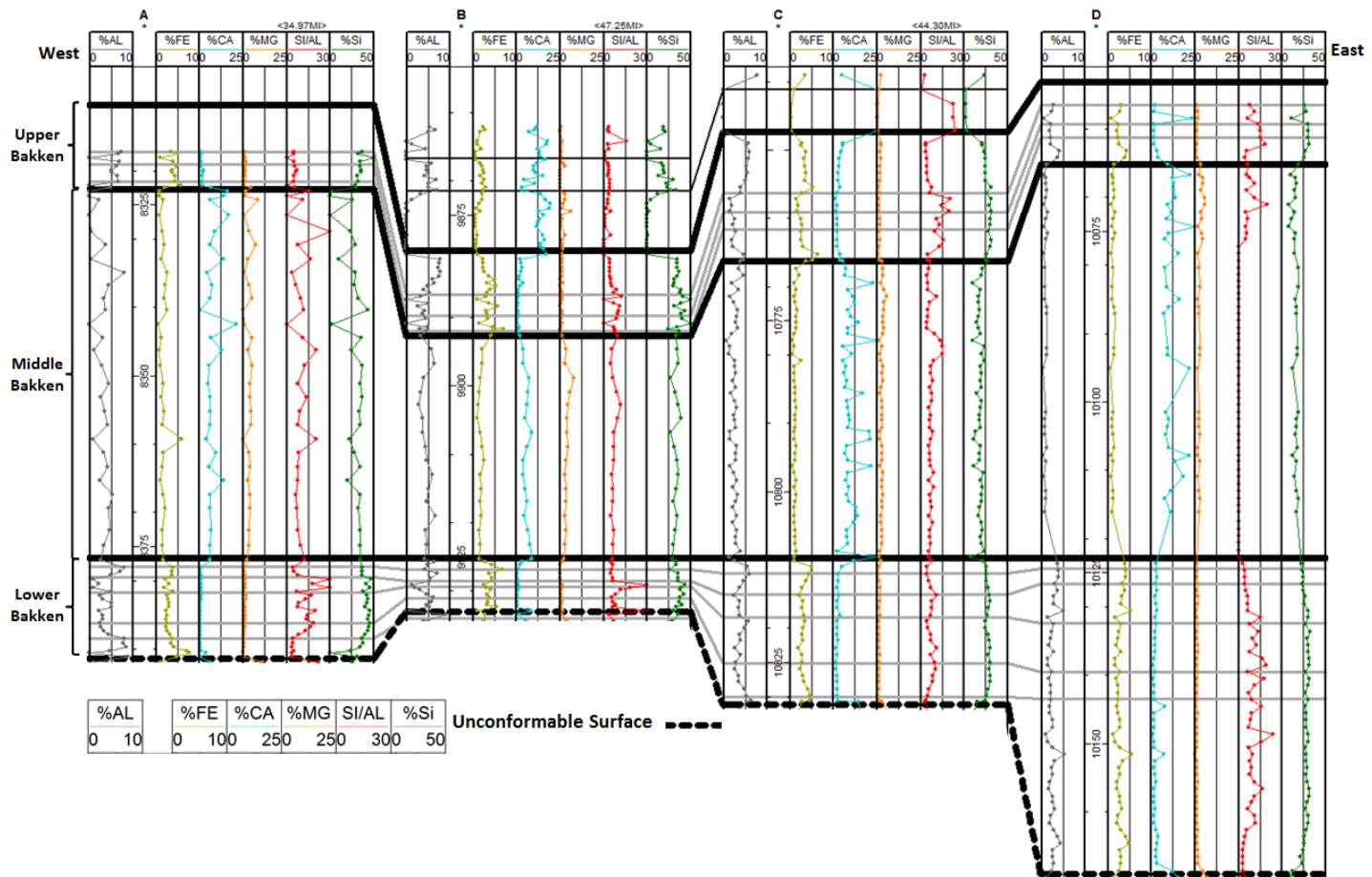


Figure 4-11 Chemostratigraphic profile of major elements from west to east for the Three Forks Formation and the lower Bakken shale i.e. %Al, %Fe, %Ca, %Mg, %Si/%Al and %Si.

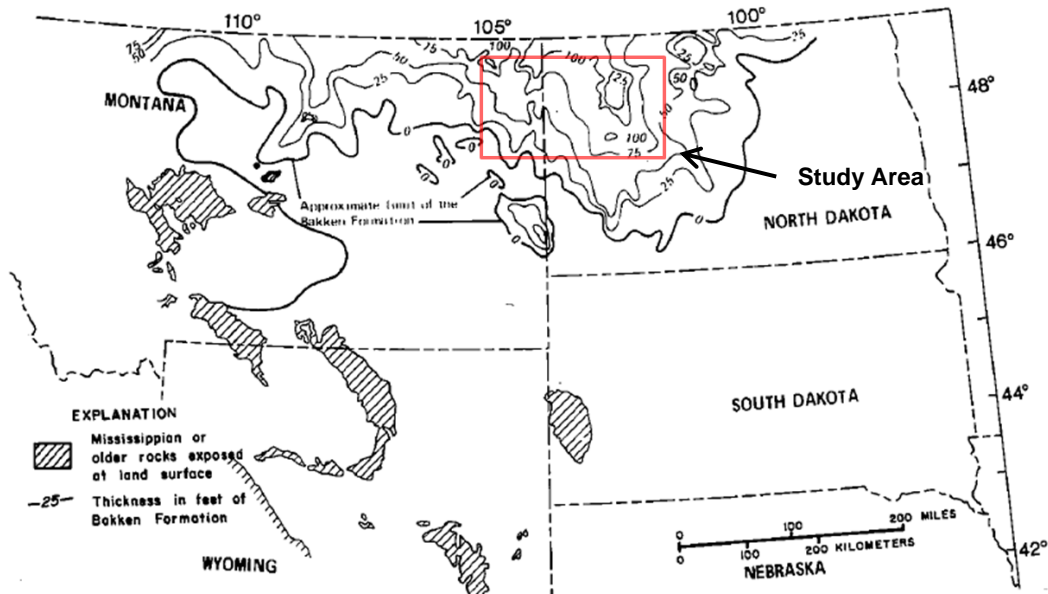


Figure 4-12 Gross thickness map and depositional limits of Bakken (modified from Peterson et. al. 1987).

At the subsurface of eastern Montana and around the inner edge of the Williston Basin the Bakken Formation thins. The thinning of the Bakken formation along the inner edges of the Williston Basin could be attributed to two tectonic processes known as subsidence and uplift. These tectonic processes would allow for exposure of older Paleozoic rocks ie. middle to early Devonian, Silurian, Ordovician to experience erosion providing a source of detrital quartz during Bakken deposition. Factors which may have also affected the volume of Si content within the upper, middle and lower Bakken intervals are weathering from uplifted mountain ranges, land plants which may deepen the extent of surface weathering and exposure of silicate rich rocks when sea level lowered (Kidder and Erwin, 2001). A secondary source for Si content along the edges and deepest parts of the Williston Basin could be attributed to biogenic silica produced from sponge's spicules and radiolarians during the Paleozoic (Young et. al. 2012, Jones et al. 1971). Radiolarians could serve as a source of biogenic silica because during Bakken deposition the semi-isolated Williston Basin was located close to the Equator (5°

to 10°N) where normally, radiolarians are most abundant. Radiolarians will compete with diatoms for limited dissolved silica (silicon dioxide) resources available in sea water so that both organisms can build exoskeletons and as they die off their tests sink and accumulate on the ocean floor as biogenic sediment (Davidson, 2012). Also, global cooling may have enhanced marine water circulation intensifying the sinking of colder waters potentially resulting in upwelling zones that favor plankton blooms. During the late Paleozoic siliceous sponges became more abundant in some paleo-upwelling areas (Beauchamp et al., 1999). Oscillatory peaks of %Al, % Si, and %Fe which are correlatable across the Williston Basin signifying the depositional controls of biogenic silica, detrital quartz, clay content distribution, and pyrite occurrences within the lower and upper Bakken Shale (Figure 4-11). However, some believe that biogenic silica alone would be an inadequate source of silica unless additional sources are considered (Savard et al., 1990; Eley et al., 1982; Jacka, 1974; and Wetzel, 1957).

Cross-plots of elemental ratios of K, Si, and Ti versus Al, identify the mineralogical characteristics of the detrital fraction in the Bakken Formation within all 4 cores (Figures 4-3, 4-4, 4-5, and 4-6). The existence of positive linear trends observed in the cross plots for the lower and upper Bakken shales for each core represents the presence of these elements in clay. Elemental cross plots for the Bakken Formation e.g. Al, Ca, Mg, and Si versus Al, display concentrations for major elements as having linear or non-linear relationships with respect to each other (Figures 4-7, 4-8, 4-9, and 4-10). Cross plots for %Ca and %Mg versus %Al do not exhibit a linear trend which may signify the presence of higher calcite and dolomite content versus clay content in the middle Bakken member. The upper and lower Bakken shale within each core however, displays extremely small amounts of %Ca and %Mg content with greater concentrations %Al associated with the mineral illite. Aluminum has been commonly utilized as a proxy for clay mineral content, i.e. illite (Ver Straeten, et. al., 2011).

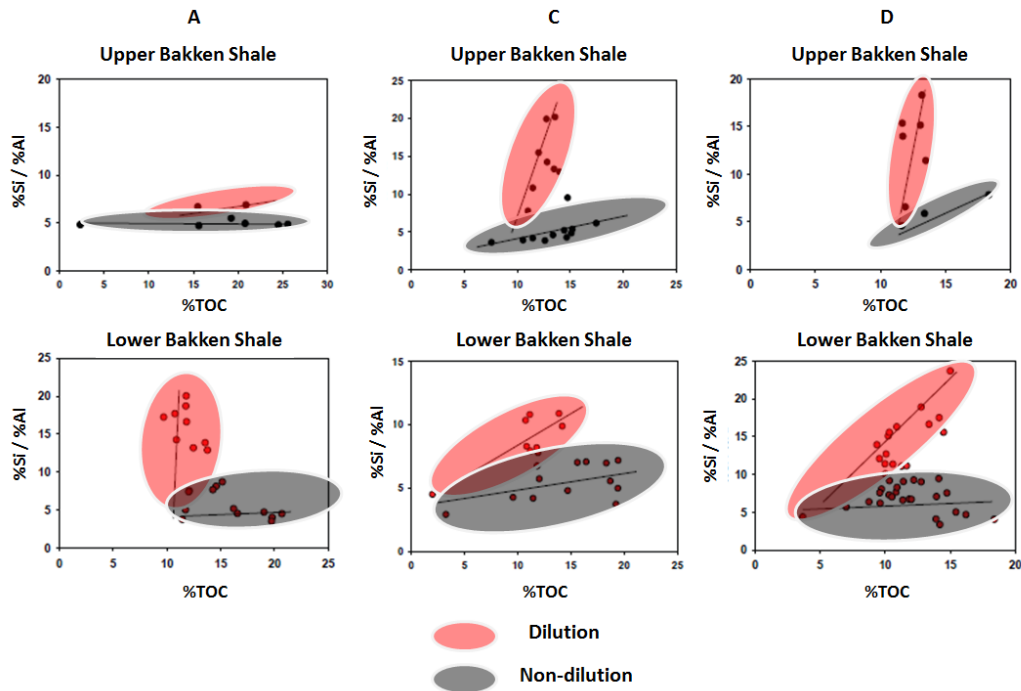


Figure 4-13 Upper and lower Bakken shale cross plot of %Si/%Al versus %TOC.

Cross-plots of %Si/%Al vs %TOC were examined to observe positive or negative linear trends for the upper and lower Bakken shales and to establish a dilution relationship with respect to Si. In core A for the upper Bakken shale there is a lack of number of data points due to early termination of coring job. Cross plots for cores A, C, and D for the lower and upper Bakken shales, display positive linear trends that represent a dilution or non-dilution of silica. This can be observed from higher Si/Al content dissipating %TOC and the opposite takes place when decreasing Si/Al amounts increases %TOC. The dilution of Si/Al along vertical linear trends versus %TOC observed from cross plots; Figure 4-13, could be linked to silica content that is derived from various sources e.g. detrital or biogenic source.

Redox-indicators geochemical proxies

Trace elements that bond to organic matter or form sulfide compounds are enriched in strata under lower dysoxic to anoxic conditions such as Mo, Mn, V, Cr, Ni, Co, Cu, U, and Th and often parallel elemental shifts with respect to TOC concentrations (Ver Straeten et. al., 2011). Redox sensitive trace elements also exhibit higher rates of transfer to sediments at lower redox potentials due to uptake by organic matter or authigenic minerals (Morford, 1999). Chemostratigraphic profiles Mo, U, V, Zn, Ni, and Cu from each core were expressed as (EF) enrichment factors to examine the redox capacity of the Bakken shales in comparison to the average marine gray shale and to demonstrate high concentrations caused by anoxic-euxinic conditions (Calvert et. al, 1993). During deposition of the Bakken shales noticeable anoxic-euxinic conditions existed throughout the Williston Basin that can be observed in the chemostratigraphic profiles (Figure 4-14). Total organic carbon was also utilized to compare any possible correlations with geochemical shifts represented by peaks that may coincide within each core separately (Figure 4-14). In general, elemental shifts represented by peaks enriched with Mo, U, V, Zn, Ni, and Cu can be observed throughout the upper and lower Bakken shale chemostratigraphic profiles (Figure 4-14). Peaks of enriched trace elements demonstrate that the Bakken shales experienced episodic anoxic-euxinic conditions during deposition (Figure 4-14). This relationship can be specifically observed from chemostratigraphic profiles of (EF) Mo, U, V, and Ni from west to east. Another observation that should be noted is the covariation and preservation of total organic carbon with periods of anoxic-euxinic conditions in cores C and D for the lower Bakken shale and core C for the upper Bakken shale e.g. (EF) V and to a lesser extent Zn (Figure 4-14). Also the geographical distribution of the cores span across the Williston Basin and show an overall increase in enrichment concentration from the following trace elements Mo, U, V, Zn, Ni, and Cu (Figure 4-14). Core intervals which are structurally

higher display significant amounts of enrichment associated with these redox-sensitive elements (Figure 4-14).

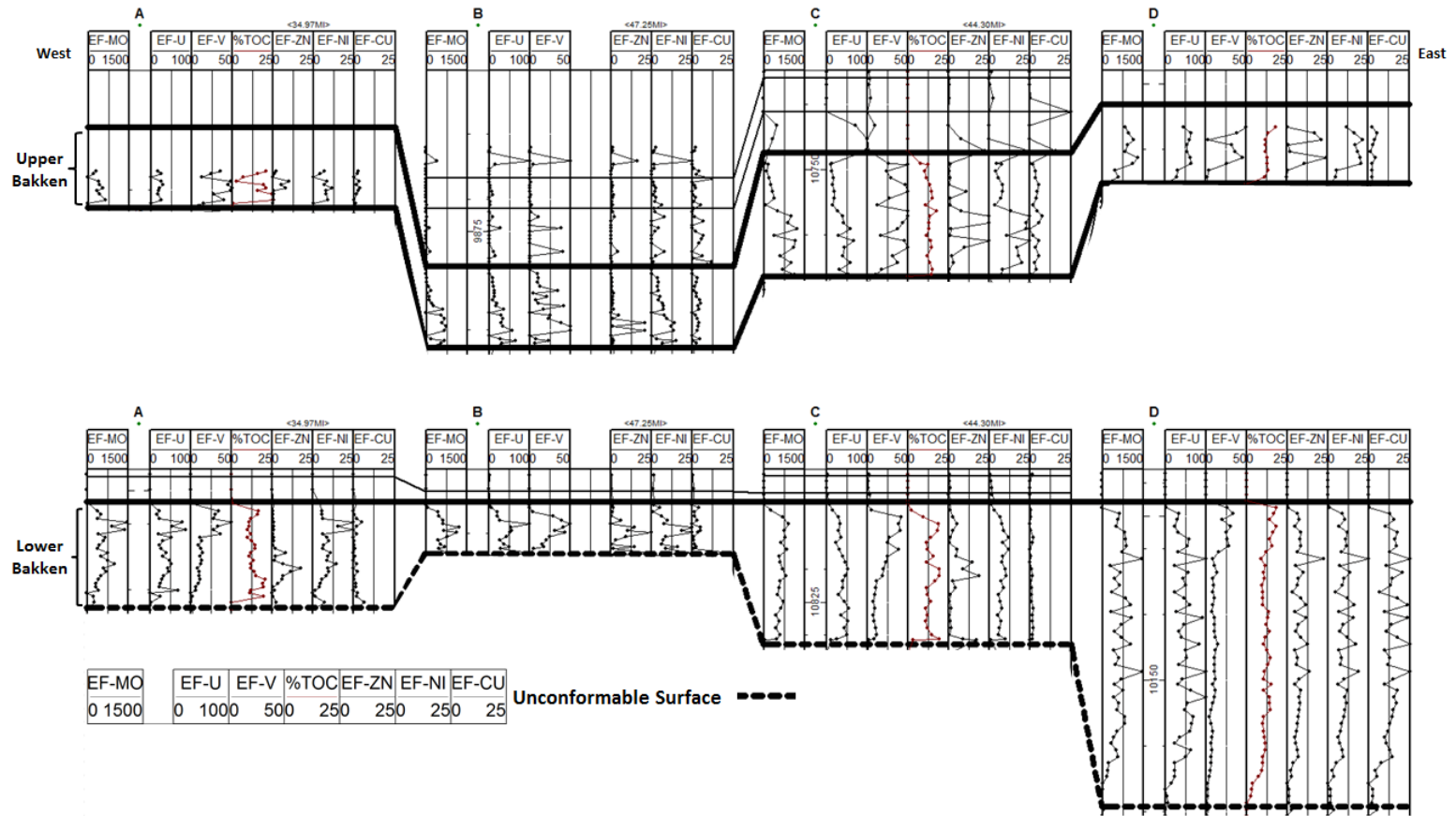


Figure 4-14 Chemostratigraphic profiles of trace elements expressed as enrichment factors (EF) were used to evaluate the redox character of the upper and lower Bakken shales in comparison with %TOC. i.e. Mo, U, %TOC, Zn, Ni, and Cu.

Conversely, higher enrichment concentrations of these same elements can be observed where the Williston basin becomes structurally deeper, i.e. C and D cores (Figures 4-14). Another observation is the strong covariation between (EF) Mo and U which is associated with attributes and processes of a depositional system to include (1) variation in benthic redox conditions, (2) the operation of particulate shuttles within the water column, and (3) the evolution of watermass chemistry. The importance of these factors in each depositional system can be assessed both from the degree of enrichment of authigenic molybdenum (Mo-auth) and uranium (U-auth) and from the (Mo/U) auth ratio of the sediment relative to the seawater Mo/U molar ratio of $\sim 7.5\text{--}7.9$ (Algeo and Tribouillard, 2009). In open-ocean systems with suboxic bottomwaters Molybdenum, uranium, vanadium, zinc, nickel, and copper increased enrichments across the Williston Basin are representative of a strong euxinic affinity, more specifically concentrations for Mo (Figure 4-14). Molybdenum concentrations are associated with anoxic-euxinic conditions during the deposition of the lower and upper Bakken shales. Recent studies suggest that increased Mo fluxes are linked to high concentrations found in silled basins (Algeo et al., 2006). Chemostratigraphic profiles of Mo, U, Zn, Ni, Cu and observed peaks of elevated concentrations within each core for the Bakken shales resulted from upwelling or highstands associated with episodic glacial periods during late-Devonian/early Mississippian time (Figure 4-14). Nutrient-enriched oxygen-depleted waters of the equatorial undercurrent for example were well established in the Pacific Ocean Basin during Late Devonian time upon the western margin of North America (Jewell, 1993). Eustatic sea level rise during the deposition of the lower and upper Bakken shale, as proposed by Smith and Bustin, 1998, could have brought in marine seawater undercurrents into the Williston Basin along its margins and also pass through the westerly structural low found in eastern Montana namely the Montana trough (Figure 4-15).

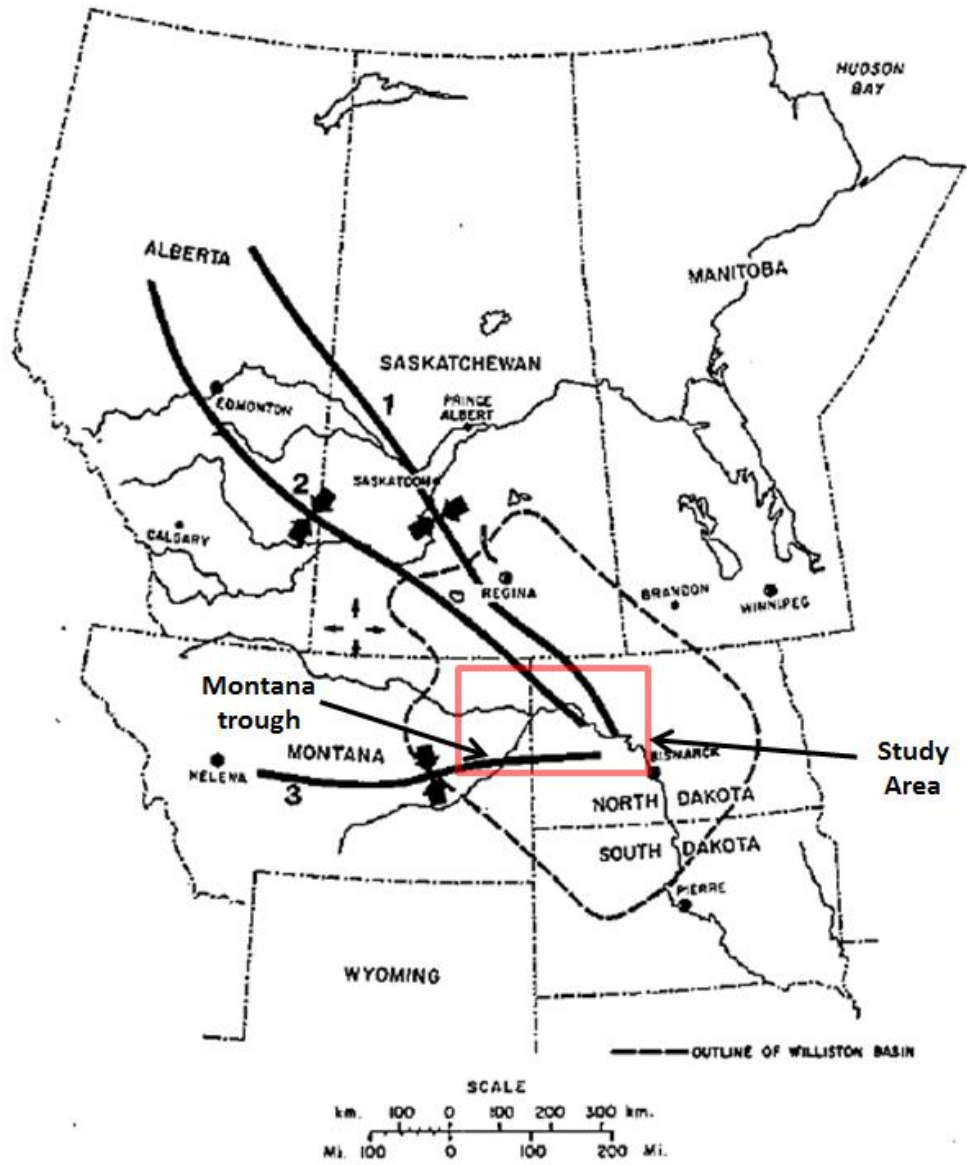


Figure 4-15 Middle to late Paleozoic axes for potential paleoceanic undercurrents during 1. Middle Devonian, 2. Upper Devonian and 3. Mississippian time (modified from Kent, 1987).

Basin Restriction

Recent research suggests that relationships between Mo-TOC concentrations are associated with basin hydrographic circulation and deep water restriction (Rowe et al., 2009). Coincidentally, modern basins can be utilized and compared to ancient basins in order to decipher the degree of paleo-basin restriction, water mass residence time and redox conditions for the Williston Basin during the late Paleozoic (Figures 4-16, 4-17, and 4-18). Modern basins comparable to the Williston Basin that have experienced varying degrees of basin restriction, water mass residence time, and redox conditions include, i.e. Saanich Inlet, Cariaco Basin, Framvaren Fjord, and the Black sea. Modern basin analogs can also shed light on hydrographic circulation which directly correlates to the type of environment impacted by biogeochemical cycles (Algeo et al. 2011). Comparisons of the geometries of these modern basins can contribute to the amount of restriction the Williston Basin may have experienced based on Mo-TOC relationships. Basin evolution was produced by simultaneous processes of subsidence and tectonic events (Sleep et al., 1980; Sandberg et al., 1982; Lambeck, 1983; DeRito et al., 1983; Quinlan and Beaumont, 1984; Johnson et al., 1985; Ross and Ross, 1985; Beaumont et al., 1987). These processes enabled the development of the basin to experience simultaneous events of varying rates of restriction and replenishment of nutrient rich paleoceanic waters contributed by the Devonian-Mississippian North American seaway (Algeo et al., 2007). During the transgression of the seaway the shallow semi-enclosed Williston basin was at the western margin of North America near the center of the epicontinental sea (Algeo et al. 2007). The geographic location of the basin is important to this research study because it allows for the delivery of trace elemental that can be utilized as proxies to identify basin restriction.

The degree of basin restriction and hydrographic conditions for the Williston basin was examined via Mo/TOC cross plots and compared to modern analogs. The

Mo/TOC ratios were examined for three cores and compared to the Black Sea, Framvaren Fjord, Cariaco Basin, and Saanich Inlet, all modern anoxic basins. All three cores A, C, and D, display similar yet different results in terms of basin restriction and Mo concentrations (Figures 4-16, 4-17, and 4-18). Recent research suggests that Mo-TOC relationships within a single environment have the potential to yield information about the temporal dynamics of basin hydrography (Algeo et. al. 2006). The modern anoxic marine basins compared to the Williston Basin in this research exhibit a spectrum of degrees of deep water restriction from weak (Saanich Inlet) to strong (the Black Sea) (Figures 4-16, 4-17, and 4-18). According to the Mo-TOC relationships between the Williston Basin and modern basins, it can be concluded that the Williston basin experienced hydrographic restriction similar to the Cariaco Basin (Figures 4-16, 4-17, and 4-18).

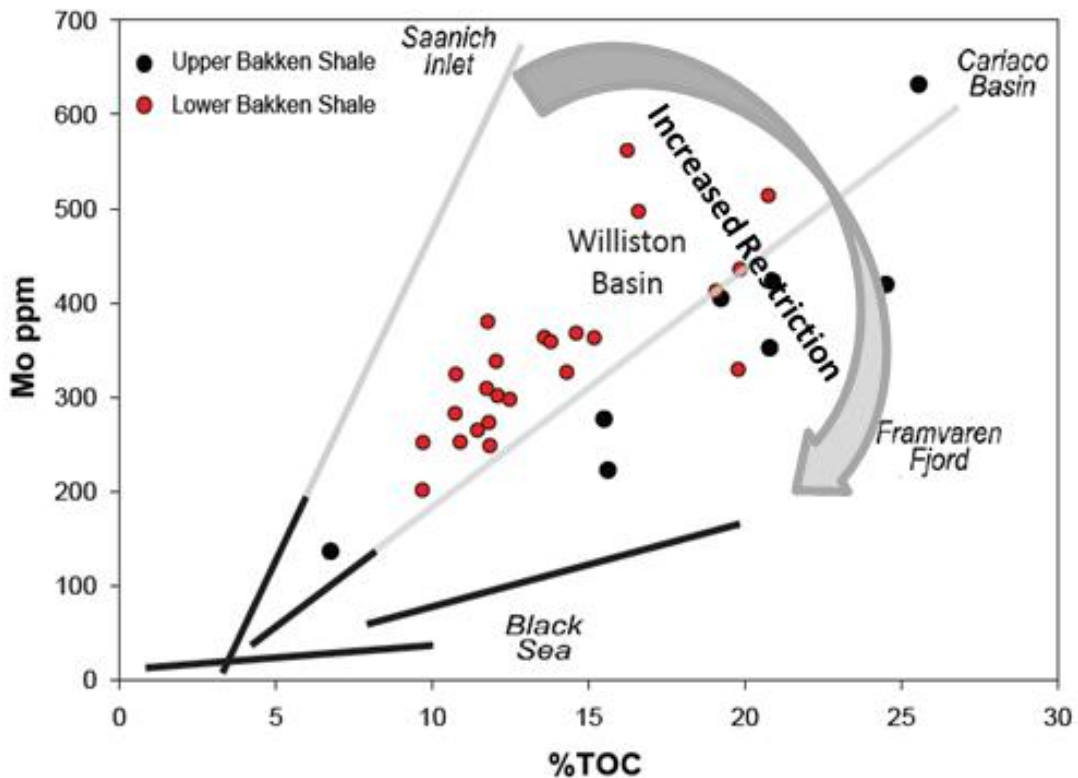
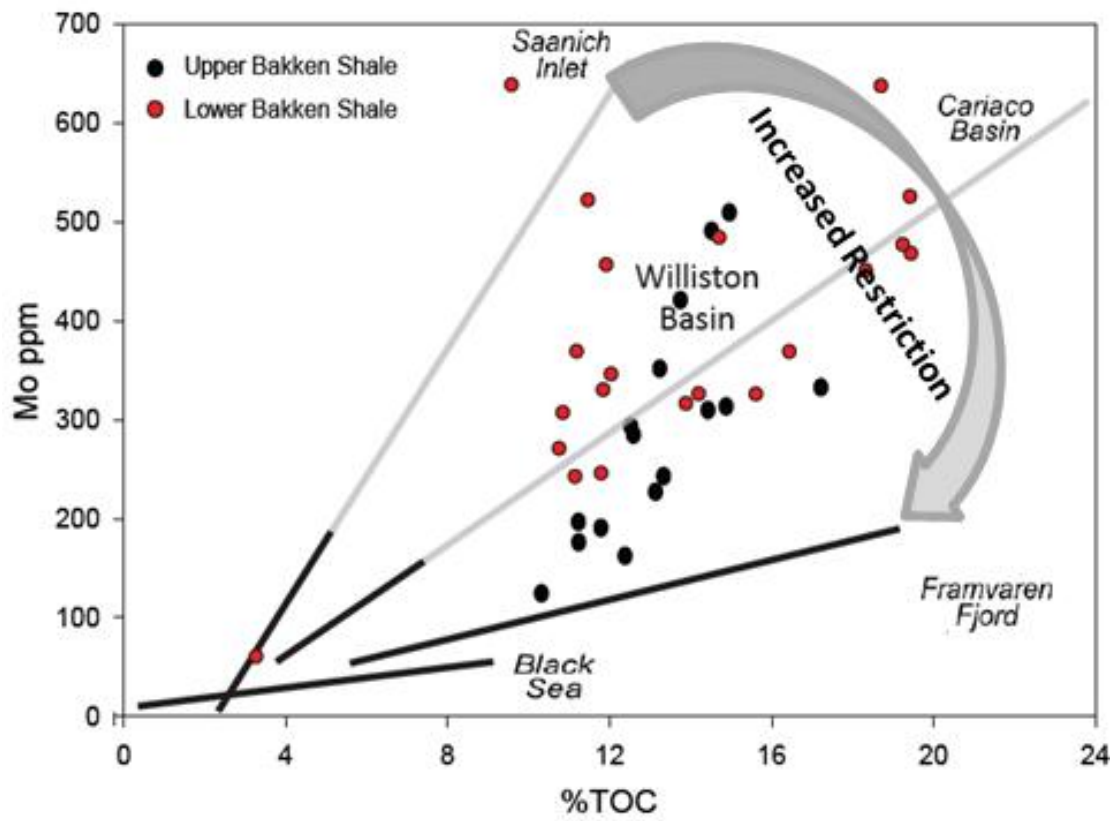


Figure 4-16 Cross plot for core A of Mo ppm versus total organic carbon of modern anoxic silled basin and the Williston Basin.



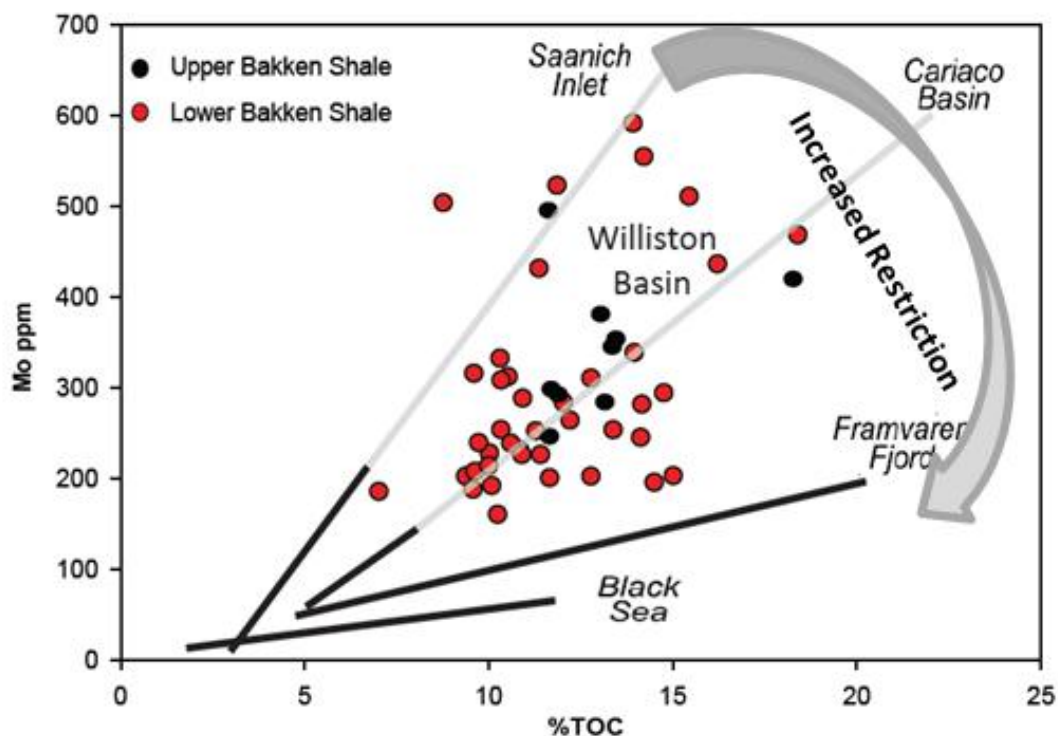


Figure 4-18 Cross plot for core B of Mo ppm versus total organic carbon of modern anoxic silled basins and the Williston Basin.

The Cariaco Basin experiences varying fluxes of surface and intermediate waters from the adjacent Caribbean Sea (Algeo et al. 2006). Inversely, during lowstands that were produced by the last glaciation, the Cariaco Basin experienced maximum exchange that was dominated by nutrient-poor surface waters, limiting primary productivity and lessening oxygen demand in the deep water mass. As sea level rose during post glacial periods, nutrient-rich intermediate waters entered the basin stimulating primary productivity and increasing oxygen demand (Algeo et al. 2006). If the Williston Basin experienced similar hydrographic conditions during post glacial periods as the Cariaco Basin, then based on proposed late Devonian-early Mississippian eustatic sea level curves it could be concluded that this ancient basin was semi-restricted (Figure 4-19). Chemostratigraphic shifts defined as peaks of Mo and TOC versus depth observed in the

Bakken shales could be linked to episodic eustatic sea level changes during late Devonian-early Mississippian time (Figures 4-20 and 4-21).

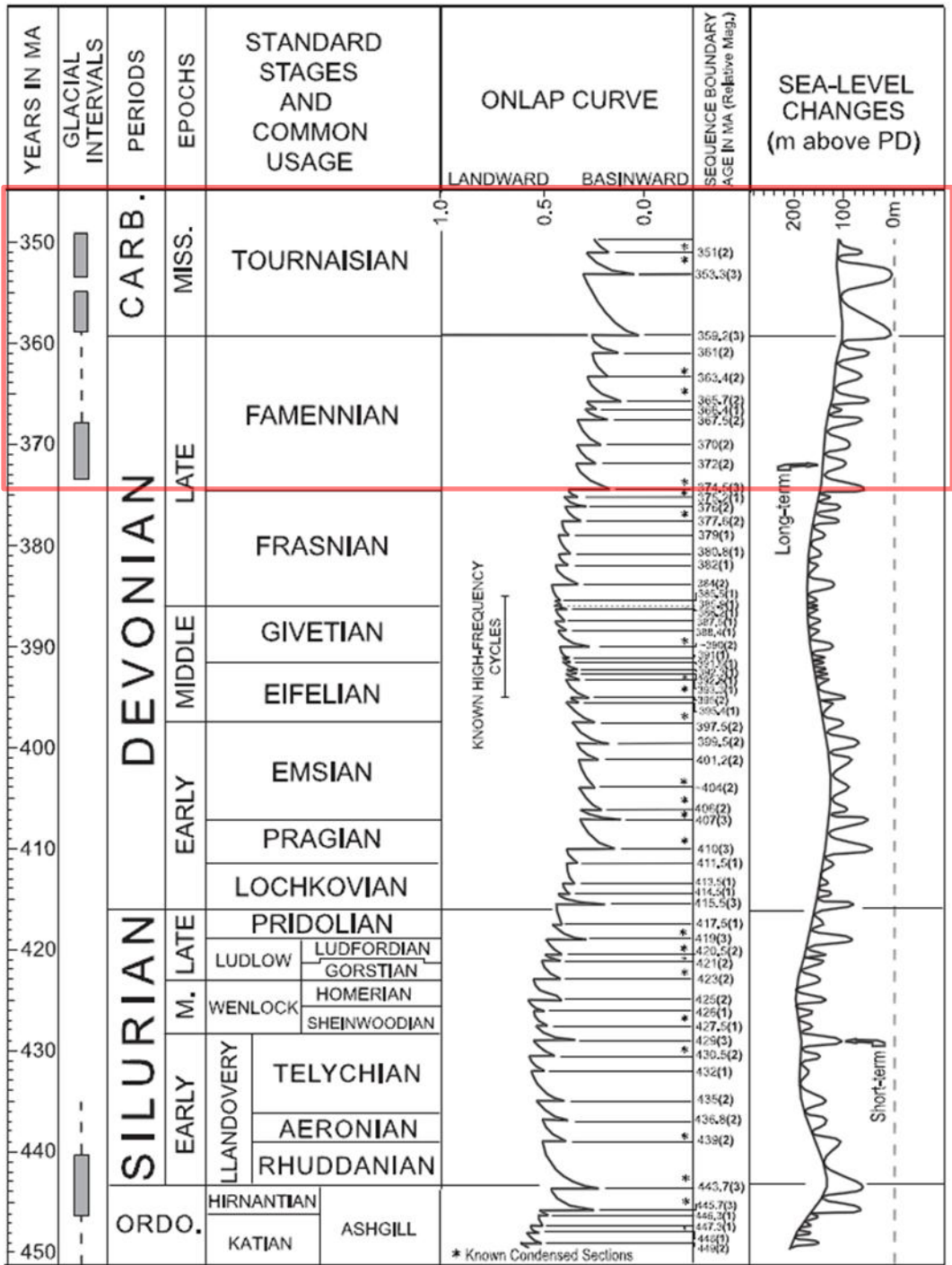


Figure 4-19. Eustatic sea level changes and associated onlap curves during late-Devonian to early-Mississippian time. (Haq *et. al*, 2008). Red box delineates the geologic time period associated with this research.

As previously discussed, Molybdenum concentrations are linked to anoxic-euxinic conditions however, according to Mo concentrations versus depth profiles of the upper and lower Bakken shales it can be concluded that paleoceanic marine waters enriched with Mo were delivered to the Williston Basin during late-Devonian to early-Mississippian time (Figure 4-20 and 4-21).

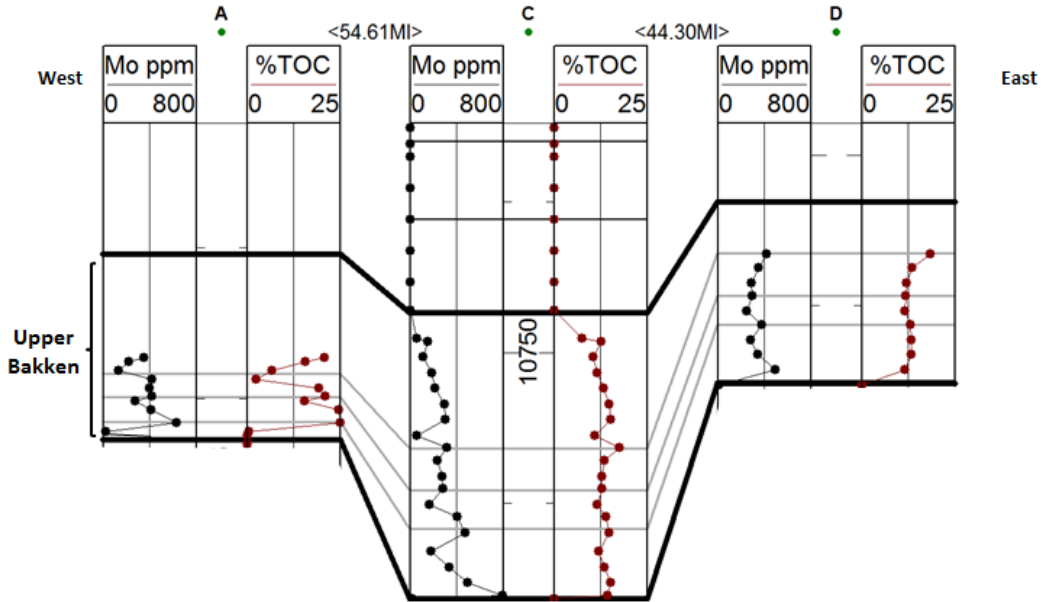


Figure 4-20. Chemostratigraphic profile of correlative geochemical shifts of Molybdenum and total organic carbon for the upper Bakken shale.

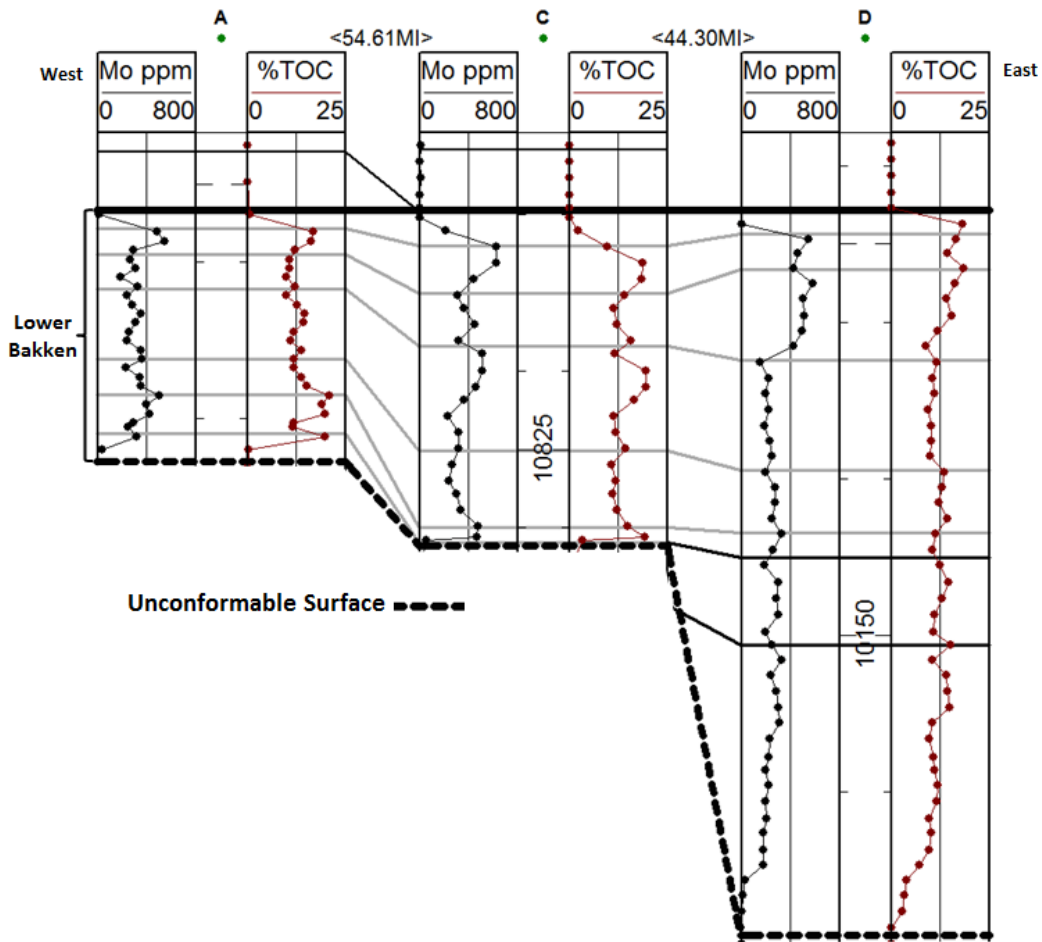


Figure 4-21 Chemostratigraphic profile of correlative geochemical shifts of Molybdenum and total organic carbon for the lower Bakken shale. Dashed line identifies an unconformable surface at the base of the lower Bakken shale.

Based on the Mo versus depth profile it could also be hypothesized that the Williston was a semi-restricted basin that experienced periodic renewed solutions of nutrient rich paleoceanic sea waters during high and low sea level stands from the Devonian-Carboniferous seaway. Also, Mo versus depth profiles for the Cariaco Basin display similar cyclical patterns of caused by Mo replenishment, similar to those observed in the Williston Basin (Figure 4-22). High enrichment of Mo and %TOC could be attributed to a rapid influx of Mo and nutrient rich paleoceanic waters inducing periods of high primary productivity as reflected by increased TOC. Furthermore, the delivery of oceanic waters

observed from periods of increase Mo and TOC introduced into the Cariaco Basin indicate continuous vertical mixing within the water column (Algeo and Lyons, 2006).

Cyclical shifts observed in Mo and TOC profiles versus depth for the lower and upper Bakken shales directly exhibit covariation identified by chemostratigraphic peaks linked to the same conditions that occurred in the Cariaco Basin, (Figure. 4-20 and 4-21). Elemental peaks of Mo and TOC influenced by hydrographic conditions and tectonic events, induced patterns of surface currents and differential high and low primary productivity during the deposition of the Bakken shales in the Williston Basin.

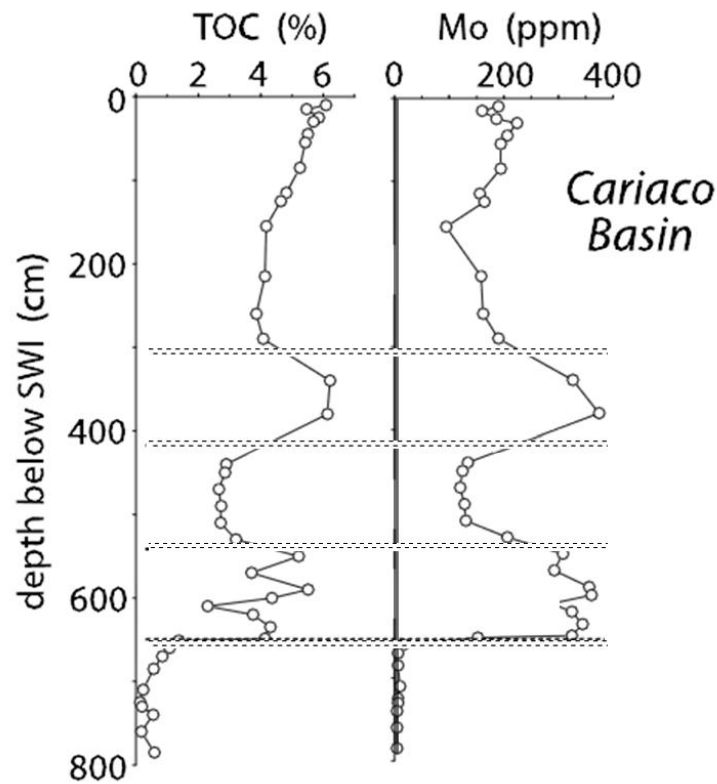


Figure 4-22. Total organic carbon and Mo versus depth below sediment-water interface for the Cariaco Basin, modified from Algeo et. al., 2006.

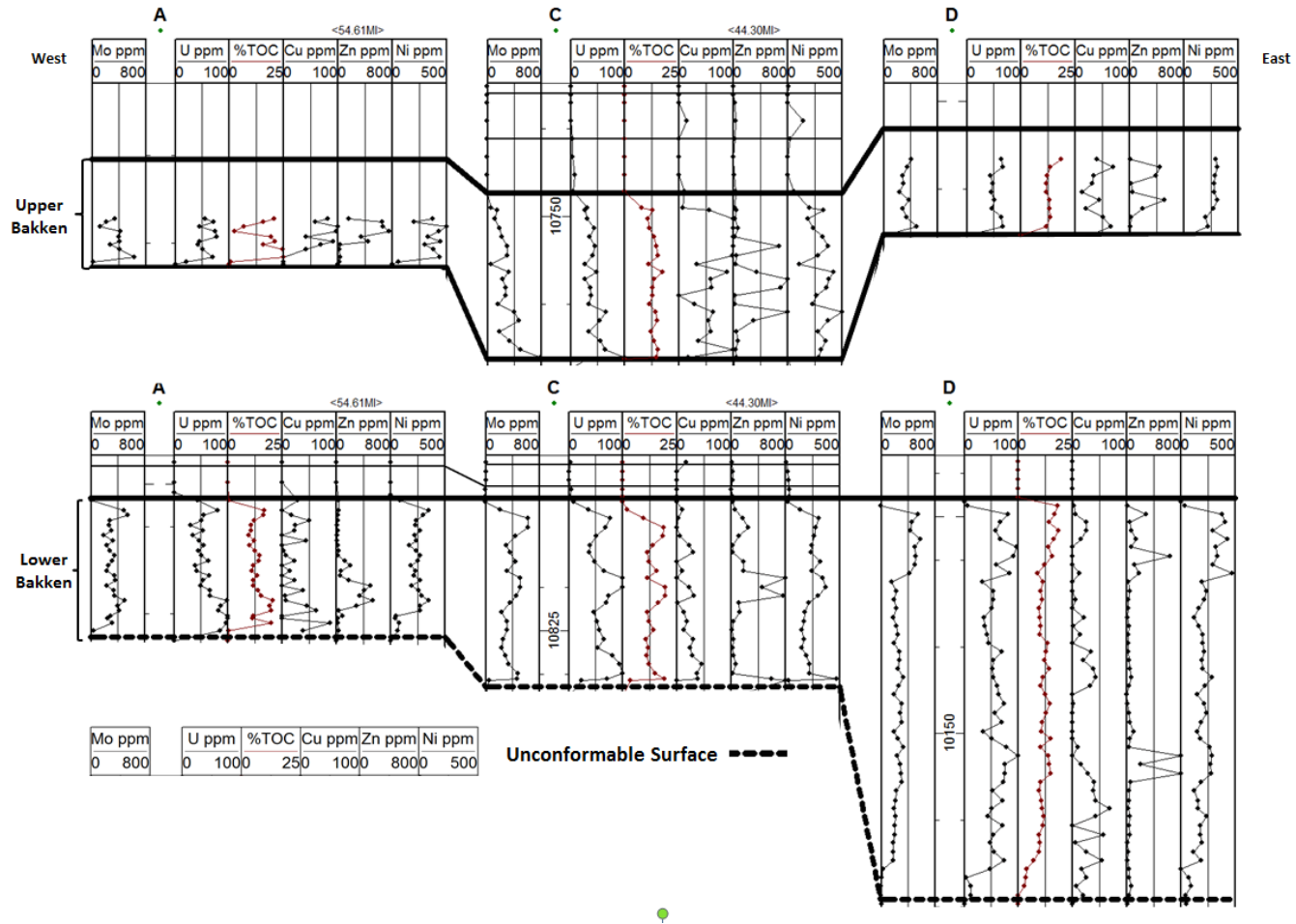
Chemostratigraphically, cores A, C, and D contain extremely high concentrations of molybdenum and TOC for the lower and upper Bakken shales (Figure 4-20 and 4-21).

Also, another observation that should be noted from the Mo and TOC versus depth profiles is the strong chemostratigraphic correlation across the Williston Basin between the A, C, and D cores from west to east for the upper and lower Bakken shales (Figure 4-20 and 4-21). Correlative geochemical shifts at the top of the lower Bakken shale display consistent patterns of Mo and TOC deposition. However, at the base of the lower Bakken shale an unconformable surface exists, which is defined as a surface of erosion or non-deposition, and it can be clearly identified by the inability to correlate elemental shifts from west to east across the Williston Basin (Figure 4-21). Core D seems to have an expanded section at the base of the lower Bakken shale which does not exist in core A and C which may be linked to a period of non-deposition in core A and C (Figure 4-21). Constant Mo concentrations that are vertically distributed versus depth, such as those observed in the Cariaco Basin are said to be a result of modern ocean waters constantly mixing, replenishing and dropping off Mo into silled reservoirs. When compared to the Bakken shale's within each examined core, increased concentrations with respect to Mo and TOC can be observed (Figure 4-20 and 4-21). Although, concentrations are uniformly high within each core it can be concluded that concentrations with respect to Mo and TOC concentrations exists in varying amounts. Based on the modern analogs and elemental results from Bakken shale's it can be concluded that during late Devonian-early Mississippian time the Williston Basin experienced the same physical contributions of Mo replenishment. In general, geologic process can be assessed to identify periods of eustatic sea level changes and intermitted tectonic events e.g. uplifts and subsidence, by utilizing elemental proxies, Mo and TOC, to identify hydrographic conditions and basin restriction.

Organic Composition (TOC and stable isotopes of organic carbon)

The richness and source of organic matter in the upper and lower Bakken shales for the A, C and D cores was examined by analyzing for TOC and stable isotopes of organic carbon. The reason for conducting such analyses on the shales is to consider the amount and production of organic matter; organic matter preservation based on influencing paleoenvironmental conditions, and examine the origin of the organic matter.

The importance for analyzing for TOC is to consider the amount and production of organic matter, organic matter preservation based on influencing paleoenvironmental conditions, and examine the origin of the organic matter content. Based on the amount TOC and geographical distribution of these cores it can be concluded that concentrations vary through the Williston Basin (Table 4, 5, and 6). Geochemical proxies were also utilized to demonstrate the correlation between high concentrations of TOC and elements which are indicators of primary productivity (Figure 4-23). Trace elements such as Mo, U, Zn, Ni, and Cu show increased enrichments and display unique covariation signatures with respect to TOC across the Williston Basin. Enrichment of Mo, U, V, Zn, Ni, and Cu in the lower and upper Bakken shales is indicative of euxinic conditions, more specifically, concentrations for Mo are attributed to anoxic-euxinic conditions which serve as a redox potential source as observed high enrichment concentrations. The strong relationship between high TOC content and enrichment of Mo, U, Zn, and Ni concentrations suggest increased production and preservation of organic matter as a result of upwelling marine during deposition (Figure 4-24).



Figures 4-23 Chemostratigraphic profiles of trace elements and %TOC were used to evaluate the covariation of Mo ppm, U ppm, Cu ppm, Zn ppm, Ni ppm with %TOC, for the lower and upper Bakken shales.

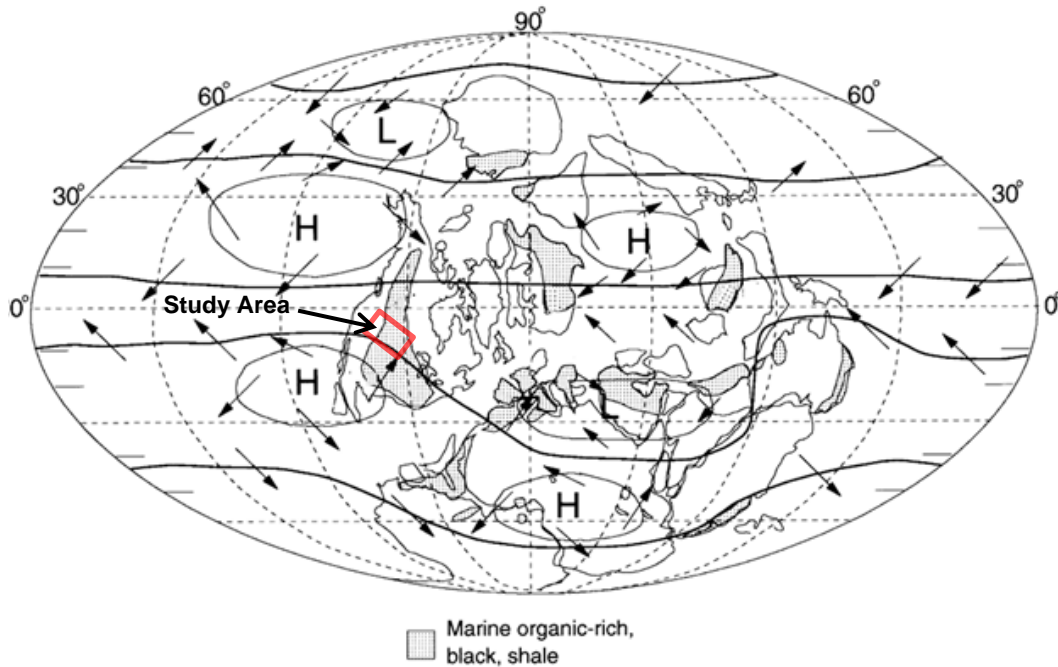


Figure 4-24. Palaeogeographical reconstruction of continents during the Famennian (after Scotese and McKerrow, 1990). Superimposed are distributions of Famennian–Tournaisian organic-rich marine mudrocks (modified from Klemme and Ulmishek, 1991), and predicted positions of atmospheric pressure cells and associated surface winds likely responsible for upwelling locations (modified from Parrish, 1982).

Mixing of the unstable water column and increased upwelling could also have been enhanced by increase wind strength during climatic cooling episodes. In addition, the down welling of cold polar waters, due to the Devonian-Carboniferous glacial climate, could have stimulated thermohaline circulation causing an increase in ocean mixing and upwelling (Caplan et al., 1999). Atmospheric and oceanic circulation patterns constructed for the Upper Devonian show a 92% correlation between organic rich mudrock facies and predicted upwelling cells along the shorelines of western North

America (Figure 4-24). Previous, research suggests that during the late Devonian geologic units throughout the Andean and intracratonic South American basins are very high in total organic carbon (TOC) values (Peters et al., 1996). Similarly, strong relationship between high TOC content and enrichment of Mo, U, Zn, and Ni concentrations suggest increased production and preservation of organic matter as a result of upwelling. This suggests that a combination of low sea-levels and increased nutrient supply brought significant increase in primary production which was subsequently preserved in shallow ocean basins, affording high organic content (Isaacson et. al., 2008).

Kerogen Type

Bakken shales were analyzed for stable carbon isotopes to identify organic source. Previous research studies have utilizing stable carbon isotopes as a tracer in hydrocarbon exploration (Van Krevelen, 1984). According to Van Krevelen 1984, hydrocarbons depends on the $\delta^{13}\text{C}$ content of the sourced material, any fractionation attendant on its formation, and any fractionation subsequent to its formation. Furthermore, past studies indicate that $\delta^{13}\text{C}$ analysis of oils and drilled samples can be utilized to correlate oil typing or oil-rock correlation (Fuex, 1976). Also, there has been plenty of research done with respect to the source for the organic content found within Bakken Formation where stable carbon isotopes were utilized for analysis and tied back to oil types (Dow, 1972; Dow, 1974; Williams, 1974; and Fuex, 1976). According to research done by Williams, 1974, the Bakken formation was analyzed via $\delta^{13}\text{C}$ by samples of oil from the reservoir and rock samples to determine a range of values associated with oil types (Figure 4-25). The range of analyzed stable carbon isotope data and TOC derived from the Bakken shale within the A, C, and D cores (Figure 26 and Tables 4,5, and 6) for this project correlates well with the range of values identified by

Williams 1974, research for $\delta^{13}\text{C}$ analysis of oil-rock correlation to Type II and Type III oils. Also, the oil generation from the Bakken shales is developed by two processes of hydrocarbon generation and hydrocarbon expulsion where these two combinations operating together is called catagenesis (Krevelen, 1984). Catagenesis is defined as the stage of geochemical conversions during burial in sedimentary basins. In this stage of increasing depth and temperature, the thermal degradation of kerogen is responsible for the generation of oil and gas. (Krevelen, 1984 and Muscio et al, 1994). This observation is important because it identifies the provenance for the organic carbon found within the examined lower and upper Bakken shales. The combination of these attributes together with a relative uniformity of kerogen type, predominately Type II makes the Bakken Shales an ideal candidate for reexamining source rocks and reservoir processes (Muscio et al, 1993). Coincidentally, research has shown that Type II kerogen is predominately made up of an alicyclic (naphthenic) nature which is formed mainly of marine organic matter (plankton) in a reducing environment (Dow, 1972; Dow, 1974; Williams, 1974; and Fuex, 1976). Research has also shown that the Bakken shale is the classical marine organic rich, oil prone source rock with abundant algal liptinite macerals (Dow, 1972; Dow, 1974; Williams, 1974; and Fuex, 1976).

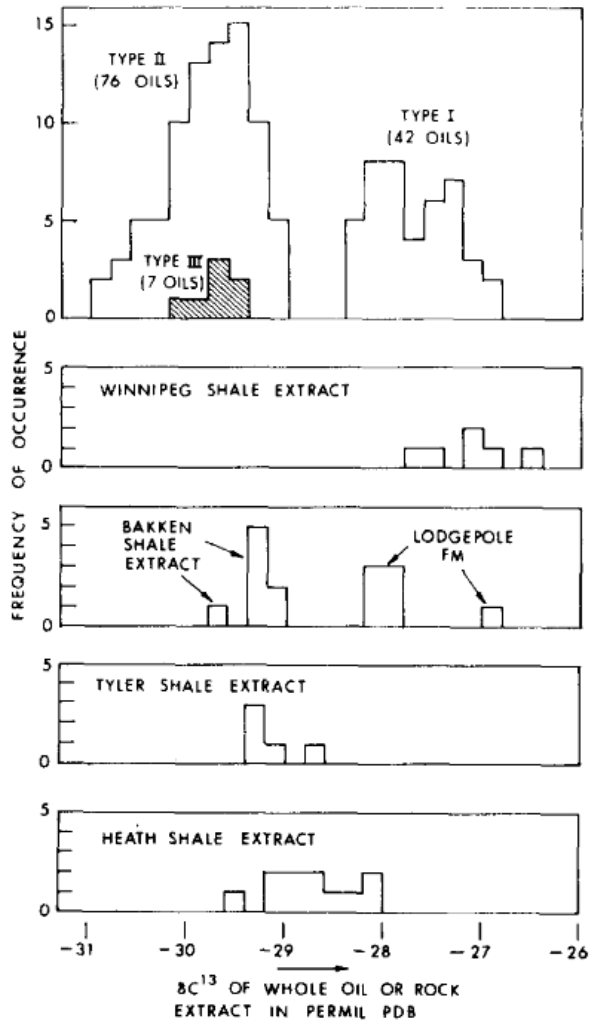


Table 4-25. Carbon isotopes of Williston Basin oil extract and rock samples (Williams, 1974 and Fuex, 1976).

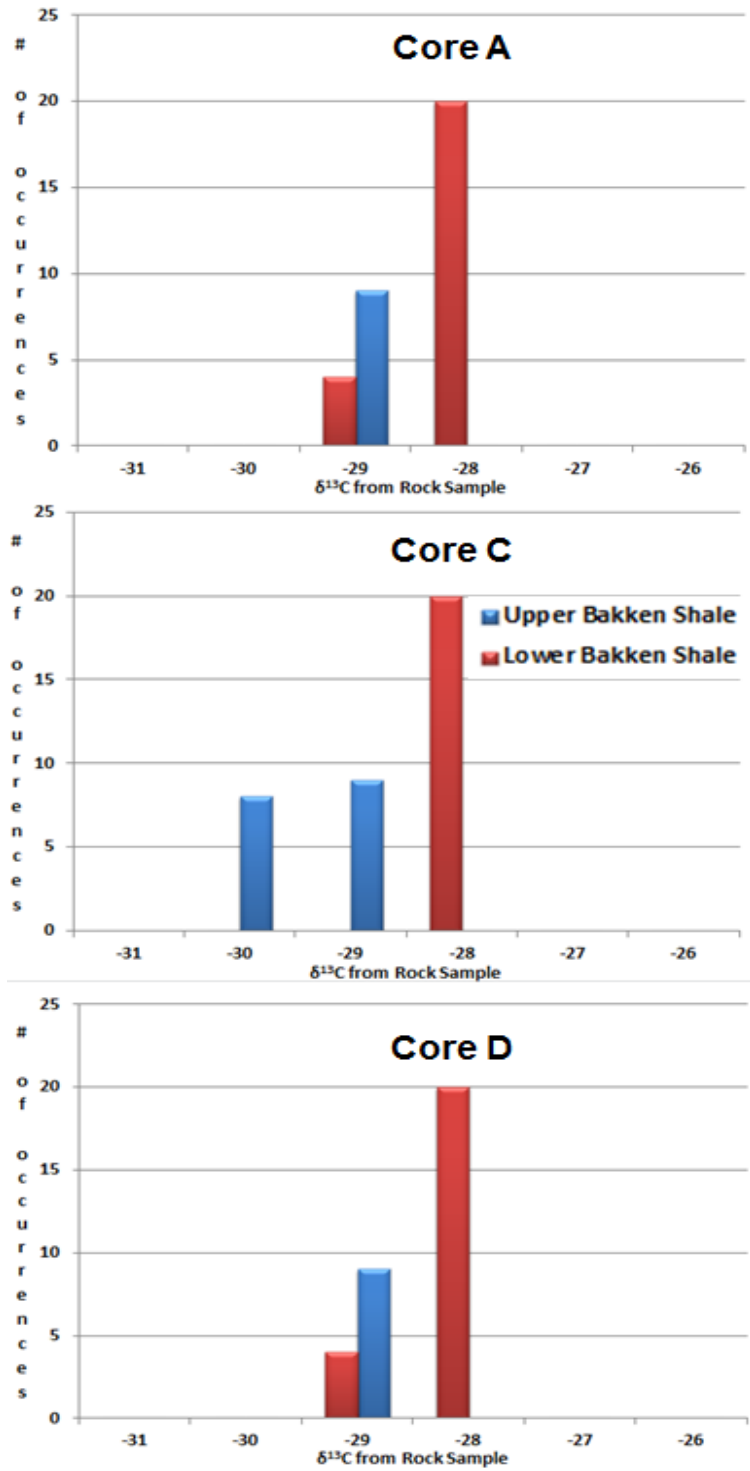


Table 4-26 Occurrences of $\delta^{13}\text{C}$ analyzed from the A, C, and D core for the Bakken shales.

Core A

Interval	Depth	%TOC	$\delta^{13}\text{C}$
Upper Bakken	8317.25	20.78	-29.91
Upper Bakken	8317.54	15.61	-29.85
Upper Bakken	8318.00	6.74	-29.99
Upper Bakken	8318.50	2.35	-29.78
Upper Bakken	8319.04	19.22	-29.83
Upper Bakken	8319.54	20.88	-29.59
Upper Bakken	8319.92	15.49	-29.67
Upper Bakken	8320.54	24.50	#REF!
Upper Bakken	8321.33	25.55	-29.47
Lower Bakken	8378.38	16.55	-28.84
Lower Bakken	8378.88	16.19	-28.94
Lower Bakken	8379.42	12.07	-28.97
Lower Bakken	8379.88	10.72	-29.10
Lower Bakken	8380.50	10.74	-28.70
Lower Bakken	8380.96	9.68	-28.79
Lower Bakken	8381.50	12.02	-29.24
Lower Bakken	8382.08	9.69	-28.79
Lower Bakken	8382.67	12.46	-29.01
Lower Bakken	8383.25	14.57	-28.95
Lower Bakken	8383.96	14.27	-28.24
Lower Bakken	8384.50	11.79	-28.96
Lower Bakken	8384.96	10.88	-29.01
Lower Bakken	8385.50	13.55	-28.80
Lower Bakken	8386.08	11.76	-28.69
Lower Bakken	8386.58	11.82	-28.15
Lower Bakken	8387.04	13.76	-28.65
Lower Bakken	8387.58	15.14	-28.06
Lower Bakken	8388.04	20.68	-28.42
Lower Bakken	8388.54	19.02	-28.31
Lower Bakken	8389.00	19.77	-28.34
Lower Bakken	8389.50	11.72	-28.44
Lower Bakken	8389.92	11.43	-28.35
Lower Bakken	8390.46	19.72	-28.30

Table 4-1 Total Organic Carbon, TOC and Stable Carbon Isotopic, $\delta^{13}\text{C}$ data on the core A.

Core C

Interval	Depth	%TOC	$\delta^{13}C$
Upper Bakken	10748.92	12.62	-30.43
Upper Bakken	10749.92	10.55	-30.29
Upper Bakken	10750.92	11.46	-30.32
Upper Bakken	10751.92	13.37	-30.20
Upper Bakken	10753.00	14.67	-29.71
Upper Bakken	10754.00	15.12	-29.50
Upper Bakken	10755.00	11.02	-29.53
Upper Bakken	10755.92	17.46	-29.83
Upper Bakken	10756.83	13.57	-30.04
Upper Bakken	10757.92	12.82	-30.00
Upper Bakken	10758.83	12.76	-30.06
Upper Bakken	10759.88	11.47	-30.01
Upper Bakken	10760.67	13.98	-29.99
Upper Bakken	10761.63	14.76	-29.77
Upper Bakken	10762.79	12.02	-29.69
Upper Bakken	10763.75	13.48	-29.81
Upper Bakken	10764.71	15.19	-29.49
Lower Bakken	10812.00	9.57	-28.89
Lower Bakken	10813.00	18.70	-28.36
Lower Bakken	10814.00	18.32	-28.60
Lower Bakken	10814.96	13.88	-28.82
Lower Bakken	10815.75	11.18	-28.74
Lower Bakken	10816.79	11.91	-28.70
Lower Bakken	10817.88	15.61	-28.74
Lower Bakken	10818.75	11.46	-28.50
Lower Bakken	10819.79	19.41	-28.39
Lower Bakken	10820.83	19.44	-28.43
Lower Bakken	10821.75	16.44	-28.45
Lower Bakken	10822.88	11.14	-28.46
Lower Bakken	10823.96	11.84	-28.34
Lower Bakken	10824.92	14.20	-28.82
Lower Bakken	10825.96	10.75	-28.76
Lower Bakken	10826.96	11.79	-28.66
Lower Bakken	10827.83	10.84	-28.42
Lower Bakken	10828.83	12.03	-28.28
Lower Bakken	10829.83	14.70	-28.25
Lower Bakken	10830.46	19.24	-28.34

Table 4-2. Total Organic Carbon, TOC and Stable Carbon Isotopic, $\delta^{13}C$ data for core C.

Core D

Interval	Depth	%TOC	$\delta^{13}C$
Upper Bakken	10056.58	18.31	-29.76
Upper Bakken	10057.50	13.48	-29.85
Upper Bakken	10058.50	11.91	-29.93
Upper Bakken	10059.33	11.71	-29.72
Upper Bakken	10060.33	11.67	-29.22
Upper Bakken	10061.25	13.07	-29.92
Upper Bakken	10062.25	13.18	-29.10
Upper Bakken	10063.25	13.38	-28.19
Lower Bakken	10124.71	16.50	-28.92
Lower Bakken	10125.58	14.21	-29.03
Lower Bakken	10126.58	18.39	-28.83
Lower Bakken	10127.54	16.21	-29.13
Lower Bakken	10128.50	13.91	-29.01
Lower Bakken	10129.58	15.44	-28.97
Lower Bakken	10130.54	11.85	-28.86
Lower Bakken	10131.50	8.76	-28.69
Lower Bakken	10132.54	11.36	-28.59
Lower Bakken	10133.58	10.24	-28.56
Lower Bakken	10134.58	10.84	-28.52
Lower Bakken	10135.58	9.37	-28.63
Lower Bakken	10136.63	10.01	-28.63
Lower Bakken	10137.58	10.07	-28.58
Lower Bakken	10138.58	9.72	-28.89
Lower Bakken	10139.58	13.37	-28.76
Lower Bakken	10140.54	12.77	-28.73
Lower Bakken	10141.54	12.02	-28.75
Lower Bakken	10142.54	14.15	-28.85
Lower Bakken	10143.54	11.27	-28.87
Lower Bakken	10144.54	10.30	-28.97
Lower Bakken	10145.50	12.20	-28.85
Lower Bakken	10146.58	14.49	-28.61
Lower Bakken	10147.63	12.77	-28.77
Lower Bakken	10148.67	10.91	-28.89
Lower Bakken	10149.79	10.52	-28.90
Lower Bakken	10150.63	15.01	-28.67
Lower Bakken	10151.54	10.32	-28.39
Lower Bakken	10152.54	13.94	-28.81
Lower Bakken	10153.54	14.12	-28.63
Lower Bakken	10154.58	14.75	-28.56
Lower Bakken	10155.58	10.33	-28.76
Lower Bakken	10156.63	9.59	-28.90
Lower Bakken	10157.75	10.59	-29.02
Lower Bakken	10158.63	10.89	-28.69
Lower Bakken	10159.58	11.65	-29.16
Lower Bakken	10160.63	11.40	-29.13
Lower Bakken	10161.67	9.62	-29.07
Lower Bakken	10162.63	9.99	-29.32
Lower Bakken	10163.71	9.56	-29.26

Table 4-3. Total Organic Carbon, TOC and Stable Carbon Isotopic, $\delta^{13}C$ data for core D.

Chapter 5

CONCLUSION

An analysis of elemental abundances was conducted using XRF, for the Bakken and Three Forks Formations. The use of elemental proxies has allowed the identification for the linkage of elemental concentrations to mineralogical make up within these formations such as calcite, dolomite, illite, and silica quartz. Geochemical proxies were used to determine various aspects of paleoceanic waters during the deposition of the upper and lower Bakken shale such as bottom water redox conditions in the Williston Basin, degree of basin restriction, mixing of elemental constituents and hydrographic conditions. Modern basin analogs were used as a scale to explain physical process i.e. tectonic events or episodic sea level changes that the Williston Basin could have experienced during late Paleozoic time. The current findings for this research project are as follows:

1. The elemental data sets derived from each of the 4 cores examined provide evidence that geochemical attributes derived from the Bakken and Three Forks Formations provide a linkage to mineralogical content within each of these formations. Linkage to the bulk mineralogy of these two formations were observed in cross plots as linear and non-linear trends demonstrating the existence of elements in clay and non-clay mineral phases, i.e. calcite, dolomite, illite, and silica quartz. The Three Forks Formation displays an overall increase in Ca concentration from west to east whereas Mg concentrations display an inverse relationship. Correlative chemostratigraphic packages within the Three Forks Formation of Al and Si content can be observed on an elemental vs. depth profile from west to east. Upward diminishing Mg concentrations and increased Ca concentrations content from west to east are related to a facies change within the Three Forks Formation. Cross-plots of elemental ratios of K, Si, Rb, and Ti versus Al,

displaying a positive linear trend is associated with trace and major elements linked to same derivation of source and linkage to the clay structure within of the Three Forks Formation for all 4 cores.

In each core the lower and upper Bakken shales display 0 to 2 weight percent Ca & Mg concentrations on average across the Williston Basin. However, the middle Bakken member displays much higher amounts of Ca and Mg ranging from 4 to 20 weight percent. The chemostratigraphy of the middle Bakken, specifically in the C and D core show higher concentrations of Ca and Mg. The concentration of Mg within the middle Bakken increases from west to east then diminishes while %Ca content increases across the Williston Basin. These geochemical shifts come about as a result of lithological changes within the middle Bakken that represent a transition from a dolomite to a dolostone facies with high amounts of calcite and quartz content.

Concentrations of %Si content observed in chemostratigraphic profiles within the lower and upper Bakken shales for cores A and B are located in eastern Montana, range between 30 to 50 weight percent. The %Si content observed in the C and D core however, range between 25 to 32 weight percent. The amounts of Si content found within each core could be related to location of each core within the Williston Basin. The Si content could have been sourced from older Paleozoic rocks e.g. middle to early Devonian, Silurian, and Ordovician that experienced erosion during Bakken deposition.

2. Elemental data expressed as enrichment factors versus depth gave insight into the redox conditions of the lower and upper Bakken shale's. Elemental shifts represented by cyclical peaks enriched with Mo, U, V, Zn, Ni, Cu and TOC for example, can be observed throughout the upper and lower Bakken shale chemostratigraphic profiles. Cyclical peaks of enriched trace elements indicate that the Bakken shales experienced episodic anoxic-euxinic conditions during deposition. This relationship can

be specifically observed from chemostratigraphic profiles of (EF) Mo, U, V, and Ni from west to east. A covariation between preservation of total organic carbon (TOC) with periods of anoxic-euxinic proxies, Mo, U, V, Zn, Ni, Cu, in cores C and D for the lower Bakken shale and core C for the upper Bakken shale exists. An overall increase in enrichment concentration can also be observed from the following trace elements Mo, U, V, Zn, Ni, and Cu. Chemostratigraphic profiles demonstrate elevated enrichment in reference to each element for the Bakken shales which may have resulted due to paleoupwelling or high stands associated with episodic glacial periods during late-Devonian/early Mississippian time.

3. A high enrichment of Mo concentrations observed in chemostratigraphic profiles may have been attributed to variable influxes of Mo rich paleoceanic marine waters. Cyclical shifts of Mo concentration demonstrates that the Williston Basin could have been semi-restricted and experienced periodic renewed solutions of nutrient rich paleoceanic sea waters from the Devonian-Carboniferous sea way, during high and low sea level stands. Covariation between high enrichment of Mo and TOC may be linked to differential high and low primary productivity variations influenced by tectonic events. Mo and TOC signatures versus depth were also utilized to compare modern basins e.g. Cariaco Basin versus the Williston Basin to demonstrate the physical process of oceanic waters constantly mixing, replenishing and dropping off Mo into these modern basin silled reservoirs. Based on a similar cyclical trends observed in chemostratigraphic profiles between modern basin analogs e.g. Cariaco Basin versus the Williston Basin, it can be concluded that during late Devonian-early Mississippian time the Williston Basin experienced the same physical contributions of Mo replenishment.

4. The lower and upper Bakken shale were analyzed for stable carbon isotopes to identify organic provenance. Stable carbon isotopic data was also utilized to identify

kerogen type and related to process of hydrocarbon generation. Based on this research and previous studies, the upper and lower Bakken shale is a rich organic mud rock that has Type II kerogen and is predominately made up of an alicyclic (naphthenic) nature that is formed mainly from marine organic matter (plankton) in a reducing environment.

Future Research

Recently, there has been geochemical research conducted on mudrocks from different geological time periods that have been able to reconstruct the paleo-geochemical environments of their time. However, further analysis should be conducted on the cores analyzed in this research project such as XRD in the upper and lower Bakken shale's that will definitively provide crystallite size, shape, and most importantly chemical composition. Further investigation should be undertaken to examine and compare late Phanerozoic mudrocks on a national and international scale with the same types of analysis found in this research project. This would not only enable the reconstruction of basin restriction, vertical mixing of paleoceanic waters within basins but also ultimately defining detailed paleo-upwelling regions around the globe.

References

- Algeo, T. J., and J. B. Maynard 2004, Trace element behavior and redox facies in core shales of Upper Pennsylvanian Kansas-type cyclothems, *Chem. Geol.*, 206, 289–318.
- Algeo, T.J., and Lyons, T.W., 2006, Mo-total organic carbon covariation in modern anoxic marine environments: Implications for analysis of paleoredox and paleohydrographic conditions: *Paleoceanography*, v. 21, p.
- Algeo, T.J., Lyons, T.W., Blakey, R.C., and Over, D.J. 2007. Hydrographic conditions of the Devonian–Carboniferous North American Seaway inferred from sedimentary Mo–TOC relationships. *Palaeogeography, Palaeoclimatology, Palaeoecology*. 256: 204–230.
- Algeo, T.J., and Maynard, J.B., 2008. Trace-metal covariation as a guide to water-mass conditions in ancient anoxic marine environments, *Geosphere*, V.4; no.5; 872- 887.
- Algeo, T.J. and Rowe, H.D. 2011, In press. Paleoceanographic applications of trace-metal concentration data. *Chemical Geology*.
- Algeo, T., Rowe, H., Hower, J.C., Schwark, L., Herrmann, A., Heckel, P., 2008. Changes in ocean denitrification during Carboniferous glacial-interglacial cycles, *Nature Geoscience* Vol 1. Macmillan Publisher Limited.
- Algeo TJ, Scheckler SE. 1998. Terrestrial-marine teleconnections in the Devonian: Links between the evolution of land plants, weathering processes, and marine anoxic events. *Philos. Trans. R. Soc. London Ser. B* 353:113–28
- Algeo, T.J., Tribouillard, N. 2009. Environmental analysis of paleoceanographic systems based on molybdenum-uranium covariation. *Chemical Geology*. 268; 211-225.
- Angulo, S., Luis A. Buatois, Halabura, Paleoenvironmental and sequence-stratigraphic reinterpretation of the Upper Devonian–Lower Mississippian Bakken Formation of subsurface Saskatchewan: integrating sedimentological and ichnological data. Saskatchewan Geological Survey, Saskatchewan Ministry of Energy and Resources, 2008, v. 1,
- Angulo, S., Luis A. Buatois, Ichnology of a Late Devonian–Early Carboniferous low-energy seaway: The Bakken Formation of subsurface Saskatchewan, Canada: Assessing paleoenvironmental controls and biotic responses, *Palaeogeography, Palaeoclimatology, Palaeoecology*, Volumes 315–316, 15 January 2012, Pages 46-60, ISSN 0031-0182, 10.1016/j.palaeo.2011.11.007.
- Bai, S., Ning, Z., 1988. Faunal change and events across the Devonian–Carboniferous boundary of Huangmao Section, Guangxi, South China. In: McMillan, N.J., Embrey, A.F., Glass, D.J. (Eds.), *Devonian of the World. Proc. Can. Soc. Pet. Geol. Int. Symp., Devonian System III*, pp. 147–157.

- Beauchamp, B., Baud, A., 2002. Growth and demise of Permian biogenic chert along northwest Pangea: evidence for end-Permian collapse of thermohaline circulation. *Palaeogeography, Palaeoclimatology, Palaeoecology* 187, 37–63.
- Beaumont, C., G. M. Quinlan, and J. Hamilton, 1987, The Alleghanian orogeny and its relationship to the evolution of the eastern interior, North America, in C. Beaumont and A. J. Tankard, eds., *Sedimentary basins and basin-forming mechanisms: Canadian Society of Petroleum Geologist Special publication 39*, p. 233-257. et al., 1987)
- Berrange, P. G., and Grill, V. E., 1974. The effect of manganese oxide scavenging on molybdenum in Saanich Inlet, British Columbia. *Mar. Chem.* 2: 125-148.
- Becker, R.T., 1992. Analysis of ammonoid palaeobiogeography in relation to the global Hangenberg (terminal Devonian) and Lower Alum Shale (Middle Tournaisian) events. *Ann. Soc. Geol. Belg.* 115, 459–473.
- Blatt, H., W. B. N. Berry, and S. Brande, 1991, *Principles of stratigraphic analysis*: Oxford, Blackwell Scientific Publications, 512 p.
- Blakey, R., 2005. North American paleogeographic maps, Late Devonian (360Ma). Retrieved June 15, 2011, <http://jan.ucc.nau.edu/rcb7/namD360.jpg>
- Bridges, et. al. Lower Mississippian lithofacies Map, Shell Oil Company. 1964
- Bohacs, K.G., 1998, Contrasting expressions of depositional sequences in mudrocks from marine to none marine environs, in J. Schieber, W. Zimmerle, and P. Sethi (eds.), *Mudstones and shales 1: basin Studies, Sedimentology, and Paleontology*, Stuttgart, Schweizerbart'sche Verlagsbuchhandlung, p. 33-78.
- Brenchley, P.J., Marshall, J.D., Carden, G.A.F., Robertson, D.B.R., Long, D.G.F., Meidla, T., Hints, L., Anderson, T.F., 1994. Bathymetric and isotopic evidence for a short-lived Late Ordovician glaciation in a greenhouse period. *Geology* 22, 295–298.
- Brown, D. L., Blankennagel, R. K., MacCrary, M., L., and Peterson, A., J., 1982, Correlation of paleostructure and sediment deposition in the Madison Limestone and associated rocks in parts of Montana, North Dakota, South Dakota, Wyoming, and Nebraska: U. S. Geological Survey Open-File Report 82-906, 71p.
- Butler, et. al. Upper Devonian lithofacies Map, Shell Oil Company. 1961
- Brumsack, H.J. 2006. The trace metal content of recent organic carbon-rich sediments: Implications for Cretaceous black shale formation. *Palaeogeography, Palaeoclimatology, Palaeoecology.* 232: 344-361.
- Calvert, S.E. and Pedersen, T.F. 1993. Geochemistry of recent oxic and anoxic marine sediments: implications for the geological record. *Marine Geology.* 113: 67–88.
- Caplan, M.L., Bustin, R.M., 1999. Devonian–Carboniferous Hangenberg mass extinction event, widespread organic-rich mudrock and anoxia: causes and consequences. *Palaeogeogr., Palaeoclimatol., Palaeoecol.*

- Carlson, C. G., and S. B. Anderson, 1965, Sedimentary and tectonic history of North Dakota part of Williston Basin: AAPG Bulletin, v. 49, p. 1833–1846.
- Carlson, C. E., 1960, Stratigraphy of the Winnipeg and Deadwood formations in North Dakota: North Dakota Geological Survey Bulletin 35, 149 p.xd
- Cawood, P. A., Alexander A., Nemchin, Freeman, M., Sircombe, K., Linking source and sedimentary basin: Detrital zircon record of sediment flux along a modern river system and implications for provenance studies, Earth and Planetary Science Letters, Volume 210, Issues 1–2, 15 May 2003, Pages 259-268
- Chen J. H., Edwards R. L., and Wasserburg G. J. (1986) ^{238}U / ^{234}U and ^{232}Th in seawater. Earth Planet. Sci. Lett. 80, 241–251.
- Chlupac, I., 1988. The Devonian of Czechoslovakia and its stratigraphic significance. In: McMillan, N.J., Embrey, A.F., Glass, D.J. (Eds.), Devonian of the World. Proc. Can. Soc. Pet. Geol. Int. Symp., Devonian System I, pp. 481–497.
- Clayton J. L. and Swetland P. J. (1978) Subaerial weathering of sedimentary organic matter. *Geochim. Cosmochim. Acta* **42**, 305–312.
- Crowley, K. D., Ahern, J. L., and Naeser, C. W., 1985, Origin and epirogenic history of the Williston basin: Evidence from fission-track analysis of apatite: *Geology*, v. 13, p. 620-623.
- Cox, J.E., Railsback, L.B, and Gordon, E.A., Evidence from Catskill pedogenic carbonates for a rapid Late Devonian decrease in atmospheric carbon dioxide concentrations Northeast. *Geol. Environ. Sci.*, 23 (2001), pp. 91–102.
- Dean, W. E., Arthure, M.A., 1998. Geochemical expressions of cyclicity in Cretaceous pelagic limestone sequences: Niobrara Formation, Western Interior Seaway. In: Dean, W.E., Arthure, M.A. (Eds.), Stratigraphy and Paleoenvironments of the Cretaceous Western Interior Seaway USA: Society of Economic Paleontologists, and Mineralogists, Concepts in Sedimentology and Paleontology, 6, pp. 227-255.
- Dean, W. E., Gardner, J. V., Piper, Z., D., Inorganic geochemical indicators of glacial-interglacial changes in productivity and anoxia on the California continental margin, *Geochimica et Cosmochimica Acta*, Volume 61, Issue 21, November 1997
- DeRito, R. F., F. A., Cozarelli, and D. S. Hodge, 1983, Mechanism of subsidence of ancient cratonic rift basins: *Tectonophysics*, v. 94, p. 141-168.
- Dow, W. G., 1972, Application of oil correlation and source rock data to exploration in Williston basin (abs.): AAPG Bulletin, v. 56, p. 615.
- Dow, W. G., 1974, Application of oil correlation and source rock data to exploration in Williston basin: AAPG Bulletin, v. 58, n. 7, p. 1253-1262.

- Ellison, S. P., Jr., 1950, Subsurface Woodford black shale, West Texas and southeast New Mexico: University of Texas, Austin, Bureau of Economic Geology Report of Investigations No. 7, 20 p.
- Ellingson, J.B., and LeFever, R.D., 1995, Depositional environments and history of the Winnipeg Group (Ordovician), Williston Basin, North Dakota: in Seventh International Williston Basin Symposium, p. 129-138.
- Eley, B. E., Jull, R. K., 1982. Chert in the Middle Silurian Fossil Hill Formation of Manitoulin Island, Ontario. *Bulletin of Canadian Petroleum Geology*, 30: 208–215
- Emlet, R.B. (1982) Echinoderm calcite: Mechanical analysis from larval spines. *Biological Bulletin*, 163, 264-275.
- Ettensohn, F. R., M. L. Miller, S. B. Dillman, T. D. Elam, K. I. Geller, D. R. Swager, G. Markowits, R. D. Woock, and L. S. Barron, 1988, Characterization and implications of the Devonian-Mississippian black shale sequence, eastern and central Kentucky, U.S.A.: pycnoclines, transgressions, regressions and tectonism, in N. J. McMillan, A. F. Embry, and D. J. Glass, eds., *Devonian of the world: Proceedings of the 2nd International Symposium on the Devonian System*, v. II Sedimentation, Canadian Society of Petroleum Geologist Memoir 14, p 323-345.
- Feist, R. (Ed.), 1990. Guide book of the field meeting, Montagne Noire 1990. Montpellier, Int. Union Geol. Sci. Subcom. Dev. Stratigr., pp. 1–69.
- Frakes, L.A., Francis, J.E., Syktus, J.I., 1992. *Climate Modes of the Phanerozoic*. Cambridge University Press, Cambridge, 274 pp.
- François Demory, Hedi Oberhänsli, Norbert R. Nowaczyk, Matthias Gottschalk, Richard Wirth, Rudolf Naumann, Detrital input and early diagenesis in sediments from Lake Baikal revealed by rock magnetism, *Global and Planetary Change*, Volume 46, Issues 1–4, April 2005, Pages 145-166
- Fuex A. N. (1977) The use of stable carbon isotopes in hydrocarbon exploration. *J. Geochem. Exploration*. 7, 155-188.
- Ganeshram, R., and T. Pedersen, Glacial-interglacial variability in upwelling and bioproductivity off NW Mexico: Implications for Quaternary paleoclimate, *Paleoceanography*, 13, 634–645, 1998
- Gerhard, L. C., Anderson, B. S., La Ferver, A., A.J., and Carlson, G. C. 1982, Geological development, origin, and energy mineral resources of Williston Basin: *AAPG Bulletin*, v. 66 p. 989-1020.
- Gerhard, L. C., and S. B. Anderson, 1988, Geology of the Williston basin (United States portion), in L. L. Sloss, ed., *Sedimentary cover-North American craton: Geological Society of America, The Geology of North America*, v. D-2, p 221-241.

Gerhard, L. C., Anderson, B. S., and Fischer, W. D., 1990. Gerhard, L. C., and S. B. Anderson. Interior Cratonic Basin. Spec. Pub.: Memoir. P 507-559.

Gradstein, F. M., Ogg, J. G. and Smith, A. G., 2004, "A geologic Time Scale" Cambridge University Press, Cambridge

Gendtwill, D.J., 1978b, Winnipegosis mounds and Prairie Evaporite Formation of Saskatchewan seismic study: in Williston Basin Symposium, 24th annual conference, Billings, Montana, 1978: Billings, Montana Geological Society, p. 121 - 130.

Grosjean, P, Adam, J, Connan, Albrecht, P., Effects of weathering on nickel and vanadyl porphyrins of a Lower Toarcian shale of the Paris basin, *Geochimica et Cosmochimica Acta*, Volume 68, Issue 4, 15 February 2004, Pages 789-804

Handford, C.R. & Loucks, R.G.: Carbonate depositional sequences and systems tracts – responses of carbonate platforms to relative sea-level changes. – In: R.G. LOUCKS & J.F. SARG (eds.): Carbonate Sequence Stratigraphy. American Association of Petroleum Geologists, Memoir, 57, 3–41, Tulsa 1993.

Haq, B.U. and S.R. Shutter, 2008, A chronology of Paleozoic sea-level changes: *Science*, v. 322, October 2008, p. 64-68.

Helz, G. R., Miller, C.V., Charnock, J. M., Mosselmans, J. L. W., Patrick, R.A.D., Garner, C.D., and Vaughan, D.J., 1996, Mechanisms of molybdenum removal from the sea and its concentration in black shales: EXAFS evidences: *Geochimica et Cosmochimica Acta*, v. 60, p. 3631–3642.

Halabura, S., 1982, Depositional environments of the Upper Devonian Birdbear Formation, Saskatchewan: Fourth International Williston Basin Symposium, Saskatchewan Geological Society Publication 6, p. 113-124.

House, M.R., 1985. Correlation of Mid-Palaeozoic ammonoid evolutionary events with global sedimentary perturbations. *Nature* 313, 17–22.

Isaacson, P. E., Hladil, J., Shen, J. W., Kalvoda, J., Grader, G., 1999. Late Devonian (Famennian) glaciation in South America and marine offlap on other continents. In: Feist, R., Talen, J.A., Daurer, A., (Eds), *North Gondwana: Mid-Palaeozoic Terranes, Stratigraphy and Biota*, Vol. 54 Abh. Geol. B. A., pp 239-257.

Isaacson, P. E., Díaz-Martínez, E., Grader, G.W., Kalvoda, J., Babek, O., Devuyst, F.X. , Late Devonian–earliest Mississippian glaciation in Gondwanaland and its biogeographic consequences, *Palaeogeography, Palaeoclimatology, Palaeoecology*, Volume 268, Issues 3–4, 24 October 2008, Pages 126-142.

Jacka, A. D., 1974. Replacement of Fossils by Length-Slow Chalcedony and Associated Dolomitization. *Journal of Sedimentary Petrology*, 44: 421–427

Jewell, P.W., 1993, Water-column stability, residence times, and anoxia in the Cretaceous North American Seaway: *Geology*, v. 21, p. 579–582.

- Johnson, G. Klapper, C.A. Sandberg. Devonian eustatic fluctuations in Euroamerica Bulletin of the Geological Society of America, 96 (1985), pp. 567–587
- Joachimski, M.M., Buggisch, W., 1993. Anoxic events in the late Frasnian — causes of the Frasnian–Famennian faunal crisis? *Geology* 21, 675–678.
- Johnson, J. G., G. Klapper, and C. A. Sandberg, 1985, Devonian eustatic fluctuations in Euramerica: Geological Society of American Bulletin, v. 96, p. 567-587.
- Jones, J. B., Segnit, E. R., 1971. The Nature of Opal. I. Nomenclature and Constituent Phases. *Journal of the Geological Society of Australia*, 18(1): 57–67
- Kaiser, S. I., Becker, R.T., Steuber T., Aboussalam S.Z., Climate-controlled mass extinctions, facies, and sea-level changes around the Devonian–Carboniferous boundary in the eastern anti-Atlas (SE Morocco) *Palaeogeography, Palaeoclimatology, Palaeoecology*, 310 (2011), pp. 340–364
- Kalvoda, J., 1986. Upper Frasnian and Lower Tournaisian events and evolution of calcareous Foraminifera — close links to climatic changes. In: Walliser, O.H. (Ed.), *Global Bio-Events: A Critical Approach*. Lect. Notes Earth Sci. 8, Springer, Berlin, pp. 225–236.
- Kidder, D.L., and Erwin, D.H., 2001, Secular distribution of biogenic silica through the Phanerozoic: Comparison of silica-replaced fossils and bedded cherts at the series level: *Journal of Geology*, v. 109, no. 4, p. 509-522.
- Klemme, H.D., Ulmishek, G.F., 1991. Effective petroleum source rocks of the world: stratigraphic distribution and controlling depositional factors. *Am. Assoc. Pet. Geol.* 75, 1809–1851.
- Kohlruss, D., Nickel, E., Facies analysis of the Upper Devonian–Lower Mississippian Bakken Formation, southeastern Saskatchewan Summary of Investigations 2009, v. 1, Saskatchewan Geological Survey: Saskatchewan Ministry of Energy and Resources, Miscellaneous Report 2009-4.1, Paper A-6 (2009) 11 p.
- Krstic, B., Grubic, A., Ramovs, A., Filipovic, I., 1988. The Devonian of Yugoslavia. In: McMillan, N.J., Embrey, A.F., Glass, D.J. (Eds.), *Devonian of the World*. Proc. Can. Soc. Pet. Geol. Int. Symp., Devonian System Memoir 14: I, pp. 499–506.
- Kuhn, P., Di Primio, R. & Horsfield, B., 2010, Bulk composition and phase behavior of petroleum sourced by the Bakken Formation of the Williston Basin.
- Lambeck, K., 1983, The role of compressive forces in intracratonic basin formation and mid-plat orogenies: *Geophysical Research Letters*, v. 10, 845-848.
- LeFever, J.A., 2005, North Dakota middle member Bakken horizontal play: Geological Investigation No. 8, North Dakota Geological Survey.
- Lyle, M., 1988, Climatically forced organic carbon burial in equatorial Atlantic and Pacific oceans. *Nature* 335, 529-532.

- Lyons, T.W., Werne, J.P., Hollander, D.J., and Murray, R.W. 2003. Contrasting sulfur geochemistry and Fe/Al and Mo/Al ratios across the last oxic-to-anoxic transition in the Cariaco Basin, Venezuela. *Chemical Geology*. 195: 131–157.
- Lochman-Balk, C., and Wilson, J., L., 1967, Stratigraphy of Upper Cambrian-Lower Ordovician subsurface sequence in the Williston Basin: *AAPG Bulletin*, v. 51, p. 883-917.
- Lobdell, F. K., 1984, Age and depositional history of the Middle Devonian Ashem Formation in the Williston Basin, Saskatchewan and North Dakota: in Lorsong, J. A., and Wilson, M. A.,(eds.), *Oil and gas in Saskatchewan: Regina, Saskatchewan Geological Society Special Publication 7*, p. 5-12.
- LoBue, C., 1982, Depositional environments and diagenesis of the Silurian Interlake Formation, Williston Basin, Western North Dakota: *Fourth International Williston Basin Symposium, Saskatchewan Geological Society Publication 6*, 29-42.
- Martin, R.E., 1996. Secular increase in nutrient levels through the Phanerozoic: implications for productivity, biomass, and diversity of the marine biosphere. *Palaios* 11, 209–219.
- Martindale, W., and OIT, N. E., 1987, Middle Devonian Winnipegosis reefs of the Tableland area of Southern Saskatchewan: [abs] in Marchant, T. (ed.), *Second International Symposium on the Devonian System, Program and Abstracts: Calgary, Alberta, Canadian Society of Petroleum Geologists*, p. 156.
- Magyar, B., H. C. Moor, and L. Sigg (1993), Vertical distribution and transport of molybdenum in a lake with a seasonally anoxic hypolimnion, *Limnol. Oceanogr.*, 38, 521– 531.
- McGhee, G.R., Jr., 1996. *The Late Devonian Mass Extinction: The Frasnian–Famennian Crisis*. Columbia University Press, New York, 303 pp.
- McLaren, D.J., Goodfellow, W.D., 1990. Geological and biological consequences of giant impacts. *Annu. Rev. Earth Planet. Sci.* 18, 123–171.
- Meijer-Drees, N.C. and D.I. Johnston, 1996, Famennian and Tournaisian biostratigraphy of the Big Valley, Exshaw and Bakken formations, southeastern Alberta and southwestern Saskatchewan, *Bulletin of Canadian Petroleum Geologist*, v. 44, p. 683-694.
- Meissner, F.F., 1978, Petroleum geology of the Bakken Formation, Williston Basin, North Dakota and Montana: *Proceedings of 1978 Williston Basin Symposium, September 24–27, Montana Geological Society, Billings*, p. 207–227.
- Meyers, P. A., 1994, Preservation of elemental and isotopic source identification of sedimentary organic matter. *Chemical Geology*, 144 289-302
- Meyers, P. A., 1997, Tenzer, G. E., Lebo, M. E., and Reuter, J. E., 1997. Sedimentary record of sources and accumulation of organic matter in Pyramid Lake, Nevada over the past 1000 years. *Limnology and Oceanography*, in press. Millero, F. J. (1996), *Chemical Oceanography*, 2nd ed., 469 pp., CRC Press, Boca Raton, Fla.

Morford, J.L., Emerson, S.R., 1999. The geochemistry of redox sensitive trace metals in sediments. *Geochim. Cosmochim. Acta* 63, 1735–1750.

Morris A.W., 1975. Dissolved molybdenum and vanadium in the northeast Atlantic Ocean. *Deep Sea Res.*, 22: 49-54.

Murphy, E.C., S.H. Nordeng, B. J. Juenker, and J.W. Hoganson, 2009, North Dakota stratigraphic column: North Dakota Geological Survey, 1 sheet.

Muscio, G.P.A., B. Horsfield, and D.H. Welte, 1994, Occurrence of thermogenic gas in the immature zone ; implications from the Bakken in-source reservoir system : *Organic Chemistry*, v. 22/3-5, p. 461-476.

Quinlan, G. M., and C. Beaumont, 1984, Appalachian thrusting, lithospheric flexure, and the Paleozoic stratigraphy of the eastern interior of North America: *Canadian Journal of Earth Science*, v. 21 p. 973-996

Perrin, N.A., 1982% Environment of deposition of Winnipegosis Formation (Middle Devonian), Williston Basin, North Dakota: [abs] *American Association of Petroleum Geologists Bulletin*, v. 66, p. 6 16-6 17.

Peters et al., 1996, K.A. Peters, K.T. Conrad, D.G. Carpenter, J.B. Wagner, J.C. Cooke, M.M. Laughlind, R.J. Enrico, L.B. Fearn, C.D. Walters, J.M. Moldovan, J.A. Ektan, P.E. Isaacson: Geochemistry, palynology, and regional geology of worldclass Upper Devonian Source Rocks, Madre de Dios Basin, Bolivia *Am. Assoc. Pet. Geol. Bull.*, 80 (1996), pp. 1323–1324

Peterson, 1993, J.A. Peterson Bakken of the north: product of a global organic “event” and a Devonian–Carboniferous backreef-mound anoxic shelf. *Abstracts, Carboniferous to Jurassic Pangea, Can. Soc. Pet. Geol.* (1993), p. 246

Peterson, J.A., and L.M. MacCary, 1987, Regional stratigraphy and general petroleum geology of the U.S. portion of the Williston Basin and adjacent areas, in Longman, M.W., ed., *Williston Basin: Anatomy of a Cratonic Oil Province: Rocky Mountain Association of Geologists*, p. 9-43

Piper, D.Z. and Calvert, S.E. 2009. A marine biogeochemical perspective on black shale deposition. *Earth-Science Reviews*. 95: 63-96.

Potts, Philip J. and Webb, Peter C. 1992. X-ray fluorescence Spectrometry. *Journal of Geochemical Exploration*. 44: 251-296.

Precht, W.F., 1986, Reservoir development and hydrocarbon potential of Winnipegosis (Middle Devonian) pinnacle reefs, mthem Elk Point Basin, North Dakota: *Carbonates and Evaporites*, v. 1, p. 83-99.

<http://micro.magnet.fsu.edu/micro/gallery/radiolarians/radiolarians.html>

Rachold, V. and Brumsack, H. J. (2001): Inorganic geochemistry of Albian sediments from the Lower Saxony basin, NW German: paleoenvironmental constraints and orbital cycles, *Palaeogeography, Palaeoclimatology, Palaeoecology* 174, pp. 123-144 .

- Richards, B. C., 1989, Upper Kaskaskia sequence-uppermost Devonian and Lower Carboniferous, in B. D. Ricketts, ed., *Western Canadian sedimentary basin, a case history: Calgary Alberta, Canadian Society of Petroleum Geologists*, p. 165-201.
- Rimmer, S.M. 2004. Geochemical paleoredox indicators in Devonian-Mississippian black shales, Central Appalachian Basin (USA). *Chemical Geology*. 206: 373-391.
- Riquier, L., Tribouvillard, N., Averbuch, O., Devleeschouwer, X. & Riboulleau, A., 2006. The Late Frasnian Kellwasser horizons of the Harz Mountains (Germany): Two oxygen-deficient periods resulting from different mechanisms. *Chemical Geology*, 233: 137-155.
- Rosenthal, L.R., 1987, The Winnipegosis Formation of the northeast margin of the Williston Basin: in Carleson, C.G. and Christopher, J.E., (eds.), *5th International Williston Basin Symposium, Saskatchewan Geological Society*, p. 37-46.
- Ross, C. A., and J. R. P. Ross, 1985, Late Paleozoic depositional sequences are synchronous and worldwide: *Geology*, v. 13, p. 194-197.
- Rousseau, R. M. 2001. Detection limit and estimate of uncertainty of analytical XRF results: *The Rigaku Journal*. 18: 33-47.
- Rowe, H., Mainali, P., Ruppel, S. 2011, Chemostratigraphy and Paleooceanography of the Late Jurassic Haynesville-Bossier System, East Texas Basin. AAPG special volume. Accepted.
- Rowe, H., Ruppel, S., Rimmer, S., Loucks, R., 2008. Core-based chemostratigraphy of the Barnett Shale, Permian Basin, Texas. *Gulf Coast Association of Geological Societies Transactions* 59, 675–686.
- Rowe, H. D.; Ruppel, S.; Rimmer, S.; Loucks, R.G. 2009. Core-based chemostratigraphy of the Barnett Shale, Permian Basin, Texas. *Gulf Coast Association of Geological Societies Transactions*. 59: 675-686.
- Rowe, H.D., Hughes, N., and Robinson, K., 'The quantification and application of hand-held energy dispersive x-ray fluorescence (ED-XRF) in mudrock chemostratigraphy and geochemistry', 2012, *Chemical Geology*.
- Sandberg, C. A., and C. R. Hammond, 1958, Devonian system in Williston basin and central Montana: *AAPG Bulletin*, v. 42, p. 2293-2334.
- Sandberg, C. A., and G. Klapper, 1967, Stratigraphy, age and paleotectonic significance of the Cottonwood Canyon Member of the Madison Limestone in Wyoming and Montana: *U.S. Geological Survey Bulletin* 1251-B, 70 p.
- Sandberg, C.A., R. C. Gutschick, R. C. Johnson, F. G. Poole, and W. J. Sando, 1982 Middle Devonian to Late Mississippian history of the overthrust belt region, western United States, in R. B. Powers, ed., *Geologic studies of the Cordilleran thrust belt: Rocky Mountain Association of Geologist*, p. 691-791.

Savard, M., Beauchamp, B., Veizer, J., 1990. Petrography of Silica in upper Paleozoic Carbonates of the Sverdrup Basin, Canadian Arctic. Current Research, Part D, Geological Survey of Canada, Paper 101-109

Schieber, J. 1998. Developing a sequence stratigraphic framework for Late Devonian Chattanooga Shale of the Southeastern U.S.A.: Relevance for the Bakken Shale. In J.E. Christopher, C.F. Gilboy, D.F. Paterson, and S.L. Bend, eds., Eight International Williston Basin Symposium, Saskatchewan Geological Society Special Publication, No. 13, pp 58-68.

Schoenlaub, H.P., 1986. Significant geological events in the Paleozoic record of the Southern Alps (Austrian Part). In: Walliser, O.H. (Ed.), Global Bio-Events: A Critical Approach. Lect. Notes Earth Sci. 8. Springer, Berlin, pp. 163–167.

Schoenlaub, H.P. and 12 others, 1992. The Devonian–Carboniferous boundary in the Carnic Alps (Austria): a multidisciplinary approach. Jahrb. Geol. Bundesanst., 135: 57–98.

Schmoker, J.W., 1996, A resource evaluation of the Bakken formation (Upper Devonian and Lower Mississippian) continuous oil accumulation, Williston Basin, North Dakota and Montana: The Mountain Geologist, v. 33/1, p. 1-10.

Scott, C., Lyons, T. W., Contrasting molybdenum cycling and isotopic properties in euxinic versus non-euxinic sediments and sedimentary rocks: Refining the paleoproxies, Chemical Geology, Volumes 324–325, 24 September 2012, Pages 19-27

Scotese, C.R., and McKerrow, W.S., 1990. Revised world maps and introduction. In: McKerrow, W.S., Scotese, C.R. (Eds.), Palaeozoic Palaeogeography and Biogeography. Geol. Soc. Mem. 12, 1–21.

Sepkoski, J.J., Jr., 1996. Patterns of Phanerozoic extinction: a perspective from global data bases. In: Walliser, O.H. (Ed.), Global Events and Event Stratigraphy in the Phanerozoic. Springer, Berlin, pp. 35–51.

Śliwiński, M.G., M.T. Whalen, M.T. and Day, J., 2010, Trace element variations in the Middle Frasnian punctata zone (Late Devonian) in the western Canada sedimentary basin — changes in oceanic bioproductivity and paleoredox spurred by a pulse of terrestrial afforestation. Geologica Belgica, 4 (2010), pp. 459–482

Sleep, N. H., J. A. Nunn, and L. Chen, 1980, Platform basins: Annual Review of Earth and Planetary Science, v. 8, 17-34.

Sloss, L. L., 1963, Sequences in the cratonic interior of North America: Geological Society of America Bulletin, v. 74, p. 93–114

Sloss, L. L. 1987, Williston Basin in the Family of Cratonic Basins, in Longman, M. W., ed., Williston basin, anatomy of cratonic oil province: Denver, Rocky Mountain Association of Geologist, p. 1-8.

- Smith, M.G., and Bustin, R.M., 1995, Sedimentology of the Late Devonian and Early Mississippian Bakken Formation, Williston Basin, *in* Vern Hunter, L.D., and Schalla, R.A., eds., Seventh International Williston Basin Symposium 1995 Guidebook: Montana Geological Society, North Dakota Geological Society, and Saskatchewan Geological Society, p. 103–114.
- Smith, M. G., R. M. Bustin, and M. L. Caplan, 1995, Sequence stratigraphy of the Bakken and Exshaw formations: a continuum of black shale formations in the Western Canada sedimentary basin, *in* L. D. V. Hunter and R. A. Schalla, eds., 7th international Williston basin symposium: Montana Geological Society Special Publication, p. 399-409.
- Smith, M.G. and R. M. Bustin, 2000, Late Devonian and Early Mississippian Bakken and Exshaw Black Shale Source Rocks, Western Canada Sedimentary Basin: A Sequence Stratigraphic Interpretation: AAPG Bulletin, v. 84/7, p. 940-960.
- Tribouillard, N., Riboulleau, A., Lyons, T., and Baudin, F. 2004. Enhanced trapping of molybdenum by sulfurized marine organic matter of marine origin in Mesozoic limestones and shales. *Chemical Geology*. 213: 385-401.
- Tribouillard, N., Algeo, T.J., Lyons, T., and Riboulleau, A. 2006. Trace metals as paleoredox and paleoproductivity indicators: an update. *Chemical Geology*. 232: 12–32.
- Tribouillard, N., Algeo, T.J., Baudin, F., and Riboulleau, A., et al. (2011), Analysis of marine environmental conditions based on molybdenum-uranium covariation - Applications to Mesozoic paleoceanography, *Chem. Geol.*, 282, 120–130
- Algeo, T.J., and N. Tribouillard, 2009, Environmental analysis of paleoceanographic systems based on molybdenum-uranium covariation: *Chemical Geology*, v. 268/3-4, p. 211-225.
- Ulmishek, G.F., 1988. Upper Devonian–Tournaisian facies and oil resources of the Russian Craton's Eastern Margin. *In*: McMillan, N.J., Embrey, A.F., Glass, D.J. (Eds.), *Devonian of the World. Proc. Can. Soc. Pet. Geol. Int. Symp., Devonian System Memoir 14: I*, pp. 527–549.
- Veevers, J.J. and Powell, CM. 1987. Late Paleozoic glacial episodes in Gondwanaland reflected in transgressive-regressive depositional sequences in Euroamerica. *Geological Society of America Bulletin*, v. 98, p. 475-487.
- Walliser, O.H., 1984b. Geological processes and global events. *Terra Cognita* 4, 17–20.
- Waters, A. J. and Maples. 1991. Mississippian Pelmatozoan Community Reorganization: A Predation-Mediated Faunal Change. *Paleobiology* Vol. 17, No. 4, pp. 400-410
- Webster, R. L., 1984, Petroleum source rocks and stratigraphy of the Bakken Formation in North Dakota: 1984 Symposium of the Rocky Mountain Association of Geologists, p. 57–81.
- Wetzel, W., 1957. Selektive Verkieselung. *Neues Jahrbuch für Geologie und Palaontologie Abhandlungen*, 105(1): 1–9

- Wilde, P., T. W. Lyons and M. S. Quinby-Hunt, 2004, Organic Proxies in Black Shales: Molybdenum: *Chemical Geology*, v. 206, p. 167-176.
- Wilson, J. L., 1967, Carbonate-evaporite cycles in lower Duprow Formation of Williston basin: *Canadian Petroleum Geologist Bulletin*, v. 15 p. 230-321.
- Van Krevelen, D. W., 1984 Organic geochemistry-old and new: *Organic Geochemistry*, v. 6, p. 1-10.
- Ver Straeten, C. E., Brett, B., Bradley B. S., 2011. Mudrock sequence Stratigraphy: A multi-proxy (sedimentological, paleobiological, and geochemical) approach, Devonian Appalachian Basin. *Palaeogeography, Palaeoclimatology, Palaeoecology* 304, 54-73.
- Vigrass, L.W., 1971, Depositional framework of the Winnipeg Formation in Manitoba and eastern Saskatchewan: *The Geological Association of Canada, Special Paper*, v. , p. 225–234
- Walliser, O.H. (1984): Pleading for a natural D/C-Boundary. *Cour. Forsch.-Inst. Senckenberg*, 67, 241–246, Frankfurt am Main.
- Waters, J. A., and C. G. Maples. 1991. Mississippian pelmatozoan community reorganization: a predator-mediated faunal change. *Paleobiology*. 17:400-410.
- Wang, K., Chatterton, B.D.E., 1993. Microspherules in Devonian sediments: origins, geological significance, and contamination problems. *Can. J. Earth Sci.* 30, 1660–1667.
- Williams J.A., 1974, Characterization of oil types in the Williston Basin: *AAPG Bulletin*, v. 58, no. 7, p. 1241-1252.
- Xu, D.Y, Zhang, Q.W., Sun, Y.Y., Yan, Z., Chai, Z.F., He, J.W., 1989. Event stratigraphy and extraterrestrial events. In: Duff, P.D., Smith, A.J. (Eds.), *Astrogeological Events in China*. Scottish Academic Press, Edinburgh, 264 pp.
- Young, G. M., Nesbitt, H.W., 1998. Processes controlling the distribution of Ti and Al in weathering profiles, siliciclastics sediments and sedimentary rocks. *Journal of Sedimentary Research* 68, 448-455
- Young, Harvey R., Rongyu Li, and Moe Kuroda. "Silicification in Mississippian Lodgepole Formation, Northeastern Flank of Williston Basin, Manitoba, Canada." *Journal of Earth Science* 23.1 (2012): 1-18.
- Ziegler, A.M., Hulver, M.L., Lottes, A.L., Schmachtenberg, W.F., 1984. Uniformitarianism and palaeoclimates: inferences from the distribution of carbonate rocks. In: Brenchley, P. (Ed.), *Fossils and Climate*. Wiley, London, pp. 3–25.
- Zheng, Y., Anderson, R. F., Van Geen, A., and Kuwabara, J. 2000, Authigenic molybdenum formation in marine sediments: a link to pore water sulfide in the Santa Barbara Basin: *Geochimica et Cosmochimica Acta*, v. 64, p. 4165–4178.

Biographical Information

David Nyrup Maldonado was born on August 12, 1978 in Brownsville, Texas. He was raised in Brownsville by his loving mother and father and is the youngest of seven children. As a young man he attended the various schools offered by the Brownsville Independent School District in Cameron County. After completing his senior year at James Pace High School, David was accepted to the University of Texas at Austin during the summer of 1996. After attending the University of Texas at Austin for a year he decided to transfer to the Baylor University in Waco, Texas where he graduated with a Bachelors of Science in Geology, May 2002. After graduation, he worked in private industry for eight years. Returning to full-time university studies in 2010, David enrolled at the University of Texas at Arlington to pursue a Master of Science degree in Geology under the supervision of Dr. Harry Rowe. He is scheduled to complete his Master's degree on December 16, 2012.